(2)

US Army Corps of Engineers

TECHNICAL REPORT HL-88-28

TOTAL SEDIMENT LOAD MEASUREMENT USING POINT-SOURCE SUSPENDED-SEDIMENT DATA

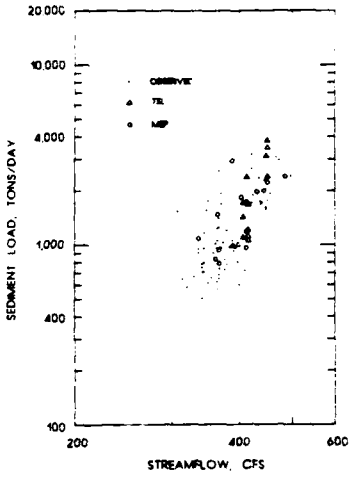

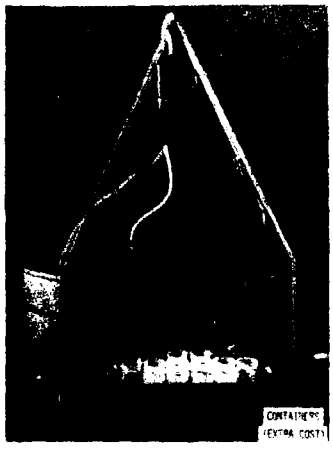

HYDRAULICS LABORATORY

by

John J. Ingram

Hydraulics Laboratory

DEPARTMENT OF THE ARMY
Waterways Experiment Station, Corps of Engineers
PO Box 631, Vicksburg, Mississippi 39181-0631

December 1988
Final Report

Prepared for US Army Engineer District, Vicksburg
Vicksburg, Mississippi 39181-0060

Unclassified

SECURITY CLASSIFICATION OF THIS PAGE

REPORT DOCUMENTATION PAGE

Form Approved
OMB No 0704-0188
Exp Date Jun 30 1986

1a REPORT SECURITY CLASSIFICATION Unclassified	1b RESTRICTIVE MARKINGS
2a SECURITY CLASSIFICATION AUTHORITY	3 DISTRIBUTION / AVAILABILITY OF REPORT Approved for public release; distribution unlimited.
2b DECLASSIFICATION / DOWNGRADING SCHEDULE	
4 PERFORMING ORGANIZATION REPORT NUMBER(S) Technical Report HL-88-28	5 MONITORING ORGANIZATION REPORT NUMBER(S)
6a NAME OF PERFORMING ORGANIZATION USAEWES Hydraulics Laboratory 6b OFFICE SYMBOL (If applicable) CEWES-HS-H	7a NAME OF MONITORING ORGANIZATION
6c ADDRESS (City, State, and ZIP Code) PO Box 631 Vicksburg, MS 39181-0631	7b ADDRESS (City, State, and ZIP Code)
8a NAME OF FUNDING / SPONSORING ORGANIZATION USAED, Vicksburg 8b OFFICE SYMBOL (If applicable)	9 PROCUREMENT INSTRUMENT IDENTIFICATION NUMBER
8c ADDRESS (City, State, and ZIP Code) PO Box 60 Vicksburg, MS 39181-0060	10 SOURCE OF FUNDING NUMBERS PROGRAM ELEMENT NO / PROJECT NO / TASK NO / WORK UNIT ACCESSION NO
11 TITLE (Include Security Classification) Total Sediment Load Measurement Using Point-Source Suspended-Sediment Data	
12 PERSONAL AUTHOR(S) Ingram, John J.	
13a TYPE OF REPORT Final report 13b TIME COVERED FROM _____ TO _____	14 DATE OF REPORT (Year, Month, Day) December 1988 15 PAGE COUNT 141
16 SUPPLEMENTARY NOTATION See reverse.	

17 COSATI CODES			18 SUBJECT TERMS (Continue on reverse if necessary and identify by block number)		
FIELD	GROUP	SUB-GROUP	Automated sampling	Sediment discharge	Suspended sediments
			Computer program	Sediment measurement	
			Point sampling	Sediment transport	

19 ABSTRACT (Continue on reverse if necessary and identify by block number)

A procedure for measuring total sediment discharge using point-source suspended-sediment data was developed. The proposed procedure, TSL (Total Sediment Load), was tested with field data from the Niobrara River at Cody, NE; Fivemile Creek at Shoshoni, WY; the Middle Loup River near Dunning, NE; the Rio Grande conveyance channel near Bernardo, NM; and Goodwin Creek near Oxford, MS. The TSL procedure was compared to the modified Einstein procedure (MEP), which uses depth-integrated suspended-sediment data for measuring total sediment discharge. The TSL procedure provides total sediment load measurements that are similar in magnitude to both turbulence flume measurements of total sediment load and MEP measurements. The similarity in results for the TSL procedure, the total sediment load measurements, and the MEP demonstrate the use of the TSL procedure as an alternative to depth-integrated suspended-sediment sampling. Results of the TSL procedure are more reliable when the point suspended-sediment samples are collected in the lower flow depth. The TSL

(Continued)

20 DISTRIBUTION / AVAILABILITY OF ABSTRACT ☒ UNCLASSIFIED/UNLIMITED ☐ SAME AS RPT ☐ DTIC USERS	21 ABSTRACT SECURITY CLASSIFICATION Unclassified
22a NAME OF RESPONSIBLE INDIVIDUAL	22b TELEPHONE (Include Area Code) / 22c OFFICE SYMBOL

DD FORM 1473, 84 MAR 83 APR edition may be used until exhausted
All other editions are obsolete

SECURITY CLASSIFICATION OF THIS PAGE
Unclassified

16. SUPPLEMENTARY NOTATION (Continued).

Available from National Technical Information Service, 5285 Port Royal Road, Springfield, VA 22161. Originally submitted in partial fulfillment of the requirements for the degree of Doctor of Philosophy in Civil Engineering to Colorado State University, Fort Collins, CO.

19. ABSTRACT (Continued).

procedure was tested and found to be reliable using point samples collected in the lower 20 to 45 percent flow depth.

The assessments of the reviewed data sets highlight advantages for selecting the TSL procedure over the MEP: realistic sediment load measurements, greater control in obtaining suspended-sediment samples, automatic sampling, the collection of near-continuous measurements, and time integration for determining the true sediment transport. Also, the use of point-source suspended-sediment samples requires less time in the field and lower sediment sampling costs.

PREFACE

The research conducted herein was performed by personnel of the Hydraulics Laboratory (HL) of the US Army Engineer Waterways Experiment Station (WES), Vicksburg, MS, at the request of the US Army Engineer District, Vicksburg (LMK), during the period November 1986 - March 1988.

The work was accomplished under the general supervision of Messrs. Frank A. Herrmann, Jr., Chief, HL; Richard A. Sager, Assistant Chief, HL; Marden B. Boyd, Chief, Waterways Division; and Glenn A. Pickering, Chief, Hydraulic Structures Division; and under the direct supervision of Dr. Bobby J. Brown, Chief, Hydraulic Analysis Branch, Hydraulic Structures Division. The study was conducted and this report was prepared by Dr. John J. Ingram, Hydraulic Analysis Branch, now Chief, Water Resources Engineering Group, Environmental Engineering Division, Environmental Laboratory, WES.

Mr. Andrew J. Bowie of the US Department of Agriculture-Agricultural Research Service, Sedimentation Laboratory, Oxford, MS, provided special assistance in obtaining data from the Goodwin Creek research catchment. Technical reviews of the report were provided by Drs. Steven R. Abt, E. V. Richardson, Daryl B. Simons, and Stanley A. Schumm, all of Colorado State University, Fort Collins, CO, and Dr. Frank M. Neilson, Hydraulic Analysis Branch.

Mr. Phil G. Combs, LMK, was the point of contact for the Vicksburg District, and Mr. David S. Biedenharn, LMK, provided assistance.

This report was also submitted to the Academic Faculty of Colorado State University, Fort Collins, CO, in partial fulfillment of the requirements for the degree of Doctor of Philosophy in Civil Engineering.

COL Dwayne G. Lee, EN, is the Commander and Director of WES. Dr. Robert W. Whalin is the Technical Director.

TABLE OF CONTENTS

TABLE OF CONTENTS (Continued)

TABLE OF CONTENTS (Concluded)

LIST OF TABLES

LIST OF FIGURES

LIST OF FIGURES (Continued)

LIST OF FIGURES (Concluded)

LIST OF SYMBOLS

Symbol	Definition
'	on J and Q designates association with the sampling depth
a	bed load layer thickness
A	ratio of bed layer thickness to water depth
A_c	cross-sectional area
c	a constant
C_a	sediment concentration for a particle having diameter D at a distance a from the streambed
C_b	the bed load sediment concentration
C_ℓ	sediment concentration at the lower boundary of Toffaleti's lower suspended load zone
C_m	sediment concentration at the lower boundary of Toffaleti's middle suspended load zone
C_{md}	middepth sediment concentration at $y = d/2$
C_p	the concentration of the suspended sediment at distance y_p above the channel bed
C_s	a variable coefficient
C_u	sediment concentration at the lower boundary of Toffaleti's upper suspended load zone
C_y	sediment concentration for a particle having diameter D at a distance y from the streambed
C_z	an empirical coefficient used in Toffaleti's method
C_0, C_1	constants
d	mean flow depth; flow depth
d_s	flow depth of a sampled vertical section in a cross section

LIST OF SYMBOLS (Continued)

Symbol	Definition
D	diameter of a particle
D_{35}	particle size at which 35 percent by weight of the bed material is finer
D_{65}	particle size at which 65 percent by weight of the bed material is finer
D_{84}	particle size at which 84 percent by weight of the bed material is finer
f	Weisbach friction factor
g	the acceleration of gravity
i_b	fraction of bed material in a given size range
i_B	fraction of bed load in a given size range
i_s	fraction of suspended material in a given size range
i_T	fraction of total load in a given size range
$i_B q_B$	rate at which a particle of diameter D moves through a unit width of the bed layer per unit of time
$i_B Q_B$	sediment discharge through the bed layer of particles of a given size range
$i_s q_s$	rate at which a particle of diameter D moves in suspension through a unit width per unit of time
$i_T q_T$	rate at which a particle of diameter D moves through a unit width of channel per unit of time
I_1	$0.216 \frac{A^{z-1}}{(1-A)^z} \int_A^1 \left(\frac{1-y}{y}\right)^z dy$
I_2	$0.216 \frac{A^{z-1}}{(1-A)^z} \int_A^1 \left(\frac{1-y}{y}\right)^z \ln y \, dy$
J_1	$\int_A^1 \left(\frac{1-y}{y}\right)^z dy$

LIST OF SYMBOLS (Continued)

Symbol	Definition
J_2	$\int_A^1 \left(\frac{1-y}{y}\right)^z \ln y \, dy$
k_s	roughness element height
k_s'	roughness element height due to grain roughness
m	a numerical constant
n	Manning's roughness coefficient
P	$2.303 \log \frac{30.2d(x)}{k_s}$
P_1	a function of w/U_* and the relative roughness $n/d^{1/6}$
q	streamflow per unit width, cubic feet per second
q_B	rate of bed load transport per unit width of cross section
q_s	sediment load in suspension per unit width
q_T	total sediment discharge per unit channel width
Q	streamflow for a cross section
Q_s	total suspended-sediment transport through a cross section
Q_s'	suspended-sediment load in the measured zone through a cross section
Q_T	total sediment load through a cross section
R	hydraulic radius
R'	the hydraulic radius with respect to grain roughness
R"	the hydraulic radius with respect to form roughness
S	energy grade line slope
S'	energy grade line slope due to grain roughness
S"	energy grade line slope due to form roughness

Symbol	Definition
S_s	the specific gravity of the sediment
S_w	water-surface slope
T	water temperature in degrees Fahrenheit
U_*	shear velocity, $\sqrt{gRS}$
U'_*	shear velocity with respect to grain roughness, $\sqrt{gRS'}$
$\overline{V}$	mean flow velocity in the cross section
V_{max}	maximum flow velocity in a vertical section
V_y	average flow velocity at a distance y from the channel bed
$\overline{V}_y$	average flow velocity in the measured vertical section
V_0, V_1	reference velocities used in the Extrapolated Data procedure
w	particle fall velocity
w_r	w for a reference grain size
w_u	w for other than the reference grain size
W	cross-sectional width
x	dimensionless parameter for transition between hydraulically smooth and rough flows
x'	dimensionless parameter with respect to grain roughness for transition between hydraulically smooth and rough flows
X	0.77Δ if $\Delta/\delta > 1.80$, 1.39δ if $\Delta/\delta < 1.80$
y	height above the streambed
y_b	the height above the channel bed for the lower boundary of suspended sediment
y_i	an integration constant
y_p	height of suspended-sediment point sample above the channel bed

Symbol	Definition
y_0	the lower limit of integration
Y	a pressure correction parameter and a function of D_{65}/δ as given by Einstein (1950, Figure 8)
z	an exponent of the equation describing the sediment concentration distribution
z_i	an exponent used in Toffaleti's method
z_r	z for a reference size
z_u	z for size ranges other than the reference size
z_v	an empirical coefficient used in Toffaleti's method
α_1, α_2	regression coefficients determined by a least squares fit using field data
β	numerical constant relevant to diffusion in turbulent flows
β_1	log 10.6
β_x	log (10.6X/Δ)
β_{x1}	log (10.6x)
δ	thickness of the laminar sublayer of a smooth wall
δ'	thickness of the laminar sublayer of a smooth wall with respect to grain roughness
Δ	D_{65}/x
ϵ_s	diffusion coefficient relevant to sediment distribution
κ	the universal von Karman constant, 0.4 for clear water
ν	kinematic viscosity
ξ	a hiding coefficient and a function of D/X as given by Einstein (1950, Figure 7)
$(\xi Y)_{RM}$	$(\delta + C_s D)/k_s$ when $D < \delta + C_s D$; D/k_s when $D \geq \delta + C_s D$
ρ_f	the density of the flow medium

LIST OF SYMBOLS (Concluded)

Symbol	Definition
ρ_s	the density of the solids
ϕ_*	the transport intensity for an individual grain size
ψ_*	the intensity of shear for an individual grain size

CHAPTER 1

INTRODUCTION

1.1 BACKGROUND

Most river and watershed improvement programs require knowledge of the total sediment load likely to exist during various flow conditions. To obtain this knowledge with sufficient accuracy, field measurements are made which include discharge and suspended-sediment measurements. Discharge measurements consist of depth and mean velocity measurements taken at selected verticals of a channel cross section from which the total discharge can be computed. Suspended-sediment measurements are usually made by sampling the concentration of suspended bed material and wash load with a depth-integrated sampler at some or all of the verticals where mean velocity is measured. With stream discharge and sediment data, estimates of the total sediment discharge are made using computational procedures such as the modified Einstein procedure (Colby and Hembree 1955), the Colby method (Colby 1957), and the Toffaleti method (Toffaleti 1969).

The acquisition of discharge and sediment data can require extensive field data collection time and manpower. To reduce time and manpower requirements, automated sampling stations may be installed which periodically record the river's stage and collect point-source suspended-sediment samples. The current practice for analyzing automatically collected point-source sediment data is to determine the suspended-sediment load using a correlation previously developed from

concurrently collected depth-integrated and point-source suspended-sediment samples.

Lane and Kalinske (1941) developed a computational procedure for determining suspended-sediment load using a point suspended-sediment sample. Since their research and the development of depth-integrated sediment load measurement procedures, the determination of sediment load from point-source suspended-sediment data using theoretically based concepts has received little attention other than by Brooks (1963). The procedure presented in this paper advances the research efforts of Lane, Kalinske, and Brooks; eliminates the need for a correlation between point-source and depth-integrated suspended-sediment samples; and permits the direct computation of "total" sediment load (suspended load plus bed load) using point-source suspended-sediment data.

1.2 RESEARCH OBJECTIVES

The goal of this research is to develop a theoretically based computational procedure for making total sediment load measurements using a point-source suspended-sediment sample. Advantages of the proposed procedure over existing procedures include the direct use of automated sampling station data and the reduced cost of data collection. To achieve this goal, the following objectives have been established:

1. Develop a procedure for computing total sediment load that uses point-source suspended-sediment measurements.

2. Compare the proposed procedure to Colby and Hembree's depth-integrated sediment load measurement procedure (Colby and Hembree 1955) using published data.

3. Apply the procedure to newly acquired data.

The proposed total sediment load computational procedure is presented in Chapter 3, and applied and evaluated in Chapter 4.

CHAPTER 2

LITERATURE REVIEW

2.1 NUMERICAL FORMULATION OF TOTAL SEDIMENT LOAD

Numerical formulations that determine total sediment load for a set of field discharge and sediment measurements generally subdivide the total load into bed load and suspended load. Bed load is sediment that rolls or slides along the channel bed, and suspended load is sediment that is supported by the upward turbulent currents and remains suspended for considerable lengths of time. The division between these two zones of transport is not sharply defined, but has commonly been referenced and applied by setting a bed load layer thickness of two grain diameters as proposed by Einstein (1950).

The total sediment discharge per unit channel width q_T with sediment load divided as bed load and suspended load, is determined by

$$q_T = \int_a^d V_y C_y dy + q_B \qquad 2.1$$

where

a = height above the channel bed where suspended load begins

d = flow depth

V_y = time-averaged flow velocity at a distance y above the channel bed

C_y = time-averaged sediment concentration at a distance y above the channel bed

q_B = bed load transport per unit width

Therefore, components which are necessary for determining total sediment load are the vertical velocity distribution, the sediment concentration distribution, and the bed load discharge.

2.1.1 Velocity Distribution

The basis for the velocity distribution used in most of the known sediment load measurement procedures is the Prandtl-von Karman velocity distribution equation (Prandtl 1926, von Karman 1930)

$$\frac{V_y}{U_*} = \frac{1}{\kappa} \ln \frac{y}{y_i} \qquad 2.2$$

where

U_* = the shear velocity, $\sqrt{gRS}$, where g is the acceleration of gravity, R is the hydraulic radius, and S is the energy grade line slope

κ = the universal von Karman constant, 0.4 for clear water

y_i = an integration constant

Variations in the application of this relation stem from derivations of the integration constant y_i. One of these formulations considers the maximum flow velocity V_{max} to occur at the channel's surface ($y = d$). Substituting V_{max} for V_y and d for y in Equation 2.2 leads to

$$\frac{V_{max}}{U_*} = \frac{1}{\kappa} \ln \frac{d}{y_i} \qquad 2.3$$

A new relation can now be derived which does not include y_i by combining Equations 2.2 and 2.3:

$$V_y = V_{max} + \frac{U_*}{\kappa} \ln \frac{y}{d} \qquad 2.4$$

which, when integrated over depth to determine the average velocity in the vertical $\bar{V}_y$, can be expressed as

$$\bar{V}_y = \frac{1}{d} \int_0^d \left(V_{max} + \frac{U_*}{\kappa} \ln \frac{y}{d} \right) dy = V_{max} - \frac{U_*}{\kappa} \qquad 2.5$$

Equations 2.4 and 2.5 can be combined and described by

$$V_y = \bar{V}_y + \frac{U_*}{\kappa} + \frac{U_*}{\kappa} \left(\ln \frac{y}{d} \right) \qquad 2.6$$

or

$$\frac{V_y}{\bar{V}_y} = 1 + \frac{U_*}{\kappa \bar{V}_y} \left(1 + \ln \frac{y}{d} \right) \qquad 2.7$$

which have both been applied in sediment measurement procedures (Lane and Kalinske 1941 and Brooks 1963).

Another variation in the derivation of y_i which has received wide application comes from the research efforts of Keulegan (1938). Keulegan used dimensional reasoning to determine y_i for hydraulically smooth and rough boundaries. For a smooth wall he considered y_i to depend solely on U_* and ν, the kinematic viscosity, such that

$$\frac{y_1 U_*}{\nu} = m \qquad 2.8$$

where m is a constant. For a hydraulically rough wall, he established a relation for y_1 in the form

$$\frac{y_1 U_*}{\nu} = f\left(\frac{k_s U_*}{\nu}\right) \qquad 2.9$$

where k_s is the height of the roughness elements. Substituting either Equation 2.8 or 2.9 into Equation 2.2 leads to

$$\frac{V_y}{U_*} = c + \frac{1}{\kappa} \ln \frac{yU_*}{\nu} \qquad 2.10$$

or

$$\frac{V_y}{U_*} = c + \frac{2.30}{\kappa} \log \frac{yU_*}{\nu} \qquad 2.11$$

where c is a constant. Keulegan applied the data collected by Nikuradse (1932, 1933) to Equation 2.11 and formulated relations for hydraulically smooth and rough pipe flow which may be applied in open channels. Keulegan's relations are

$$\frac{V_y}{U_*} = 5.5 + 5.75 \log \frac{yU_*}{\nu} \qquad 2.12$$

for hydraulically smooth flow, and

$$\frac{V_y}{U_*} = 8.5 + 5.75 \log \frac{y}{k_s} \qquad 2.13$$

for hydraulically rough flow. (Keulegan used $\kappa = 0.40$ when he developed Equations 2.12 and 2.13.)

Keulegan similarly formulated relations for the mean flow velocity, $\overline{V}$ in trapezoidal cross sections. He determined

$$\frac{\overline{V}}{U_*} = 3.5 + 5.75 \log \frac{RU_*}{\nu} \qquad 2.14$$

for hydraulically smooth flow in pipes of circular cross section, and

$$\frac{\overline{V}}{U_*} = 3.0 + 5.75 \log \frac{RU_*}{\nu} \qquad 2.15$$

for flow between smooth parallel walls of infinite extent. The mean of these two relations may be applied in hydraulically smooth open channel flow. The mean of Equations 2.14 and 2.15 is

$$\frac{\overline{V}}{U_*} = 3.25 + 5.75 \log \frac{RU_*}{\nu} \qquad 2.16$$

For hydraulically rough channels, Keulegan formulated

$$\frac{\overline{V}}{U_*} = 6.25 + 5.75 \log \frac{R}{k_s} \qquad 2.17$$

using the experimental results of Bazin (1865).

The sediment measurement procedures which use Keulegan's velocity formulations apply them as they were presented by Einstein (1950). Einstein modified the velocity distribution Equations 2.12 and 2.13 and the mean cross-sectional velocity Equations 2.16 and 2.17 using Nikuradse's (1933) data. These modified relations are

$$\frac{V_y}{U_*} = 5.75 \log\left[30.2\left(\frac{yx}{k_s}\right)\right] \qquad 2.18$$

and

$$\frac{\overline{V}}{U_*} = 5.75 \log\left[12.27\left(\frac{Rx}{k_s}\right)\right] \qquad 2.19$$

where x is a dimensionless parameter for transitioning between smooth and rough flow and a function of k_s/δ which is presented in Figure 4 of Einstein (1950). (δ is the thickness of the laminar sublayer of a smooth wall, $11.6\nu/U_*$.)

2.1.2 Sediment Concentration Distribution

The differential equation for suspended sediment of uniform size, shape, and density in two-dimensional, uniform, turbulent flow is

$$C_y w + \varepsilon_s \frac{dC_y}{dy} = 0 \qquad 2.20$$

where w is the particle fall velocity, ε_s is a diffusion coefficient, and the remaining variables are as previously defined. If ε_s were constant from the flow surface to the channel bed, Equation 2.20 could be integrated to yield

$$\frac{C_y}{C_a} = \exp\left[-\frac{w}{\varepsilon_s}(y - a)\right] \qquad 2.21$$

where C_a is a referenced suspended-sediment concentration at the distance a above the streambed. However, the diffusion coefficient is not constant over depth and can be shown to be

$$\varepsilon_s = \beta \kappa U_* \frac{y}{d}(d - y) \qquad 2.22$$

where β is a numerical constant relevant to diffusion in turbulent flows (Vanoni 1975).

Lane and Kalinske (1941) assumed ε_s to be constant over depth to obtain an expression which was more convenient to use than Equation 2.22. They assumed the average ε_s in any vertical section could be described as

$$\varepsilon_s = \frac{U_* d}{15} \qquad 2.23$$

When this expression is placed into Equation 2.21, the sediment distribution equation becomes

$$\frac{C_y}{C_a} = \exp\left[- \frac{15w}{U_*} \frac{(y - a)}{d} \right] \qquad 2.24$$

An expression for sediment distribution which considers the diffusion coefficient ε_s to vary with flow depth can be derived by substituting Equation 2.22 into Equation 2.20. The derived expression is

$$C_y w + \beta \kappa U_* \frac{y}{d} (d - y) \frac{dC_y}{dy} = 0 \qquad 2.25$$

Separating the variables and integrating Equation 2.25 yields

$$\frac{C_y}{C_a} = \left[\left(\frac{d - y}{y} \right) \left(\frac{a}{d - a} \right) \right]^z \qquad 2.26$$

where

$$z = \frac{w}{\beta \kappa U_*} \qquad 2.27$$

Equation 2.26 was developed by Rouse (1937) and is used by several sediment measurement procedures (Colby and Hembree 1955, Brooks 1963, Allen and Barnes 1975, Burkham and Dawdy 1980, and Shen and Hung 1983).

2.1.3 Bed Load Transport

Sediment in transport within the bed layer is called the bed load. Einstein (1950) developed an equation to compute this mode of sediment transport which is based on the probability that a particle will move from its position on the bed and another particle will settle in its place. Einstein's bed load equation is

$$i_B q_B = \phi_* i_b \rho_s g^{3/2} D^{3/2} (S_s - 1)^{1/2} \qquad 2.28$$

where

$i_B q_B$ = rate at which a particle of diameter D moves through a unit width of the bed layer per unit of time

ϕ_* = the transport intensity for an individual grain size D

i_b = the bed material fraction for a given size range

i_B = the fraction of bed load for a given size range

ρ_s = the density of the solids

S_s = the specific gravity of the sediment

To apply Equation 2.28 for a given grain diameter, Einstein assumed that all the parameters on the right side of the equation were constant except for ϕ_*. The intensity of transport ϕ_* was established to be a function of the intensity of shear ψ_* for individual grain diameters. The function which relates ψ_* and ϕ_* is presented by Einstein (1950, Figure 10) where ψ_* is determined by

$$\psi_* = \xi Y \left(\frac{\beta_1^2}{\beta_x^2} \right) \frac{\rho_s - \rho_f}{\rho_f} \frac{D}{R' S} \qquad 2.29$$

where ξ is a hiding coefficient and a function of D/X as given by Einstein (1950, Figure 7), Y is a pressure correction parameter and a function of D_{65}/δ as given by Einstein (1950, Figure 8), and

$\beta_1 = \log 10.6$

$\beta_x = \log (10.6X/\Delta)$, where $X = 0.77\Delta$ if $\Delta/\delta > 1.80$ and $X = 1.39\delta$ if $\Delta/\delta < 1.80$ and $\Delta = D_{65}/x$ where D_{65} is the grain size for which 65 percent by weight of the bed material is finer

ρ_f = the density of the flow medium

R' = the hydraulic radius with respect to grain roughness

Equations 2.28 and 2.29 have experienced two significant modifications as they have been applied in total sediment measurement procedures. The first of these modifications was made by Colby and Hembree (1955) in the development of their procedure which has become known as the modified Einstein procedure. Colby and Hembree modified Equations 2.28 and 2.29 as follows: The quantity ψ_* for an individual grain size D is computed using the larger value of the two relations

$$\psi_* = 1.65 \frac{D_{35}}{RS} \qquad 2.30$$

and

$$\psi_* = 0.66 \frac{D}{RS} \qquad 2.31$$

where D_{35} is the grain size for which 35 percent by weight of the bed material is finer. Colby and Hembree arbitrarily divided ϕ_* of Equation 2.28 by 2 to fit their observed total load data more closely.

The second significant modification to Einstein's Equations 2.28 and 2.29 was made by Burkham and Dawdy (1980). In Burkham and Dawdy's study, the relation for ψ_* was redeveloped and the need to divide ϕ_* of Equation 2.28 by 2 was eliminated. The basis for the new ψ_* relation was Einstein's (1950) equation for a uniform particle size

$$\psi_* = \frac{\rho_s - \rho_f}{\rho_f} \frac{D}{R'S} \qquad 2.32$$

which Burkham and Dawdy changed to

$$\psi_* = 1.65 \frac{k_s}{RS} \qquad 2.33$$

where k_s replaces the uniform particle size; ρ_s is 5.17 slugs/ft^3; ρ_f is 1.95 slugs/ft^3; and R replaces R'. Burkham and Dawdy developed an equation for a nonuniform bed material size gradation with the assumption that Einstein's hiding coefficient and lift correction parameter can be represented by the single parameter $(\xi Y)_{RM}$. The resulting relation for ψ_* for a nonuniform size gradation is

$$\psi_* = 1.65(\xi Y)_{RM} \left(\frac{\beta_1}{\beta_{x1}} \right)^2 \frac{k_s}{RS} \qquad 2.34$$

where

$$\beta_1 = \log 10.6 \qquad 2.35$$

$$\beta_{x1} = \log 10.6x \qquad 2.36$$

$$(\xi Y)_{RM} = \frac{\delta + C_s D}{k_s} \quad \text{when } D < \delta + C_s D \qquad 2.37$$

$$= \frac{D}{k_s} \quad \text{when } D \geq \delta + C_s D$$

and

$$C_s = -0.62 + 3.12(D_{65}\ D_{35})^{1/2} \qquad 2.38$$

Burkham and Dawdy developed Equation 2.38 using data sets from the Niobrara and the Middle Loup Rivers of Nebraska.

2.2 SEDIMENT LOAD MEASUREMENT PROCEDURES

Sediment discharge measurement of streams is necessary to determine sediment loads and to develop or check sediment discharge relationships. If sediment were uniformly distributed within a channel cross section, the measurement and calculation of sediment discharge could easily be computed as the product of a known sediment concentration and stream discharge. However, sediment is not uniformly distributed, and a measurement and computational procedure is therefore required to determine total sediment loads.

2.2.1 Sediment Load Calculations using Point Sampled Data

The earliest known record of suspended-sediment sampling is the work of Gorsse and Subuors in 1808 for the Rhone River at Arles, France

(US Inter-Agency Committee on Water Resources, Subcommittee on Sedimentation 1940). From 1808 thru the 1930's, suspended-sediment samples were primarily collected from one or more points in the vertical. Two theoretically based procedures which can apply such samples for computing suspended-sediment load have been developed by Lane and Kalinske (1941) and Brooks (1963).

2.2.1.1 Lane and Kalinske. Following the development of turbulence suspension theory (O'Brien 1933, Christiansen 1935, Richardson 1937, and Rouse 1937) and the Prandtl-von Karman velocity distribution equation (Equation 2.2), Lane and Kalinske (1941) applied these theories to determine suspended-sediment load using a point suspended-sediment sample. Lane and Kalinske proposed that the point sample could be obtained from any level in a vertical section; however, they suggested that the sample should be collected from the lower half-depth.

Lane and Kalinske applied the Prandtl-von Karman logarithmic function for the vertical velocity distribution, Equation 2.7. Lane and Kalinske modified Equation 2.7 using von Karman's constant κ equal to 0.4 and applying Manning's formula for hydraulic roughness

$$\bar{V} = \frac{1.486}{n} R^{2/3} S^{1/2} \qquad 2.39$$

where n is the Manning's roughness coefficient. The resulting form of Equation 2.7 for a unit width of a wide cross section ($d \approx R$) is

$$\frac{V_y}{\bar{V}_y} = 1 + \frac{1.7n\sqrt{g}}{d}\left(1 + \ln \frac{y}{d}\right) \qquad 2.40$$

Lane and Kalinske substituted Equations 2.40 and 2.24 (a sediment distribution equation) into the integral

$$q_s = \int_0^d C_y V_y dy \qquad 2.41$$

to obtain

$$q_s = \bar{V}_y C_a d \int_0^1 \frac{V_y}{\bar{V}_y} \exp\left[-15\left(\frac{w}{U_*}\right)\frac{(y-a)}{d}\right] dy \qquad 2.42$$

where q_s is the total suspended-sediment load per unit width and C_a is the sampled sediment concentration from any point in the vertical. By taking $\exp[15(wa)/(U_* d)]$ out of the integral, Lane and Kalinske showed

$$q_s = qC_a P_1 \exp\left(15\frac{wa}{U_* d}\right) \qquad 2.43$$

where q is the streamflow in cubic feet per second per unit width and P_1 is a function of w/U_* and the relative roughness $n/d^{1/6}$. Lane and Kalinske provided a graphical solution for P_1.

2.2.1.2 Brooks. Since the research of Lane and Kalinske, the advancement of determining sediment load from point samples of suspended sediment using theoretically based concepts received little attention until the research efforts of Brooks (1963). Assuming the velocity

distribution in Equation 2.7 and the concentration distribution portrayed in Equations 2.26 and 2.27 (with $\beta = 1$), Brooks obtained

$$q_s = C_{md} \int_{y_0}^{d} \left(\frac{d-y}{y}\right)^z \left[\overline{V}_y + \frac{U_*}{\kappa}\left(1 + \ln \frac{y}{d}\right)\right] dy \qquad 2.44$$

where C_{md} is the middepth sediment concentration at $y = d/2$ and y_0 is the lower limit of integration.

Brooks proposed three possible ways to select the lower limit of integration, y_0. The first limit is Einstein's (1950) suggestion that sediment is not suspended closer to the bed than two particle diameters (2D). Another possible limit is the height above the bed where $V_y = 0$, according to the logarithmic velocity profile. This second limit prevents unintentional negative contributions to the suspended-sediment load integral, $q_s = \int_{y_0}^{d} V_y C_y dy$, if y_0 is greater than 2D. A third possible limit is when the concentration, determined by the extrapolation of the suspended load equation, is equal to the concentration of the size fraction in the bed. Brooks recommended the largest height of these three limits as the most reasonable choice for the limit to integration.

2.2.2 Conventional Suspended-Sediment Measurement

Following the development and improvement of depth-integrated suspended-sediment samplers in the 1940's, the convention for obtaining suspended-sediment data became depth-integrated sampling. Depth-integrated sampling is limited to sampling the stream section referred to as the measured zone. The measured zone, under most conditions, is

within the region of suspended-sediment transport. The unmeasured zone contains both suspended load and bed load. To include the unmeasured sediment load in total sediment load computations, various methods have been developed. The most common of these procedures are the modified Einstein procedure (Colby and Hembree 1955), the Colby method (Colby 1957), and the Toffaleti method (Toffaleti 1969). Of these, the modified Einstein procedure has received the most attention for sediment load measurements (Schroeder and Hembree 1956, Colby and Hubbell 1961, Lara 1966, Bowie, Bolton, and Murphree 1972, Burkham and Dawdy 1980, and Shen and Hung 1983).

2.2.2.1 Modified Einstein Procedure. The modified Einstein procedure was developed by Colby and Hembree (1955) to determine a channel's total sediment load through the combination of conventional suspended-sediment discharge measurements and a bed material transport formula. The modified Einstein procedure enables the computation of a channel's unmeasured load which can be added to a measured load for the estimation of total load. The procedure accomplishes this objective using depth-integrated suspended-sediment samples and Einstein's bed-load function (1950). Data required to use the procedure include depth-integrated suspended-sediment samples, streamflow measurements, bed material gradations, and water temperature. Computational components of the modified Einstein procedure include Einstein's modifications to Keulegan's open channel velocity relationships (Equations 2.18 and 2.19 with $k_s = D_{65}$ and flow depth replacing hydraulic radius), Rouse's sediment concentration profile relation (Equation 2.26), and a modified Einstein's bed load function

$$i_B q_B = \frac{\phi_*}{2} i_b \rho_s g^{3/2} D^{3/2} (\rho_s - 1)^{1/2} \qquad 2.45$$

Colby and Hembree arbitrarily divided ϕ_* of Equation 2.45 by two in order for their sediment load calculations to agree with their total sediment load measurements. Substituting Equations 2.18, 2.26, and 2.45 into Equation 2.1 produces the sediment load equation for size intervals

$$i_T q_T = \int_a^d C_a \left[\left(\frac{d - y}{y} \right) \frac{a}{d-a} \right]^z 5.75 U_* \log\left(\frac{30.2yx}{k_s} \right) dy + i_B q_B \qquad 2.46$$

where i_T is the fraction of total load in a given size range and i_B is the fraction of bed load in a given size range. Einstein (1950) transformed Equation 2.46 to

$$i_T q_T = 11.6 U_* C_a a \left[2.303 \log\left(\frac{30.2xd}{k_s} \right) I_1 + I_2 \right] + i_B q_B \qquad 2.47$$

in which

$$I_1 = 0.216 \frac{A^{z-1}}{(1 - A)^z} \int_A^1 \left(\frac{1 - y}{y} \right)^z dy \qquad 2.48$$

$$I_2 = 0.216 \frac{A^{z-1}}{(1 - A)^z} \int_A^1 \left(\frac{1 - y}{y} \right)^z \ln (y)\, dy \qquad 2.49$$

and A is a dimensionless expression equal to a/d .

According to Einstein (1950), the product $11.6U_*$ is the effective flow velocity for transporting the bed material in the bed layer. Therefore, in addition to Equation 2.45, bed material transport in the bed layer may be expressed by

$$i_B q_B = 11.6U_* C_a a \qquad 2.50$$

Substitution of Equation 2.50 into Equation 2.47 leads to

$$i_T q_T = i_B q_B \left(PI_1 + I_2 + 1\right) \qquad 2.51$$

in which

$$P = 2.303 \log \frac{30.2xd}{k_s} \qquad 2.52$$

Before Equation 2.51 can be applied to determine the total sediment load, the value for z must be determined. The value for z is obtained by trial and use of the measured suspended-sediment discharge for the dominant size interval of the measured zone.

Colby and Hembree reasoned that the ratio of the suspended-sediment load of the measured zone Q_s' to the suspended-sediment load for the entire suspended-sediment load zone Q_s could be represented by

$$\frac{Q_s'}{Q_s} = \frac{PJ_1' + J_2'}{PJ_1 + J_2} \qquad 2.53$$

where

$$J_1 = \int_A^1 \left(\frac{1 - y}{y}\right)^z dy \qquad 2.54$$

$$J_2 = \int_A^1 \left(\frac{1 - y}{y}\right)^z \ln y \, dy \qquad 2.55$$

and a single prime mark designates association with the measured zone. Equation 2.53 is rewritten with the substitution of the relation for the total suspended-sediment load,

$$Q_s = i_B Q_B (PI_1 + I_2) \qquad 2.56$$

where $i_B Q_B$ is the sediment discharge through the bed layer of particles of a given size range. Substitution of Equation 2.56 into Equation 2.53 leads to

$$\frac{Q_s'}{i_B Q_B} = \frac{I_1}{J_1}(PJ_1' + J_2') \qquad 2.57$$

where Q_s' is determined from measurements and $i_B Q_B$ is computed using the product of channel width and Equation 2.45. Equation 2.57 is used to compute z by trial for the dominant size interval of the bed load and suspended load. The values of z for the other size ranges are computed using the following relation determined by Colby and Hembree:

$$z_u = z_r\left(\frac{w_u}{w_r}\right)0.7 \qquad 2.58$$

where

$z_u = z$ for size ranges other than the reference size

$z_r = z$ for the reference size

$w_u = w$ for size ranges other than the reference size

$w_r = w$ for the reference size

2.2.2.2 Colby's Method. Colby (1957) established several empirical relationships for estimating total sediment discharge using the same type of stream measurements used in developing the modified Einstein procedure. Colby's procedure is simpler to apply than the modified Einstein procedure, although it does not compute the sediment load for individual size fractions and it is sensitive to the mean velocity. Data required for this empirical procedure which estimates unmeasured sediment load are the mean flow velocity, the stream width, the mean flow depth, and the measured mean suspended-sediment discharge concentration. The total sediment discharge is the sum of the measured and unmeasured sediment loads.

2.2.2.3 Toffaleti's Method. Toffaleti (1969) suggested that his procedure "offers a means of reducing the cost, time, and manpower requirements...in connection with continuing sediment observation stations." He further suggested that his procedure could be used to compute total sand load which can be added to wash load measured from three combined samples to determine total sediment load. Wash load is that part of the total sediment discharge that is composed of particle sizes finer than those represented in the channel bed.

Toffaleti deviated from other total sand load computation procedures with his division of the flow depth into four zones of sediment transport: (1) the bed zone of relative thickness $2D/d$; (2) the lower suspended zone from $2D/d$ to $y/d = 1/11.24$; (3) the middle suspended zone from $y/d = 1/11.24$ to $y/d = 1/2.5$; and (4) the upper suspended zone from $y/d = 1/2.5$ to the flow surface. For each of the three suspended load zones, the sediment concentration distribution of each sediment size fraction is expressed as power relations. Toffaleti's relations for the upper, middle, and lower zones, respectively, are

$$C_y = C_u\left(\frac{y}{d}\right)^{-1.5z_i} \tag{2.59}$$

$$C_y = C_m\left(\frac{y}{d}\right)^{-z_i} \tag{2.60}$$

$$C_y = C_\ell\left(\frac{y}{d}\right)^{-0.756z_i} \tag{2.61}$$

where

$$z_i = \frac{w\bar{V}_y}{C_z S_w d} \tag{2.62}$$

$$C_z = 260.67 - 0.667T \tag{2.63}$$

where

C_u, C_m, C_ℓ = sediment concentration at the lower boundaries of the upper, middle, and lower suspended load zones, respectively

S_w = water-surface slope

T = water temperature

C_ℓ also equates to the bed layer concentration.

The velocity profile for the flow depth is represented by the power relation

$$V_y = (1 + z_v)\bar{V}_y\left(\frac{y}{d}\right)^{z_v} \qquad 2.64$$

where the exponent z_v is the empirical relation

$$z_v = 0.1198 + 0.00048T \qquad 2.65$$

Toffaleti developed an empirical relationship for the sand load in the lower suspended zone to make his sediment load computation procedure complete. This empirical relationship provides a necessary boundary condition to compute the sand load for each of the other transport zones.

The following input is required for the Toffaleti model: the average velocity in the vertical, the hydraulic radius, water temperature, stream width, bed material size fraction, D_{65} of the bed material, water-surface slope, and the kinematic viscosity of the water-sediment mixture.

2.2.2.4 Burkham and Dawdy's Method. Burkham and Dawdy (1980) revised the modified Einstein procedure (Colby and Hembree 1955) by eliminating some of the empirical adjustments. Burkham and Dawdy's revision eliminates the need to arbitrarily divide Einstein's bed load transport intensity factor, ϕ_* of Equation 2.28, by 2 (Equation 2.45). Values for ϕ_* are taken directly from Einstein's curve relating ψ_* to ϕ_* (Einstein 1950, Figure 10), and ψ_* is determined by Equation 2.34. The equivalent sand roughness k_s of Equations 2.18, 2.19, and 2.52 was determined to be $5.5D_{65}$ rather than D_{65} (Burkham and Dawdy 1976). With these variations, the computation steps parallel those of Colby and Hembree (1955).

Burkham and Dawdy compared their revision of the modified Einstein procedure to the original modified Einstein procedure using data sets from the following sites: Niobrara River near Cody, Nebraska; Middle Loup River at Dunning, Nebraska; Fivemile Creek near Riverton, Wyoming; Fivemile Creek near Shoshoni, Wyoming; and Rio Grande conveyance channel near Bernardo, New Mexico. For these data sets, Burkham and Dawdy found no significant difference in the sediment discharges computed by these two procedures. However, both procedures did significantly underestimate sediment loads on the Rio Grande conveyance channel for periods when the bed form was flat or in transition. Also, these two procedures significantly overestimated sediment loads for two sites on Fivemile Creek in Wyoming where Burkham and Dawdy believe the bed forms were probably dunes, flat, or in transition at different times.

2.2.2.5 Shen and Hung's Method. Shen and Hung (1983) revised the modified Einstein procedure (Colby and Hembree 1955) with two major modifications. The first modification applies the research of Lara

(1966) which proposed a nonlinear relationship between z and w. Shen and Hung proposed that the relationship between z and w can be described as

$$z = \alpha_1 w^{\alpha_2} \tag{2.66}$$

where α_1 and α_2 are regression coefficients determined by a least squares fit using field data. Equation 2.66 permits a variation from Colby and Hembree's proposed relation (Equation 2.58) which suggests

$$\alpha_1 = z_r \left(\frac{1}{w_r}\right)^{0.7} \tag{2.67}$$

and

$$\alpha_2 = 0.7 \tag{2.68}$$

and requires the selection of a single sediment reference size. Shen and Hung's least squares fit, Equation 2.66, removes the subjectivity in selecting a single reference size and permits the determination of a more reliable relationship. Shen and Hung show that z does not vary with w raised to the 0.7 power. The other modification is an optimization procedure to minimize the difference between the measured and calculated suspended-sediment loads in the sampled zone.

2.2.2.6 Extrapolated Data Procedure. Allen and Barnes (1975) proposed a modification to conventional suspended-sediment load

measurement. Their procedure permits the direct measurement of the zones previously classified as measured and unmeasured. The direct measurements are made using a combination of depth-integrated and point sediment samples in vertical sections. The depth-integrated samples are used to determine the sediment load in the measured zone, and the point samples are used to determine the suspended-sediment load in the zone not measured by the depth-integrated sampler. The addition of these two loads equate to the total suspended-sediment load. Data required to determine the unmeasured load are point concentration and velocity data from two or more depths in each vertical section. These point concentration and velocity data are plotted on log-log plots to determine coefficients for the concentration and velocity relationships

$$C_y = C_0\left(\frac{d - y}{y}\right)^z \qquad 2.69$$

and

$$V_y = V_0 y^m \qquad 2.70$$

respectively, where

C_0 = concentration at $(d - y)/y = 1.0$

$z = \log C_1/C_0$ where C_1 is the concentration at $(d - y)/y = 10.0$

V_0 = velocity at $y = 1.0$ on the distance scale

$m = \log V_1/V_0$ with V_1 being the velocity at $y = 10.0$ on the distance scale

The product of Equations 2.69 and 2.70 is integrated over the unmeasured zone to determine the unmeasured load

$$q_s = C_0 V_0 \int_{2D\ ft}^{0.3\ ft} y^m \left(\frac{d - y}{y}\right)^z dy \qquad 2.71$$

The lower limit of integration was chosen to follow the suggestion of Einstein (1950) and the upper limit of integration was chosen as 0.3 ft because nearly all of Allen and Barnes' depth-integrated samples were taken to that elevation.

2.3 CHAPTER SUMMARY

The review of the literature shows that the vertical velocity distribution, the sediment concentration distribution, and the bed load discharge are necessary computational components for determining the total sediment load. The basis for determining the vertical velocity distribution by most of the known sediment load measurement procedures is the Prandtl-von Karman velocity distribution equation (Equation 2.2). Most of the reviewed conventional measurement procedures apply the Keulegan (1938) form of the vertical velocity distribution equation as it was modified by Einstein (1950) in Equations 2.18 and 2.19. The concentration profile relationship applied in many of these same procedures is Equation 2.26, which was developed by Rouse (1937). The bed load discharge is commonly computed with a form of the Einstein bed load function (Einstein 1950), which permits the determination of the concentration at the lower limit of the suspended-sediment zone.

CHAPTER 3

MODEL FORMULATION

3.1 NUMERICAL COMPONENTS

Conventional total sediment load measurement procedures use depth-integrated suspended-sediment samples. The total sediment load measurement procedure formulated in this chapter makes use of point-source suspended-sediment samples. The similarity between these procedures is the use of relations for a vertical velocity distribution, a suspended-sediment concentration profile, and bed load transport. For these components, the proposed procedure applies Einstein's modifications to Keulegan's mean and point velocity relations (Equations 2.18 and 2.19), Rouse's sediment concentration distribution relation (Equation 2.26), and Burkham and Dawdy's modified form of Einstein's bed load function (Equations 2.28 and 2.34). The primary feature that sets the proposed procedure apart from other methods is the direct computation of z for Equation 2.26 using a point sample of suspended sediment. When Equation 2.26 is applied, z is the only unknown, provided the suspended-sediment concentration is known at a known depth and the sediment concentration at the lower suspended-sediment boundary is calculated. Section 3.1.2 and Appendix A provide greater detail on the calculation of z.

3.1.1 Velocity Distribution Function

The velocity distribution and mean velocity equations used by the reviewed conventional sediment load measurement procedures are

Equations 2.18 and 2.19, respectively. Variations in the application of these two equations come from the use of different relations for k_s.

Einstein (1950) suggested $k_s = D_{65}$ as a good rule of thumb for application in Equations 2.18 and 2.19. Einstein's rule has been applied by each of the conventional sediment measurement procedures using these equations except for the modification proposed by Burkham and Dawdy (1980). Burkham and Dawdy (1976) analyzed the data of Barnes (1967) and Limerinos (1970) and determined that $k_s = 5.5D_{65}$. Burkham and Dawdy (1976) also indicated that the use of a larger referenced particle size improves the prediction of the mean velocity and velocity distribution. If a larger particle size is to be used, Burkham and Dawdy agree with the use of $k_s = 3.3D_{84}$ as applied by Limerinos. The Limerinos relationship for k_s is compatible with van Rijn's (1982) review of published k_s relationships and recommendation that $k_s = 3D_{90}$ for grain roughness.

Literature shows for movable-bed streams that k_s is variable and dependent upon flow regime (Nordin and Dempster 1963, van Rijn 1982). The lower limit of k_s results from grain roughness during upper regime flow (i.e., plane bed and antidunes), and the upper limit of k_s results from both grain and form roughness during lower regime flow (i.e., ripples and dunes). The importance of form roughness was demonstrated by Nordin and Dempster (1963) with their study of the Middle Rio Grande, New Mexico. Nordin and Dempster calculated for the Middle Rio Grande an average maximum k_s of $400D_{65}$.

The velocity distribution of the proposed procedure uses Equations 2.18 and 2.19 as in most of the conventional sediment measurement procedures (Colby and Hembree 1955, Burkham and Dawdy 1980, and Shen and

Hung 1983). A variation in the proposed procedure from the conventional procedures is the provision for a variable k_s and the use of D_{84} of the bed material as a reference size. A variable k_s makes it possible to account for both grain and form roughness. The larger referenced bed material size improves the prediction of the mean velocity and velocity distribution as indicated by Burkham and Dawdy (1976). The reference size multiplier may be selected based on the judgment of the investigator or determined using the measured stream hydraulics and computational procedures such as Einstein (1950) and Brownlie (1981, 1983). The Einstein and Brownlie procedures predict the resistance to flow over movable boundaries with bed forms. The use of Einstein's and Brownlie's procedures to determine k_s is presented in Appendix A.

3.1.2 Concentration Profile

The suspended-sediment concentration profile in the proposed procedure is determined according to Equation 2.26. The use of Equation 2.26 for determining the concentration profile is similar to most conventional sediment measurement procedures (Colby and Hembree 1955, Burkham and Dawdy 1980, and Shen and Hung 1983) and varies only in the determination of z. The calculation for z is based upon the sampled suspended-sediment concentration and the calculation of the bed load concentration using Burkham and Dawdy's (1980) modification of Einstein's bed load function. Values for z are directly computed using the modified form of Equation 2.26

$$z = \frac{\log\left(\frac{C_b}{C_p}\right)}{\log\left(\frac{d - y_b}{y_b}\,\frac{y_p}{d - y_p}\right)} \qquad 3.1$$

where

C_b = the bed load sediment concentration,

C_p = the concentration of the suspended sediment at distance y_p above the channel bed,

y_b = the height above the channel bed for the lower boundary of suspended sediment

y_p = the height of suspended-sediment point sample above the channel bed

The lower boundary for suspended sediment is set at the largest of two possible limits. The first limit is Einstein's (1950) suggestion that sediment is not suspended closer to the bed than two particle diameters (2D). The other limit is the height above the bed where $V_y = 0$, according to Equation 2.18. This latter limit prevents unintentional negative contributions to the suspended-sediment load integral,

$$q_s = \int_{y_b}^{d} V_y C_y \, dy \text{ , if } y_b \text{ is greater than 2D.}$$

3.1.3 Bed Load Function

Burkham and Dawdy's (1980) modified form of Einstein's bed load function (Equations 2.28 and 2.34) is applied to compute the bed load. Burkham and Dawdy's modification is chosen because it permits the computation of bed load for individual sediment size fractions and assists in the elimination of arbitrarily dividing ϕ_* by 2 as in Equation 2.45 (compare to Einstein's equation, Equation 2.28).

To apply Equation 2.34, the product of hydraulic radius and energy slope RS must be determined. Einstein (1950) recommended that the product RS should be separated into R'S and R"S, where $R = R' + R''$, and R" is the hydraulic radius due to form roughness. Einstein based his recommendation for the separation of R into two parts on reasoning

that flow energy is transformed into energy of turbulence which may be separated into two forms. The first form of turbulence is caused by the rough wall and stays in the vicinity of the boundary material. The second form of turbulence corresponds to shape resistance and occurs at a considerable distance away from the grains. Einstein further reasoned that the energy due to the first form affects the bed load motion and the energy due to the second form does not contribute to the bed load motion.

The division of R into R' and R" leads to added numerical calculations and was not applied by Colby and Hembree (1955) nor any of the subsequent sediment measurement methods. The proposed procedure applies Einstein's reasoning to separate the flow energy; however, the product RS , is separated into RS' and RS" (as suggested by Meyer-Peter and Muller 1948 and Vanoni and Brooks 1957), where

$S = S' + S"$

S' = the energy slope due to grain roughness

$S"$ = the energy slope due to form roughness

Equation 2.34 may now be written as

$$\psi_* = 1.65(\xi Y)_{RM} \left(\frac{\beta_1}{\beta_{x1}}\right)^2 \frac{k_s}{RS'} \qquad 3.2$$

and the product RS' is computed using the modified form of Equation 2.19,

$$\frac{\bar{V}}{\sqrt{gRS'}} = 5.75 \log\left(12.27 \frac{Rx'}{k_s'}\right) \qquad 3.3$$

where k_s' is the effective roughness element height due to grain roughness and x' is a function of k_s'/δ' which is presented in Figure 4 of Einstein (1950), and $\delta' = (11.6\nu)/U_*'$. Note that Equation 3.3 provides the same computational results as the conventional sediment measurement procedures when bed forms are insignificant.

3.2 MODEL DESCRIPTION

The computational relations in the proposed procedure apply Einstein's modifications to Keulegan's (1938) mean and point velocity relations (Equations 2.18, 2.19, and 3.3), the suspended-sediment concentration distribution Equation 2.26, and Burkham and Dawdy's (1980) modified form of Einstein's bed load function (Equations 2.28 and 3.2). The basic data requirements, computation steps, and computation results are similar to the modified Einstein procedure and its revisions. The major difference in the proposed procedure is the collection of suspended-sediment data from a point sample rather than from a depth-integrated sample. The data requirements and computation steps for the proposed procedure are summarized in the following sections of this chapter.

3.2.1 Basic Data

To effectively apply the proposed procedure, the basic data for each total sediment load measurement are to represent the field conditions at the time of suspended-sediment sampling. The basic data for the proposed procedure are the streamflow for the sampled cross section; the sampled cross section width, cross-sectional area, and hydraulic radius; the flow depth of the sampled vertical; the height above the channel bed where the point sample was obtained; the concentration of the suspended-sediment sample; the fraction of bed

material in individual size intervals; the fraction of suspended material in individual size intervals; and the water temperature.

3.2.2 Computation Steps

The general application of the computation components and field data for determining total sediment load is presented in detail in Appendix A. The Fortran 77 computer code for these computations is provided in Appendix B. A summary of the computations used with the basic data for the proposed procedure is presented in step form as follows:

Step 1. Compute the bed load for a unit width of flow for each bed material size interval (Equations 2.28 and 2.34-2.38).

Step 2. Using the results of step 1, compute the concentration in the bed load zone for each bed material size interval (Equation A.9).

Step 3. Determine the exponent z of Equation 2.26 for each sediment size interval using the concentration of the suspended-sediment sample and the concentration in the bed load zone determined in step 2.

Step 4. Using the results of step 3, develop a linear regressed relationship for z as a function of particle fall velocity (Equation A.12).

Step 5. Recompute the bed load zone concentration for each sediment size interval using the sampled suspended-sediment concentrations, the relationship for z developed in step 4, and Equation 2.26.

Step 6. Recompute the bed load for a unit width of flow for each sampled suspended-sediment size interval using the results of step 5 (Equation A.15).

Step 7. Determine the total sediment load for a unit width of flow for each sediment size interval using Equation 2.51, the computed bed load, and the relationship for z developed in step 4.

Step 8. Compute the total sediment load for the channel by multiplying the sum of the results from step 7 by the width of the sampled cross section (Equation A.18).

3.3 CHAPTER SUMMARY

A procedure for measuring total sediment load using suspended-sediment data collected at one point has been developed. The procedure advances the research efforts of Lane and Kalinske (1941) and Brooks (1963), eliminates the need for a correlation between point-source and depth-integrated suspended-sediment samples, and permits the direct computation of total sediment load using point-source suspended-sediment data. The proposed procedure applies Einstein's (1950) modification to Keulegan's (1938) mean and point velocity relations, the suspended-sediment concentration distribution equation developed by Rouse (1937), and Burkham and Dawdy's (1980) modified form of Einstein's bed load function. The data required for application of the proposed procedure include descriptors of the streamflow, the channel geometry, the bed material, and the point-source suspended-sediment sample.

CHAPTER 4

MODEL EVALUATION

4.1 GENERAL

This chapter compares the proposed sediment load measurement procedure to the total sediment load field data and the modified Einstein procedure. The computational step solution and computer code listing for the proposed procedure are provided in Appendices A and B, respectively. The proposed procedure and computer code are identified as TSL (Total Sediment Load).

4.2 BASIC DATA

The TSL procedure is compared to observed total sediment load data and the modified Einstein procedure using data from four selected river reaches: the Niobrara River at Cody, Nebraska (Colby and Hembree 1955); Fivemile Creek at Shoshoni, Wyoming (Colby, Hembree, and Rainwater 1956); the Middle Loup River near Dunning, Nebraska (Hubbell and Matejka 1959); and the Rio Grande conveyance channel near Bernardo, New Mexico (Culbertson, Scott, and Bennett 1972). These data sets were selected because of their use in the development and evaluation of the modified Einstein procedure. Also, the selected data sets provide the suspended-sediment point samples required for application of the TSL procedure.

4.3 COMPARISON TO TOTAL SEDIMENT LOAD MEASUREMENTS

The referenced data sets provide sediment data for both normal and total sediment load sampling stations. The "normal" sediment sampling

stations are located in channel reaches with a uniform cross section and uniform flow. The total sediment load sampling stations are located downstream of the normal sampling stations at natural channel constrictions or man-made turbulence flumes wherein depth-integrated suspended-sediment samples are assumed to represent all of the sediment in transport.

4.3.1 Niobrara River

Colby and Hembree (1955) describe the study reaches, the data collection, and the data for the Niobrara River near Cody, Nebraska. Colby and Hembree used the Niobrara River data to develop the modified Einstein procedure. The data include depth-integrated suspended-sediment samples which were concurrently collected at the normal and contracted sections for comparison of the modified Einstein procedure to the total sediment load. The data also include point-integrated suspended-sediment samples which were collected to assess the suspended-sediment concentration distribution. The point samples, however, were not collected concurrently with the total sediment load measurements. Therefore, for this study, comparisons of the TSL procedure to the total sediment load measurements are made by comparing sediment load versus streamflow relationships.

Total sediment loads observed at the contracted section of the Niobrara River are plotted against streamflow in Figure 4.1. The scatter of points in Figure 4.1 shows a trend of increasing sediment load with increasing streamflow and can be regressed to the function,

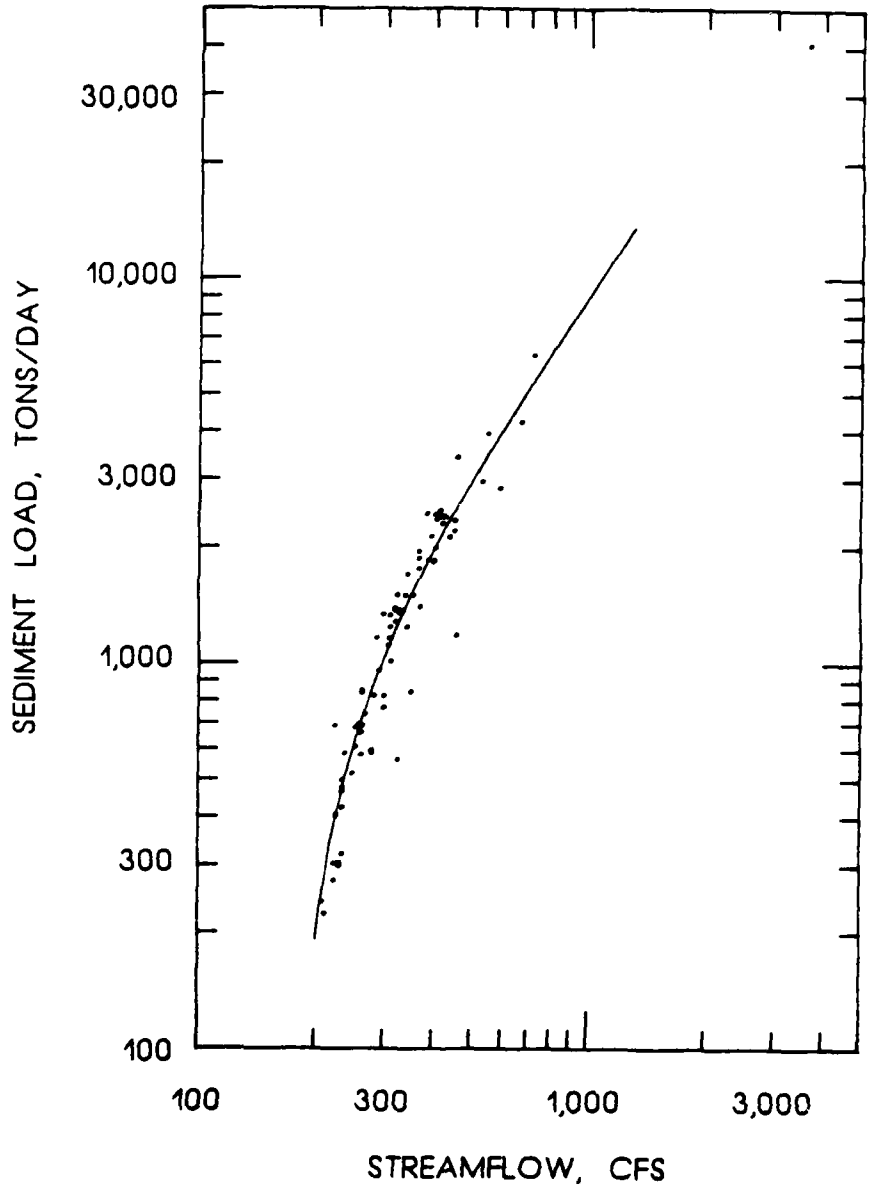

Figure 4.1. Observed total sediment load versus streamflow for the Niobrara River. The curve represents Equation 4.1.

$$Q_T = 0.003672Q^2 + 6.639Q - 1282.0 \qquad 4.1$$

where Q_T is the total sediment load in tons per day and Q is the streamflow in cubic feet per second. The coefficient of correlation r^2 for Equation 4.1 is 0.89.

Comparison of the observed total sediment loads and the total sediment loads estimated by Equation 4.1 is provided in Figure 4.2. Figure 4.2 shows 87 percent of the observed sediment loads to be within ±50 percent of the sediment load estimated by Equation 4.1. This percentage difference is an indicator of the accuracy of an attempt to determine a sediment load relationship for the Niobrara River.

Total sediment loads computed by the TSL procedure using point samples at the normal section are plotted against streamflow in Figure 4.3. The scatter of points in Figure 4.3 shows a trend of increasing sediment load with increasing streamflow. The distribution of sediment load magnitudes for a given range of streamflow in Figure 4.3 is greater than the distribution in Figure 4.1. This increased distribution may result from more samples or the sensitivity of the point sampler's location. The point samples for Figure 4.3 were taken from the lower 14 to 90 percent of the flow depths (0.5 to 3.1 ft above the channel bed).

Lane and Kalinske (1941) recommended that suspended-sediment point samples should be collected from the lower half-depth. Point sample measurements used to further assess the TSL procedure were from the lower third flow depth to be well within Lane and Kalinske's recommendation. For example, data for samples collected in the lower third of the flow depths (0.5 ft above the channel bed) are plotted in Figure 4.4.

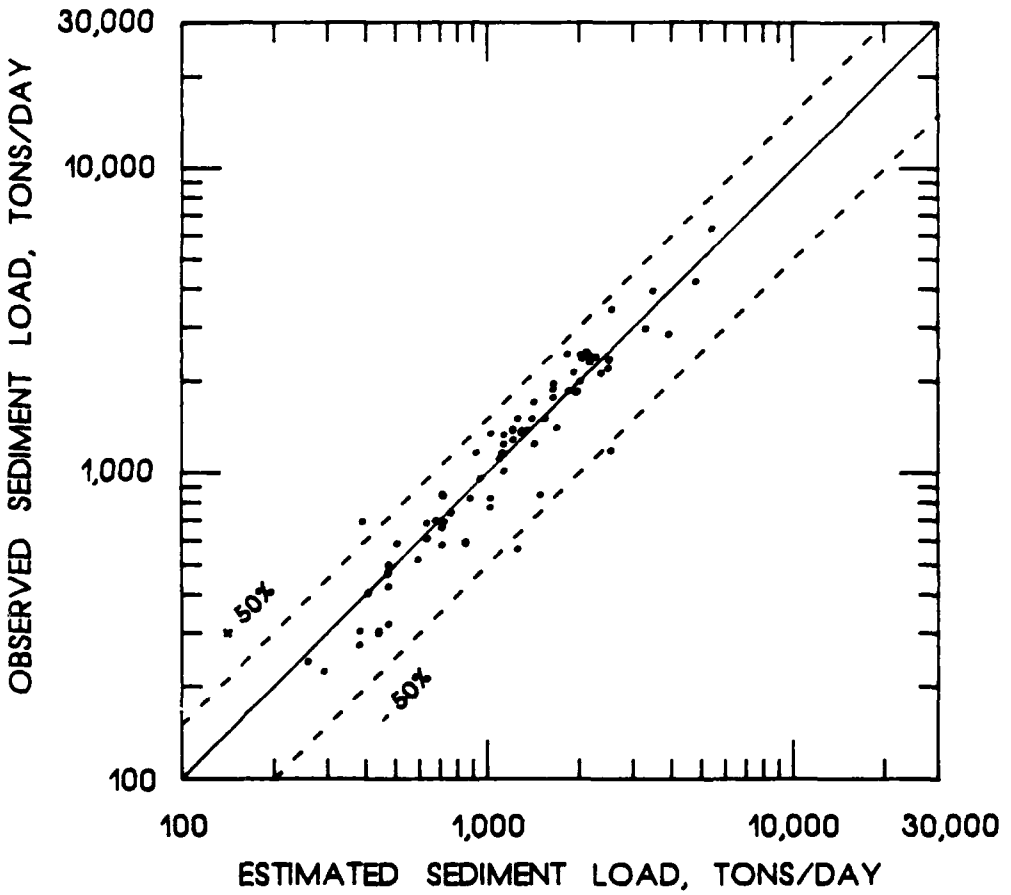

Figure 4.2. Observed sediment load versus estimated sediment load for the Niobrara River.

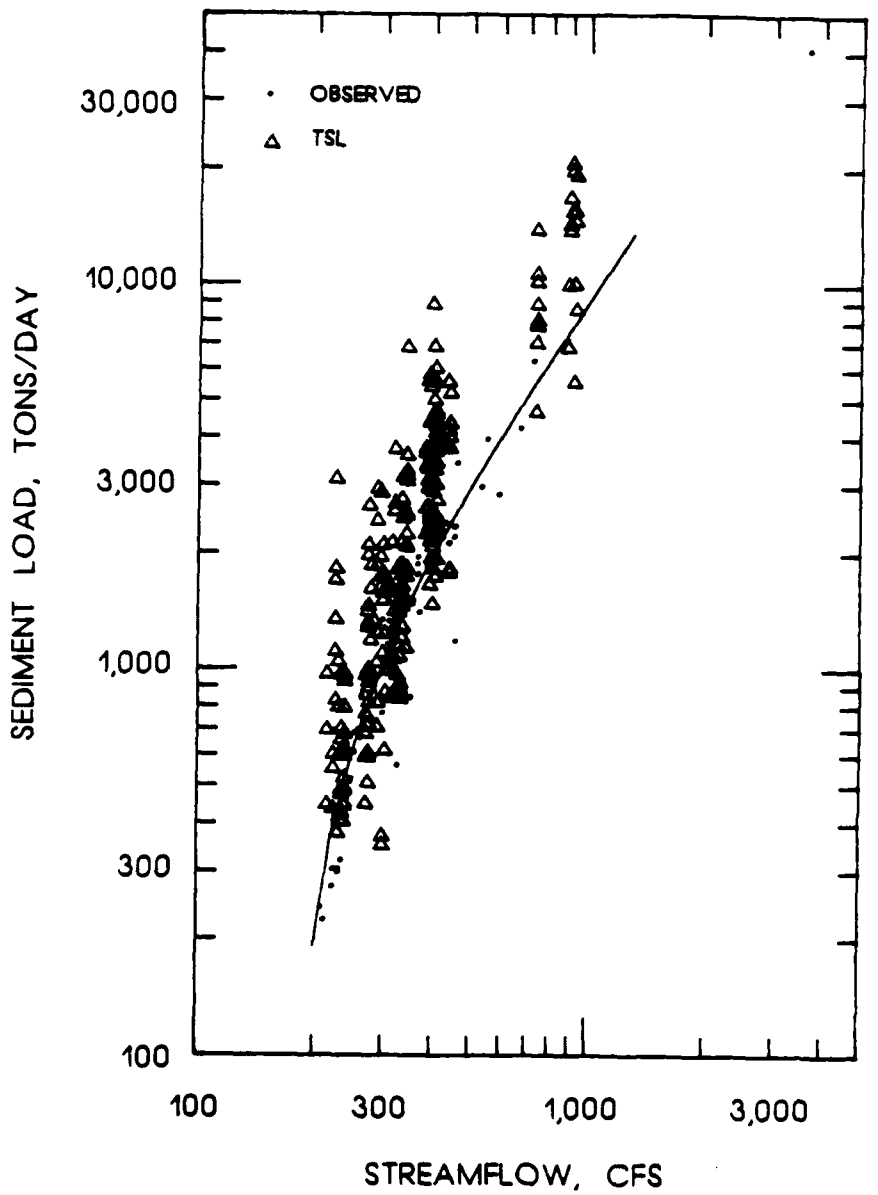

Figure 4.3. Total sediment load determined by TSL versus streamflow for the Niobrara River using point samples from the lower 14-90 percent flow depth and the Limerinos procedure to determine k_s. The curve represents Equation 4.1.

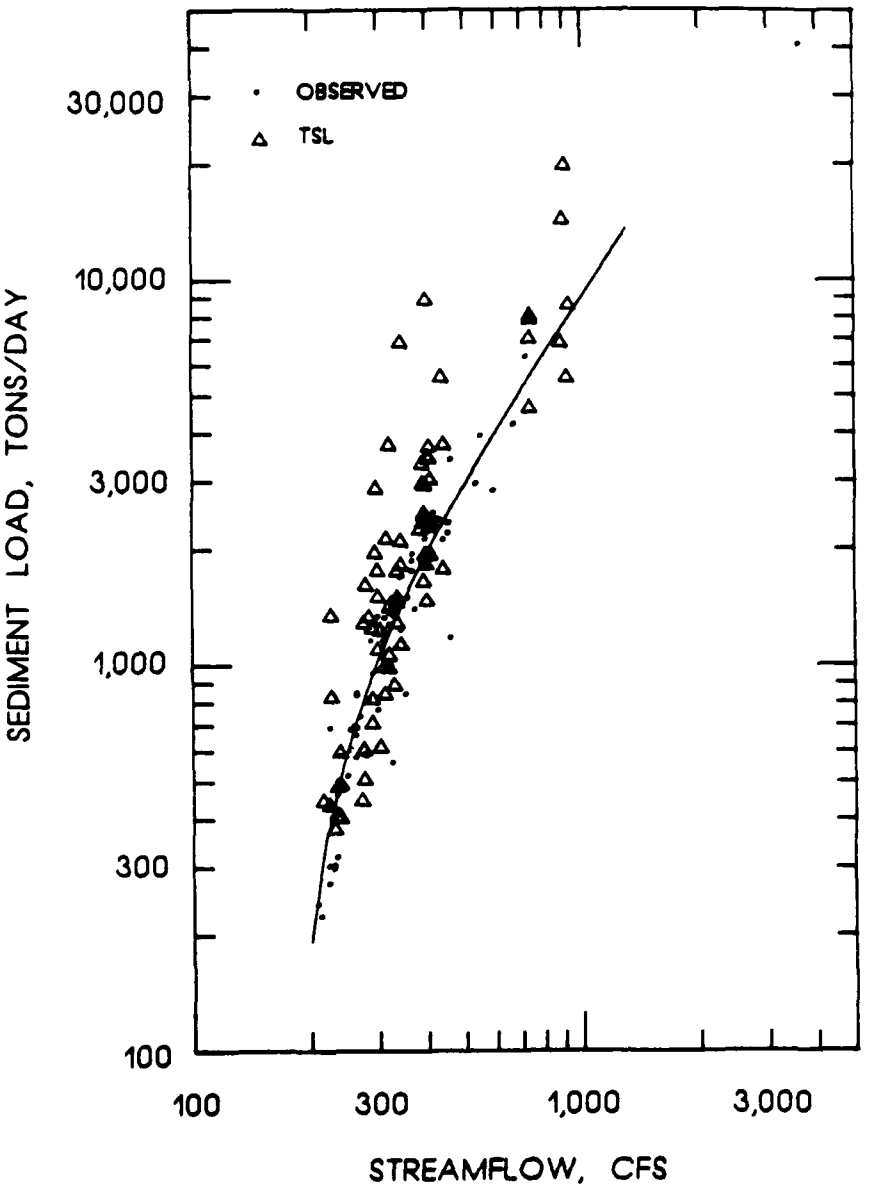

Figure 4.4. Total sediment load determined by TSL versus streamflow for the Niobrara River using point samples from the lower one-third flow depth and the Limerinos procedure to determine k_s. The curve represents Equation 4.1.

The scatter of points in Figure 4.4 is reduced from the level of scatter in Figure 4.3. The reduction of data scatter in Figure 4.4 may be attributed to greater reliability in sampling sediment concentrations in the lower flow depth as Lane and Kalinske recommended. At locations further from the channel bed the sediment concentration and flow velocity may deviate from the theoretical profiles due to factors such as macroturbulence.

The data of Figure 4.4 are replotted in Figure 4.5 to assess the relationship between the TSL procedure and the estimated total sediment loads as represented by Equation 4.1. Figure 4.5 shows 73 percent of the sediment loads determined by TSL to be within ±50 percent of the sediment load estimated by Equation 4.1. These values are a measure of the accuracy of TSL only if Equation 4.1 is the true sediment load relationship for the Niobrara River near Cody, Nebraska.

Figures 4.4 and 4.5 show that 9 percent of the sediment loads determined by the TSL procedure are at least 100 percent greater than the observed sediment loads as represented by Equation 4.1. The largest of these deviations occur at the larger streamflows. The assessment of these deviations is limited due to the limited observed data in the larger streamflow range. If additional observed data are acquired for the larger streamflows, the deviations of the TSL sediment loads from a corrected representative sediment load relationship may not be as significant as they now appear. For example, these deviations would be smaller if the corrected sediment load relationship would indicate larger sediment loads for the larger streamflows. Also, if additional observed data would display greater variability about a regressed

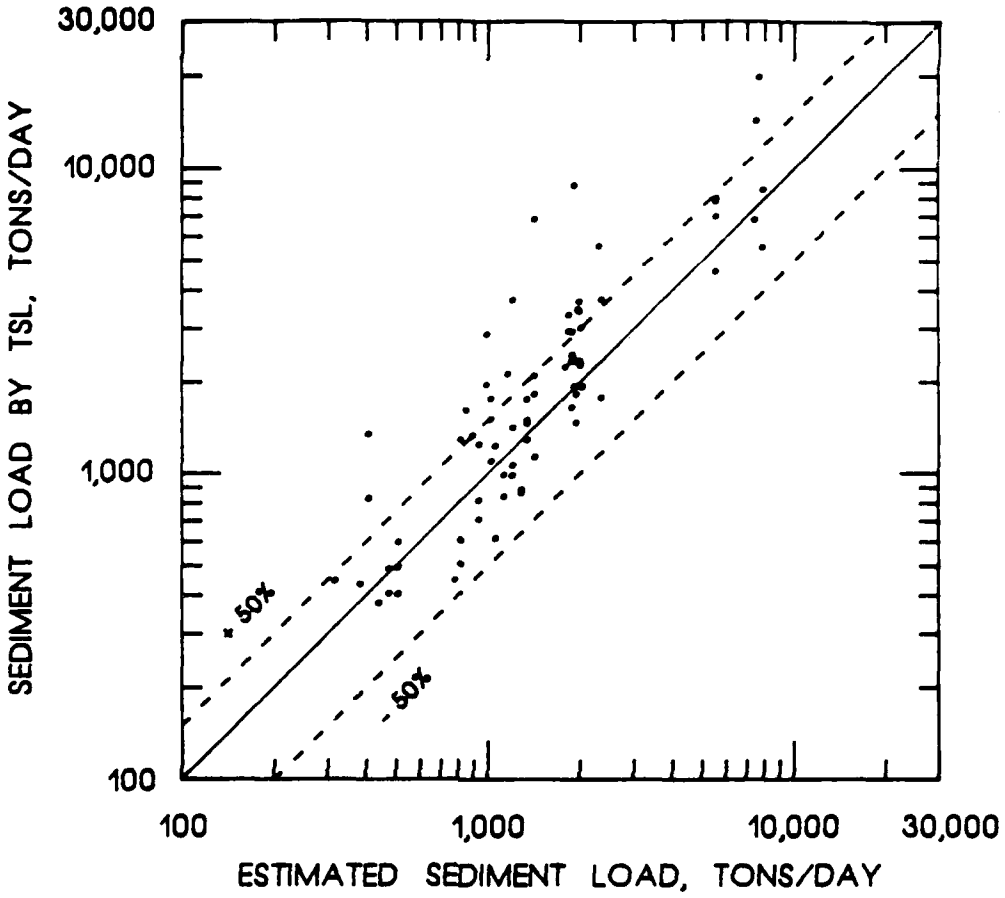

Figure 4.5. Sediment load determined by TSL using point samples from the lower one-third flow depth and the Limerinos procedure to determine k_s versus estimated sediment load for the Niobrara River.

sediment load function, the significance of the variability in the TSL sediment loads would be lessened.

Assuming the TSL deviations are departures from the true sediment load relationship for the Niobrara River, the deviations may be attributed to measurement error or spikes in the instantaneous point concentrations. Measurement errors or instantaneous spikes would be removed when TSL measurements are collected with near-continuous sampling. Continuous point-source suspended-sediment sampling and the TSL procedure

enable time integration for the measurement of the true total sediment load. Time integration results in an average of consecutive total sediment load measurements about a near-constant streamflow.

Figure 4.6 provides insight into the results of time integration for the determination of a river's total sediment load. The sediment loads of Figure 4.6 are average TSL sediment loads for 100-cfs-streamflow class intervals. The sediment loads shown in Figure 4.6 are within the ±50 percent deviation of the observed sediment loads about Equation 4.1 as shown in Figure 4.2. Therefore, the deviations of Figures 4.4, 4.5, and 4.6 are acceptable.

The Niobrara River data were used to assess the importance of estimating the roughness element height k_s due to both grain and form roughness. Section 3.1.1 discussed the importance of estimating the value for k_s to be used in the velocity distribution function, Equation 2.18. The Limerinos (1970), the Einstein (1950), and the Brownlie (1981, 1983) roughness prediction procedures may be used to determine k_s and are provided as options in the computer program, TSL. The sediment loads determined by TSL with these procedures are presented in Figures 4.4, 4.5, 4.7, 4.8, 4.9, and 4.10. These figures show similar degrees of scatter in the higher discharge range about the observed sediment loads and those calculated by Equation 4.1. The discussion relevant to the scatter in the higher discharge range remains the same as the previous discussion on Figures 4.4 and 4.5. The sediment loads in the lower discharge range are affected more by the differing roughness prediction procedures than those in the upper discharge range. The different sediment load estimates in the lower discharge range are

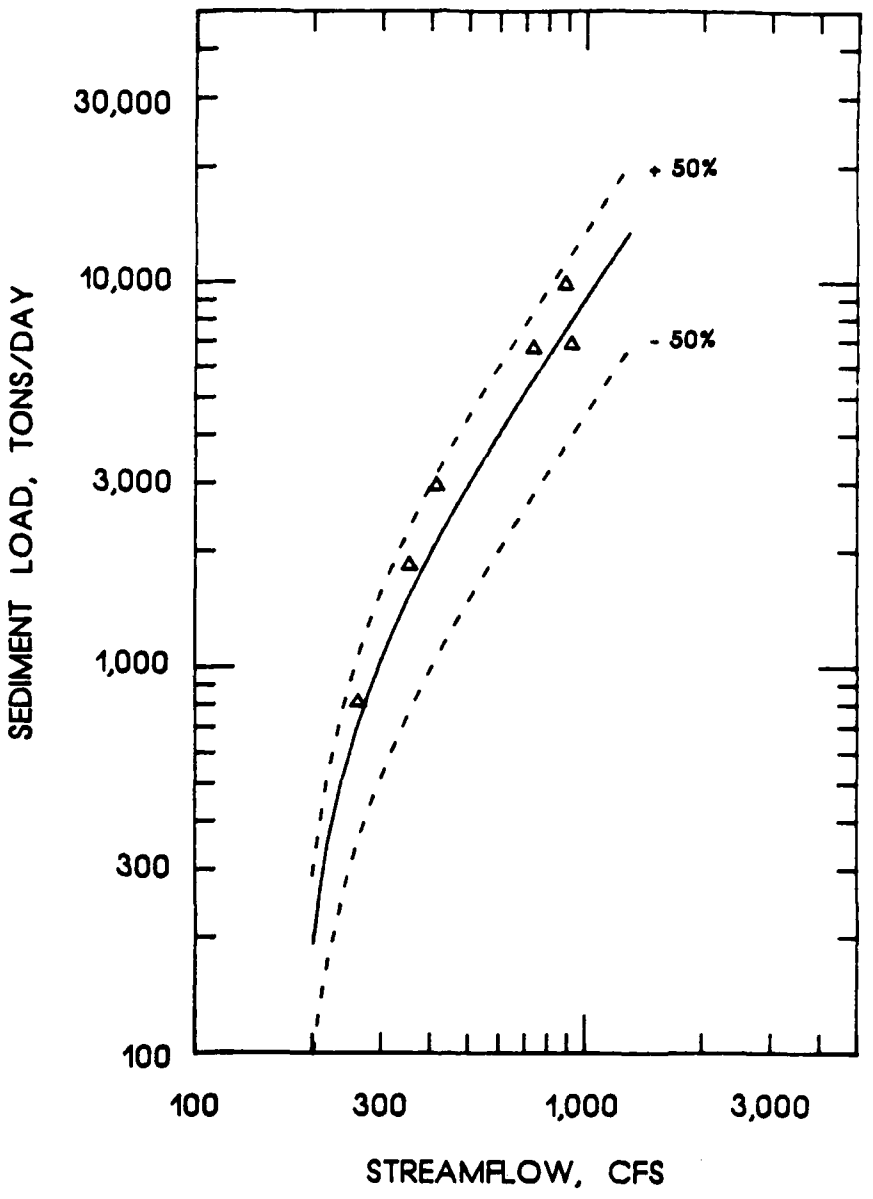

Figure 4.6. Average total sediment loads for the TSL procedure versus streamflow for the Niobrara River. The solid curve represents Equation 4.1.

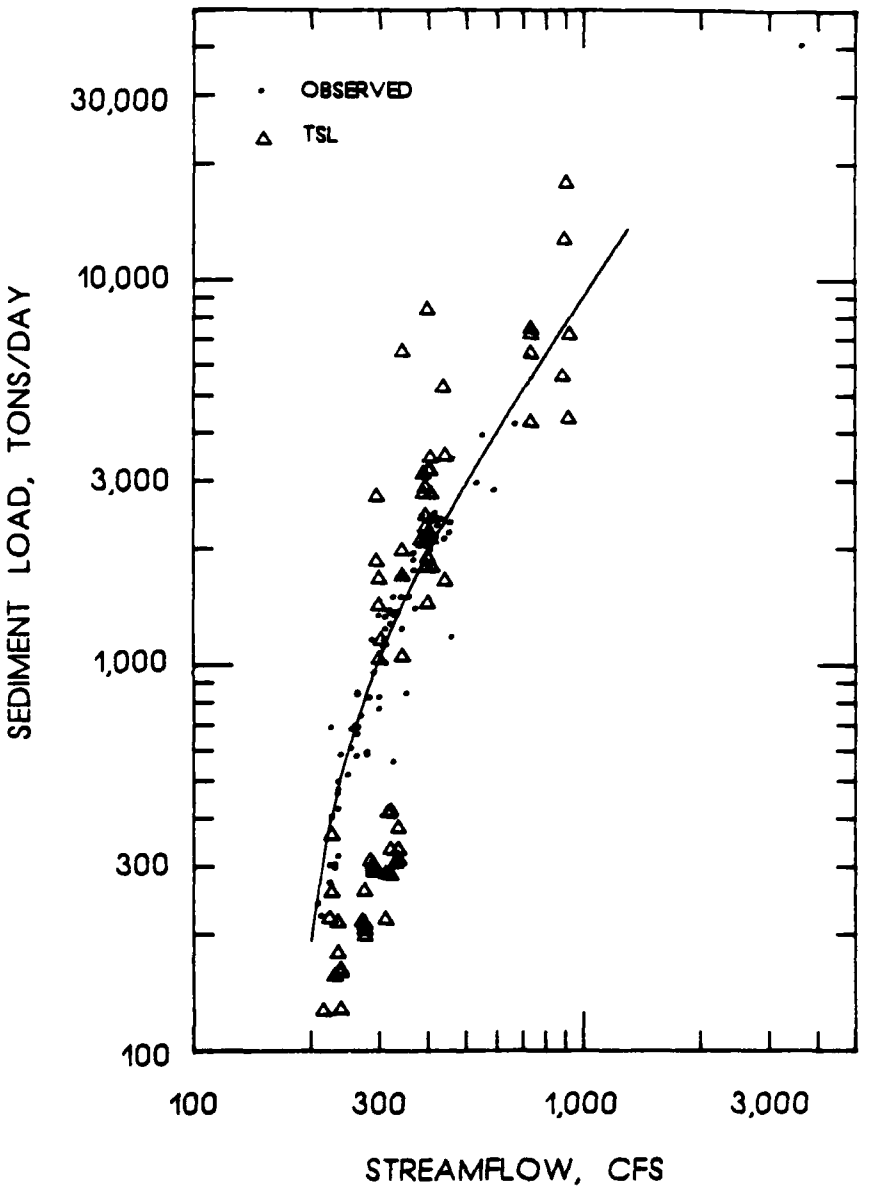

Figure 4.7. Total sediment load determined by TSL versus streamflow for the Niobrara River using point samples from the lower one-third flow depth and the Brownlie procedure to determine k_s. The curve represents Equation 4.1.

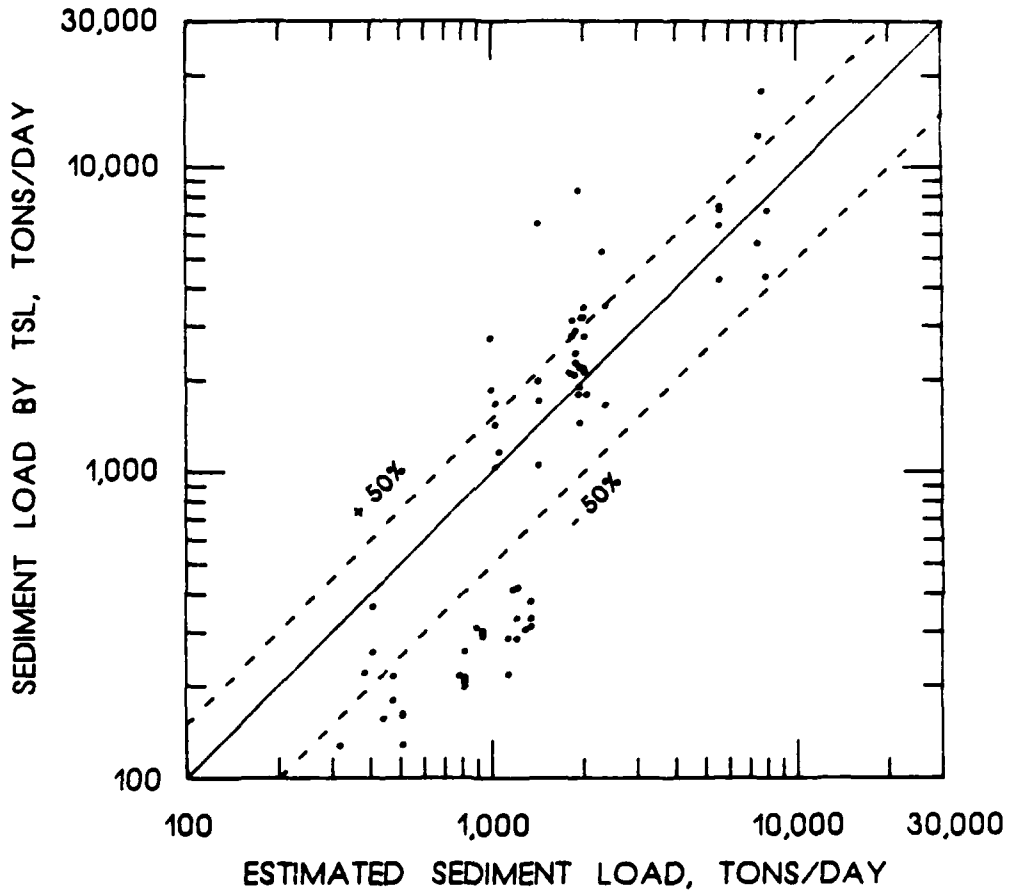

Figure 4.8. Sediment load determined by TSL using point samples from the lower one-third flow depth and the Brownlie procedure to determine k_s versus estimated sediment load for the Niobrara River.

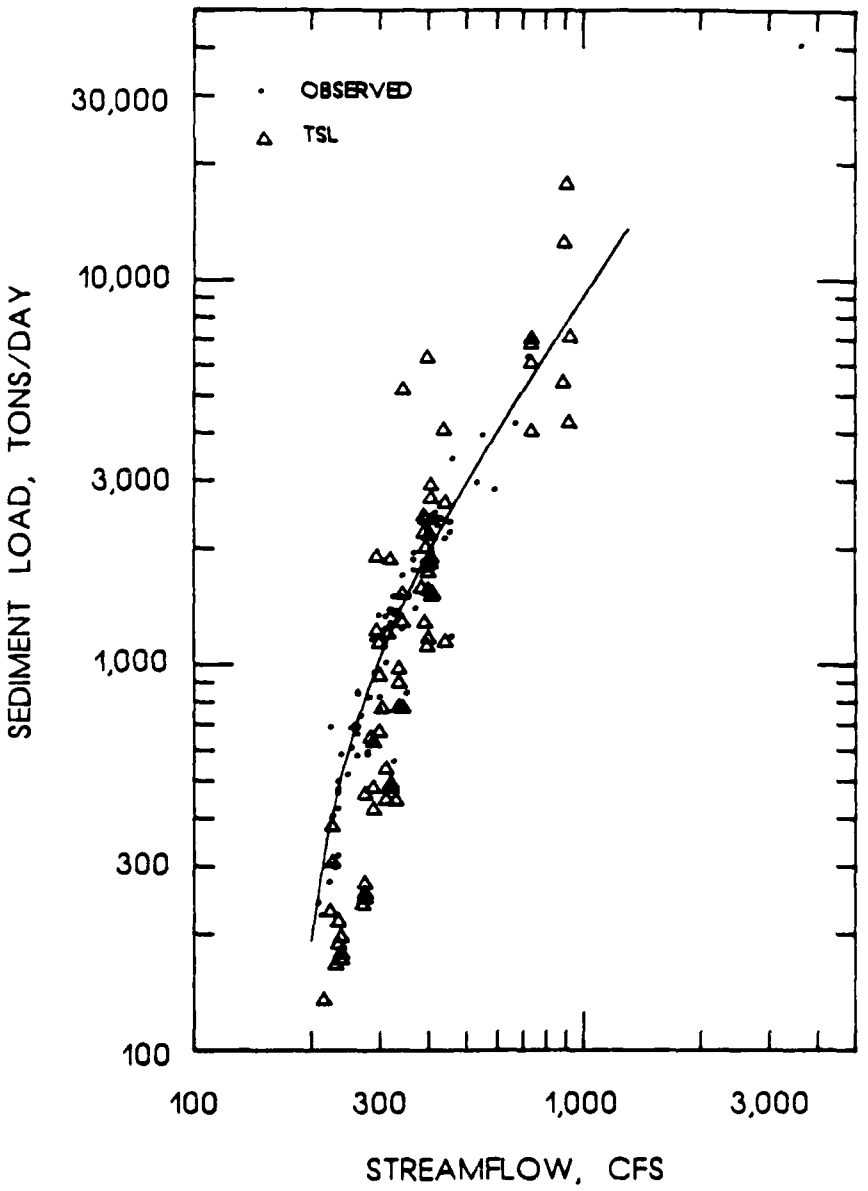

Figure 4.9. Total sediment load determined by TSL versus streamflow for the Niobrara River using point samples from the lower one-third flow depth and the Einstein procedure to determine k_s. The curve represents Equation 4.1.

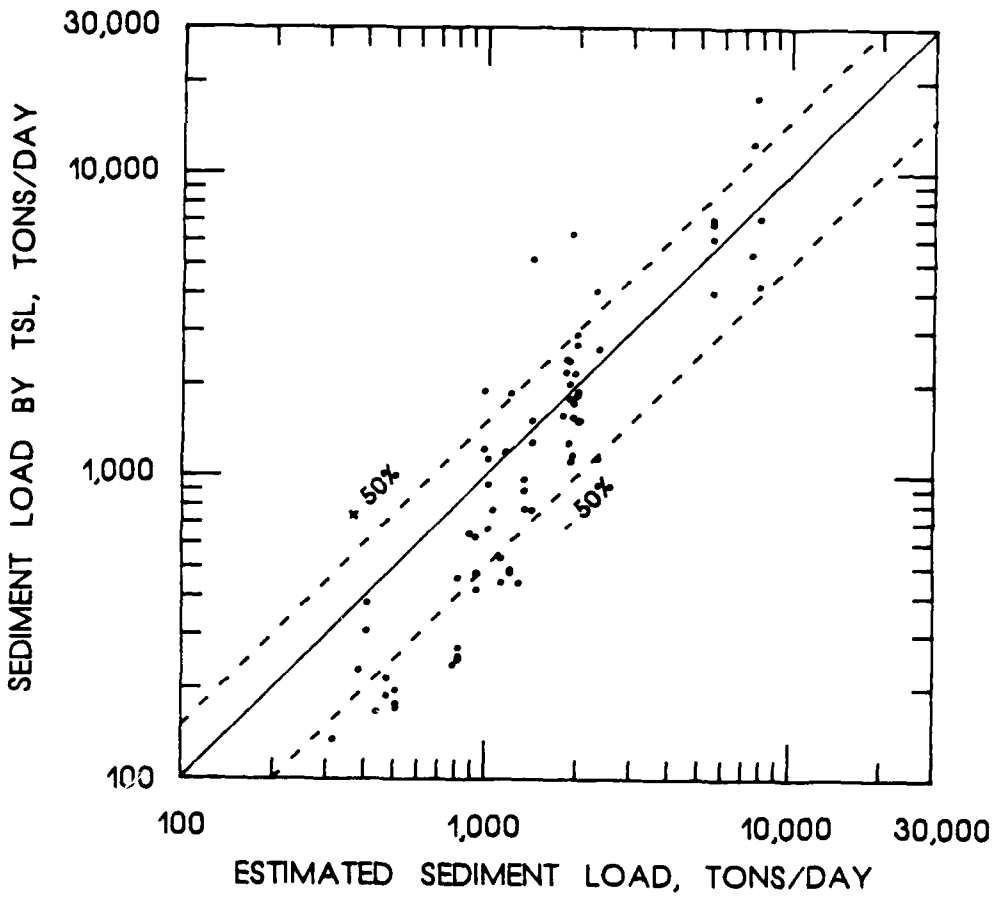

Figure 4.10. Sediment load determined by TSL using point samples from the lower one-third flow depth and the Einstein procedure to determine k_s versus estimated sediment load for the Niobrara River.

attributed to the Einstein and the Brownlie procedures estimating larger roughness element heights than the Limerinos procedure. A larger roughness element height prediction leads to a decreased estimate of total sediment load for the same point-source suspended-sediment sample. In summary, Figures 4.4, 4.5, and 4.7-4.10 indicate that total sediment load measurement by TSL is sensitive to the selection of the roughness height prediction method. The analyses of these figures encourage the selection of the Limerinos procedure.

4.3.2 Fivemile Creek

Colby, Hembree, and Rainwater (1956) describe the study reaches and the sediment data for Fivemile Creek near Shoshoni, Wyoming. Channel geometry and streamflow rating data are available in the files of the US Geological Survey, Cheyenne, Wyoming. Channel geometry and streamflow rating data for Fivemile Creek are presented in Appendix C as they were used for this analysis.

Colby, Hembree, and Rainwater's report presents depth- and point-integrated suspended-sediment data for normal and contracted sections. The depth-integrated suspended-sediment data at the contracted section are assumed to represent all of the sediment in transport. The point-integrated suspended-sediment data were not collected concurrently with the total sediment load measurements. Therefore, comparison of the TSL procedure to the total sediment load measurements is made with sediment load versus streamflow relationships.

Total sediment loads observed at the contracted section of Fivemile Creek are plotted against streamflow in Figure 4.11. The scatter of points in Figure 4.11 shows a trend of increasing sediment load with increasing streamflow. A single function for the plotted data is not

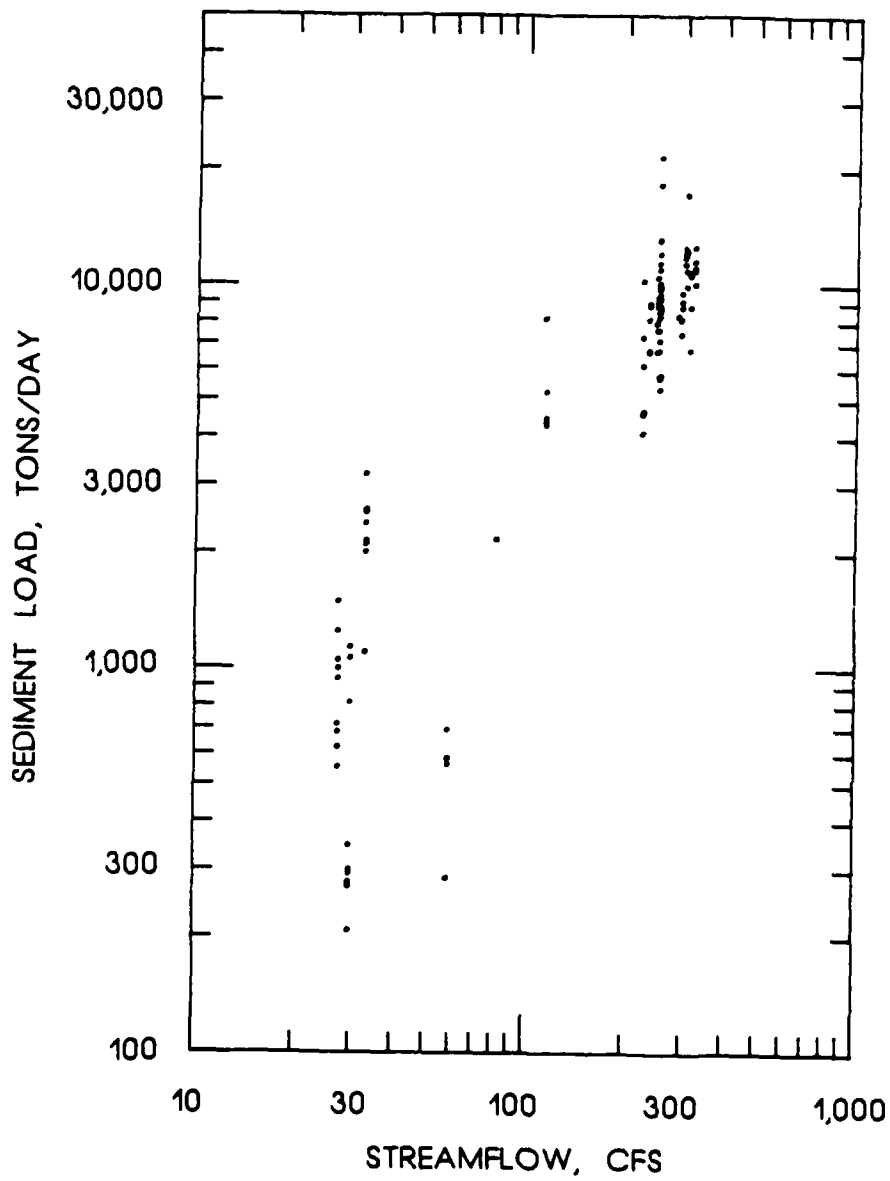

Figure 4.11. Observed total sediment load versus streamflow for Fivemile Creek.

evident; therefore, results of the TSL procedure are compared by plotting both the observed and TSL data sets in Figure 4.12. The suspended-sediment point samples for Figure 4.12 were from the lower 10 to 33 percent of the flow depths (0.2 to 0.4 ft above the channel bed). Most of the sediment load data in Figure 4.12 indicate good agreement between the observed and TSL data sets. Some of the TSL measurements are lower than the observed sediment loads in the larger streamflow range. These lower sediment load measurements may represent true sediment loads at the time each point-source suspended-sediment sample was obtained. Suspended-sediment samples for the observed and TSL measurements were not concurrently collected; therefore, this latter explanation cannot be further assessed. Other possible explanations for the low TSL measurements include sampling error or an improper calculation by TSL for bed load, suspended-sediment concentration distribution, or velocity profile. The possibility of improper calculation by TSL is minimized when consideration is given to the other TSL data, which match the distribution of the observed sediment loads. In summary, Figure 4.12 indicates good agreement between the observed and TSL data sets.

4.3.3 Middle Loup River

Hubbell and Matejka (1959) describe the study reaches, the data collection, and the data for the Middle Loup River at Dunning, Nebraska. Hubbell and Matejka's report provides depth- and point-integrated suspended-sediment data for normal sections and a turbulence flume. The depth-integrated suspended-sediment data from the turbulence flume are assumed to represent all of the sediment in transport. The point-integrated suspended-sediment data were not collected concurrently with the total sediment load measurements. Therefore, comparison of the TSL

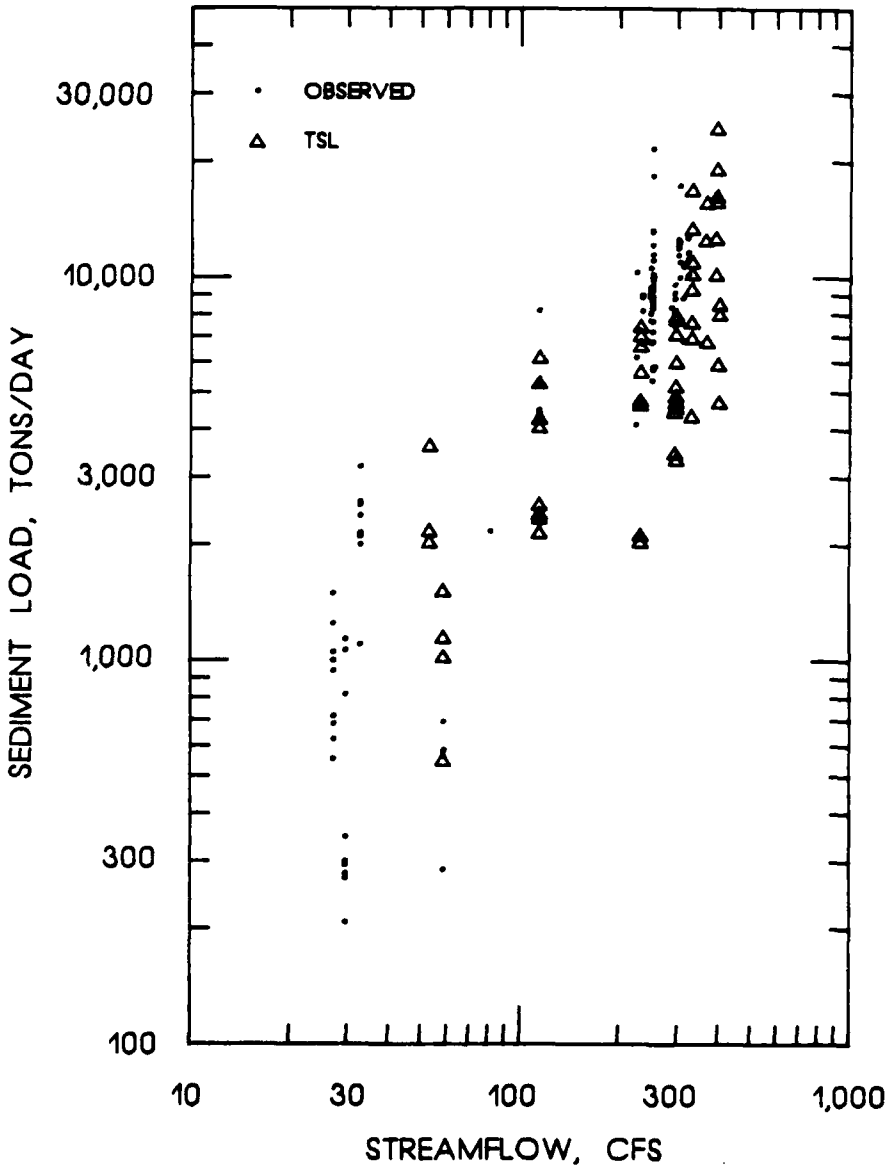

Figure 4.12. Total sediment load determined by TSL versus streamflow for Fivemile Creek using point samples from the lower one-third flow depth and the Limerinos procedure to determine k_s.

procedure to the total sediment load measurements is made by comparing sediment load versus streamflow relationships.

Total sediment loads observed at the turbulence flume of the Middle Loup River are plotted against streamflow in Figure 4.13. Results of the TSL procedure for the reported point-source suspended-sediment data are assessed by plotting the observed and TSL sediment load sets in Figure 4.14. The suspended-sediment point samples for Figure 4.14 were from the lower 19 to 33 percent of the flow depths (0.2 to 0.4 ft above the channel bed). Figure 4.14 shows good agreement between the available observed and TSL data sets.

4.3.4 Rio Grande Conveyance Channel

Culbertson, Scott, and Bennett (1972) describe the study reaches, the data collection, and the data for the Rio Grande conveyance channel near Bernardo, New Mexico. Culbertson, Scott, and Bennett's report provides depth-integrated suspended-sediment data for normal sections and a weir structure. Point-integrated suspended-sediment data for a narrow discharge range are also presented for the sampled sections in the report. The point suspended-sediment samples were not collected concurrently with the total sediment load measurements.

Total sediment loads observed at the weir structure of the Rio Grande conveyance channel are plotted against streamflow in Figure 4.15. Results of the TSL procedure for suspended-sediment point samples are compared to the observed data in Figure 4.16. The point samples for these TSL measurements came from the lower 6 to 32 percent of the flow depths (0.3 to 1.2 ft above the channel bed). The distribution of the TSL sediment loads is greater in Figure 4.16 than the observed sediment loads. The greater distribution may be attributed to the use of

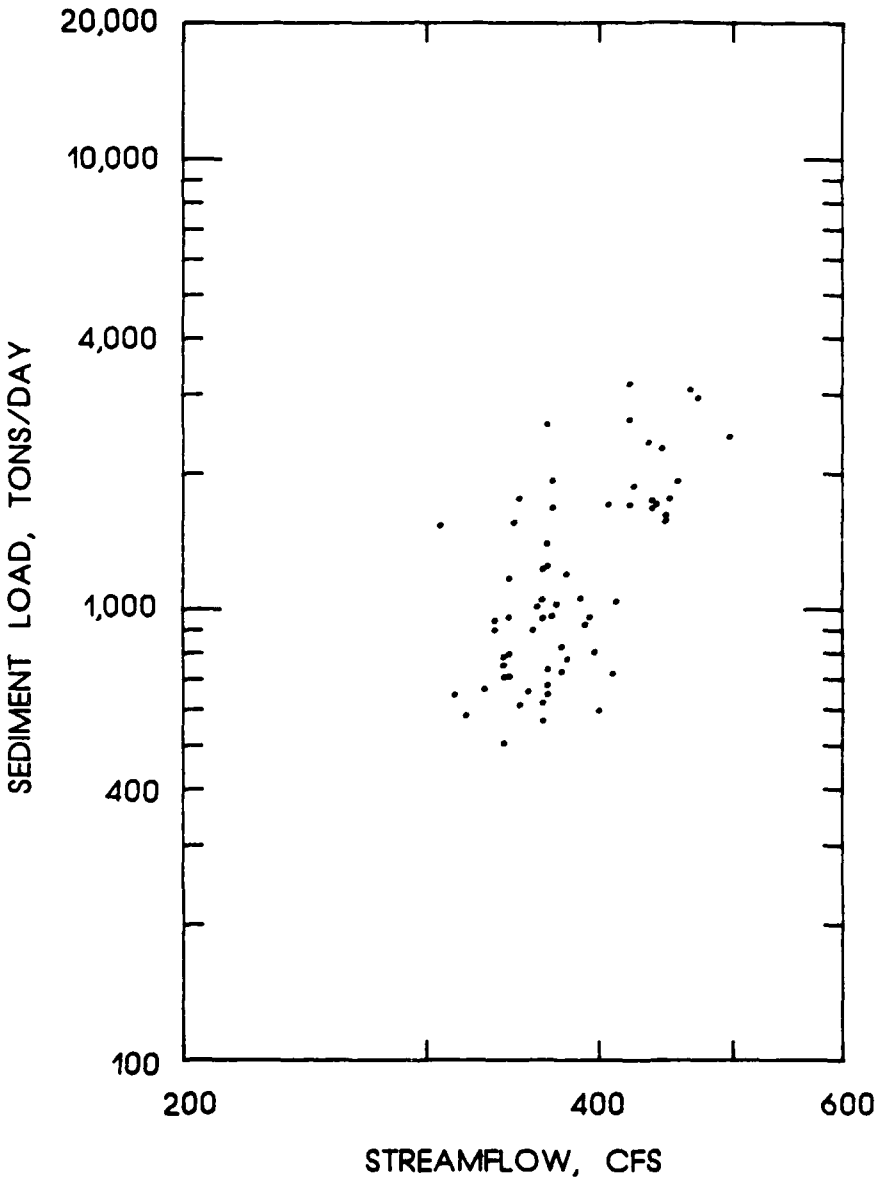

Figure 4.13. Observed total sediment load versus streamflow for the Middle Loup River.

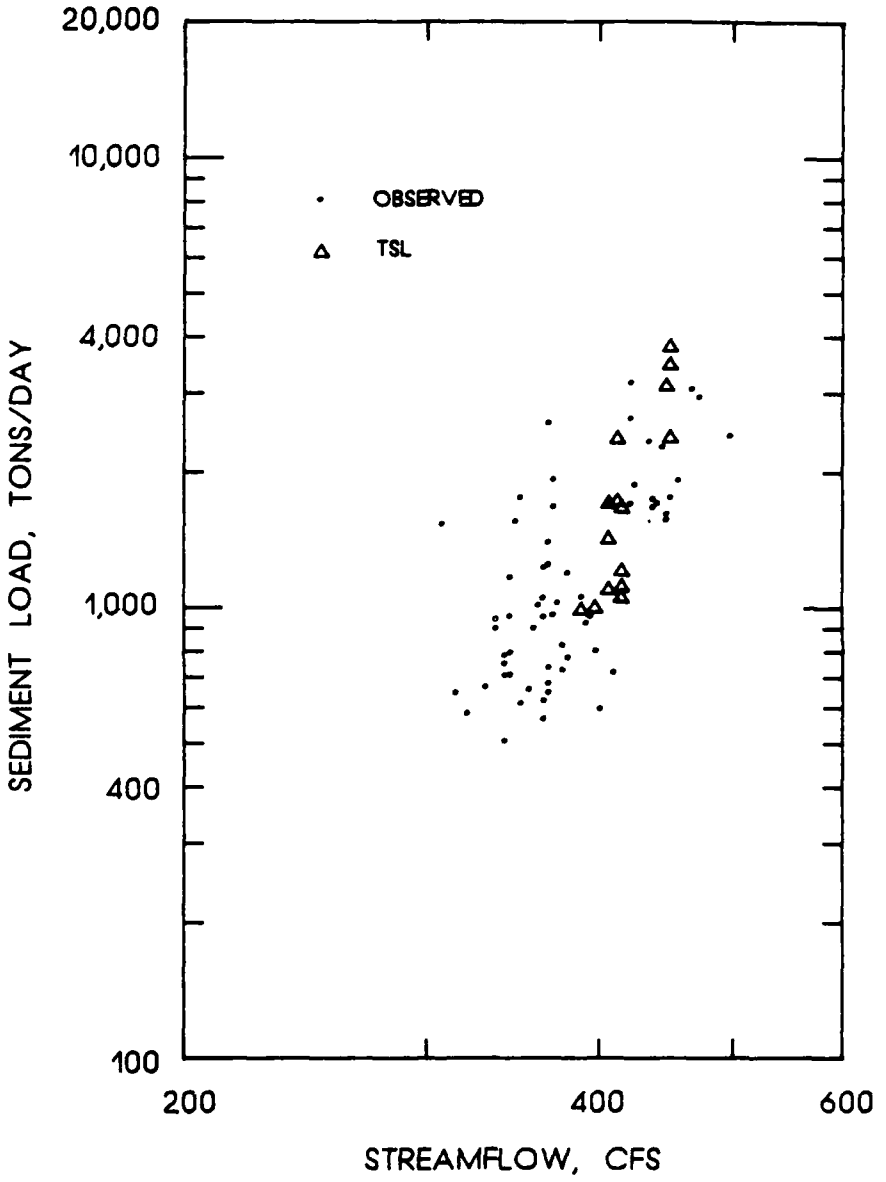

Figure 4.14. Total sediment load determined by TSL versus streamflow for the Middle Loup River using point samples from the lower one-third flow depth at section C and the Limerinos procedure to determine k_s .

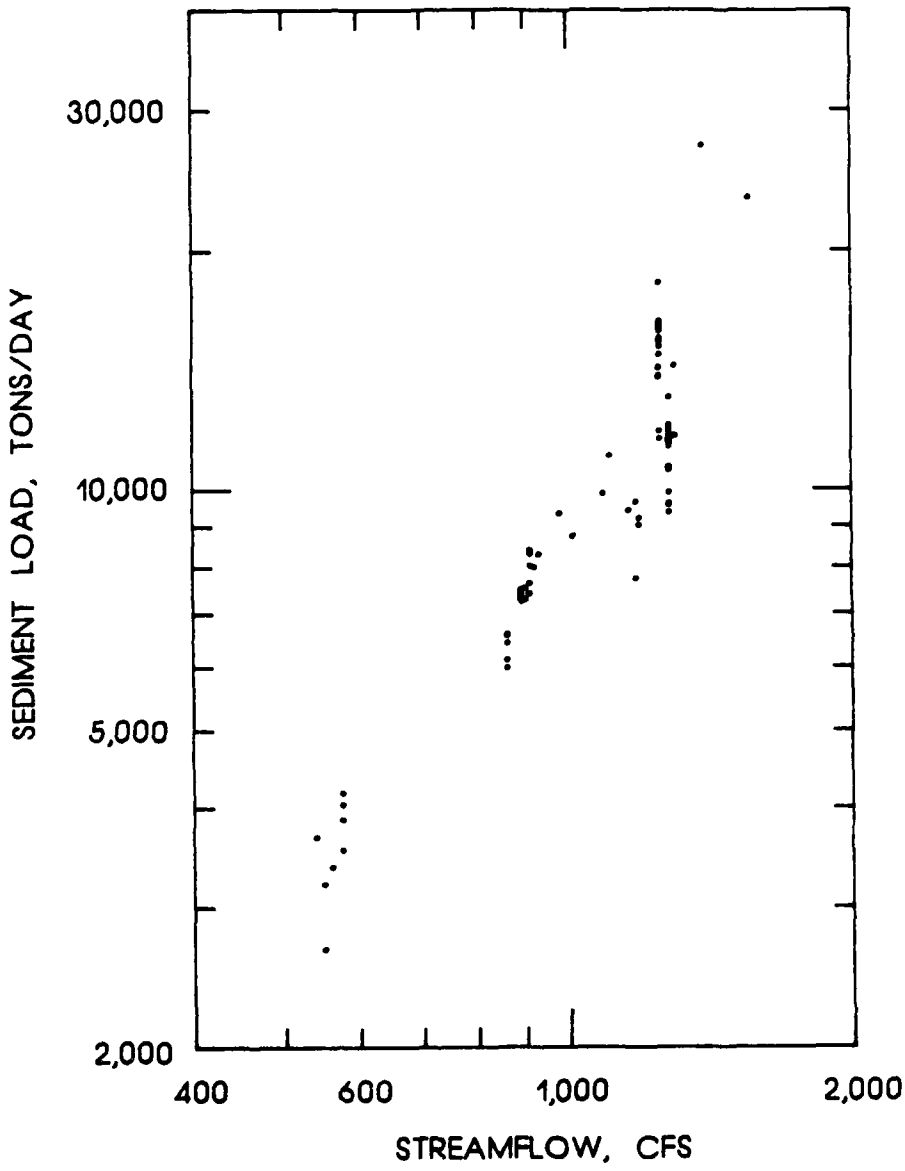

Figure 4.15. Observed total sediment load versus streamflow for the Rio Grande conveyance channel.

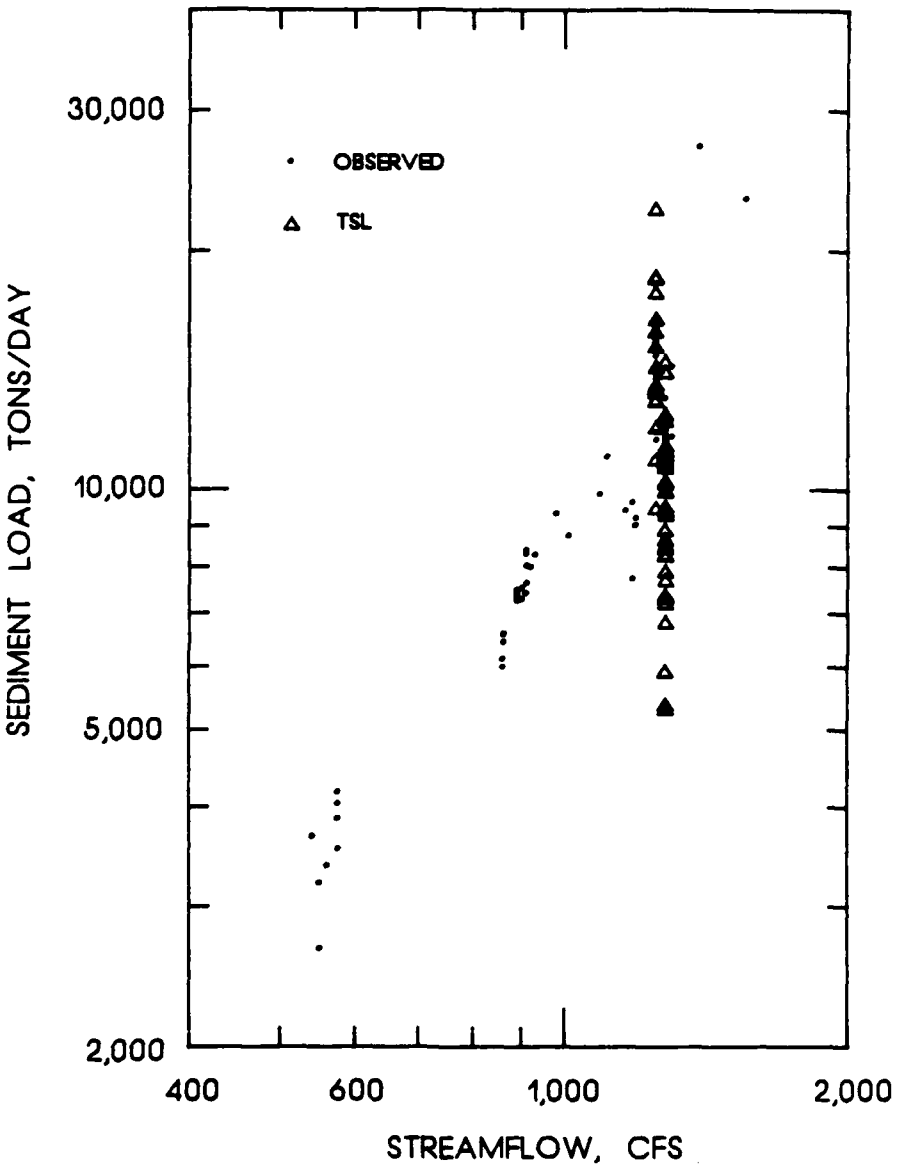

Figure 4.16. Total sediment load determined by TSL versus streamflow for the Rio Grande conveyance channel using point samples from the lower 6 to 32 percent flow depth and the Limerinos procedure to determine k_s.

point-source suspended-sediment samples which were collected too close to the channel bed. Point samples collected near the channel bed may inadvertently include bed load and bed material. Also, point samples collected close to the channel bed may exhibit greater variance than other point samples due to the same processes that influence the stochastic nature of bed load transport.

The use of point samples collected near the channel bed was assessed by plotting TSL results for point samples taken from the lower 20 to 32 percent of the flow depths (0.8 to 1.2 ft above the channel bed). The lower limit of 20 percent was selected to be well above the previous lower limit of 6 percent. The plot of TSL measurements using these point samples is presented in Figure 4.17. Figure 4.17 shows better agreement between the observed and TSL data sets than Figure 4.16.

In summary, the TSL measurement procedure is improved when the point samples are obtained in the lower flow depth but not too close to the channel bed. Point-source suspended-sediment samples collected in the lower 20 to 32 percent flow depth provide reliable data for the TSL procedure.

4.4 COMPARISON TO MODIFIED EINSTEIN PROCEDURE COMPUTATIONS

One of the objectives of this research was to compare the TSL procedure to the modified Einstein procedure (MEP). For this comparison, results of the MEP as applied to the published data are plotted with the observed total sediment load measurements in Figures 4.18 and 4.20 thru 4.22. Direct comparison of the TSL procedure to the MEP is provided in Figures 4.20 thru 4.22. Figures 4.18 and 4.20 thru 4.22 are for the

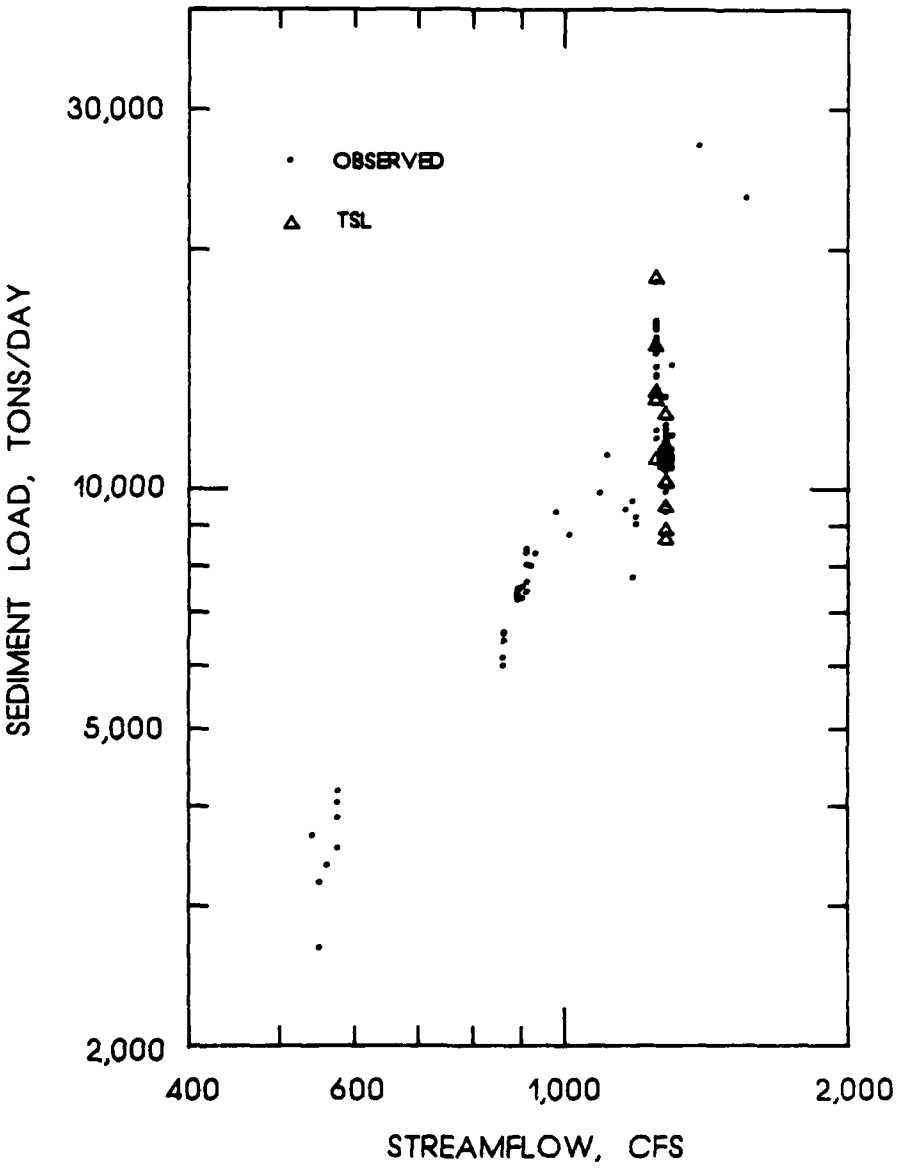

Figure 4.17. Total sediment load determined by TSL versus streamflow for the Río Grande conveyance channel using point samples from the lower 20 to 32 percent flow depth and the Limerinos procedure to determine k_s .

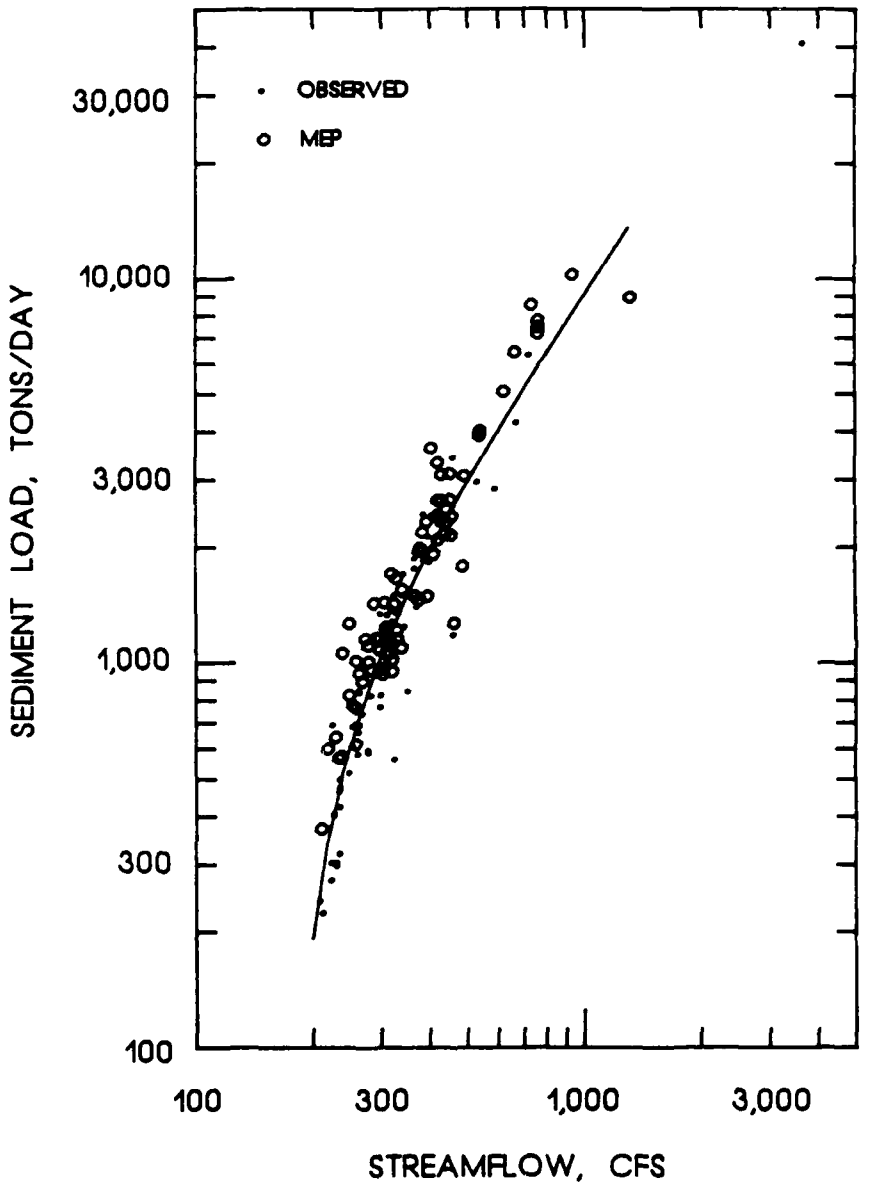

Figure 4.18. Total sediment load determined by MEP versus streamflow for the Niobrara River. The curve represents Equation 4.1.

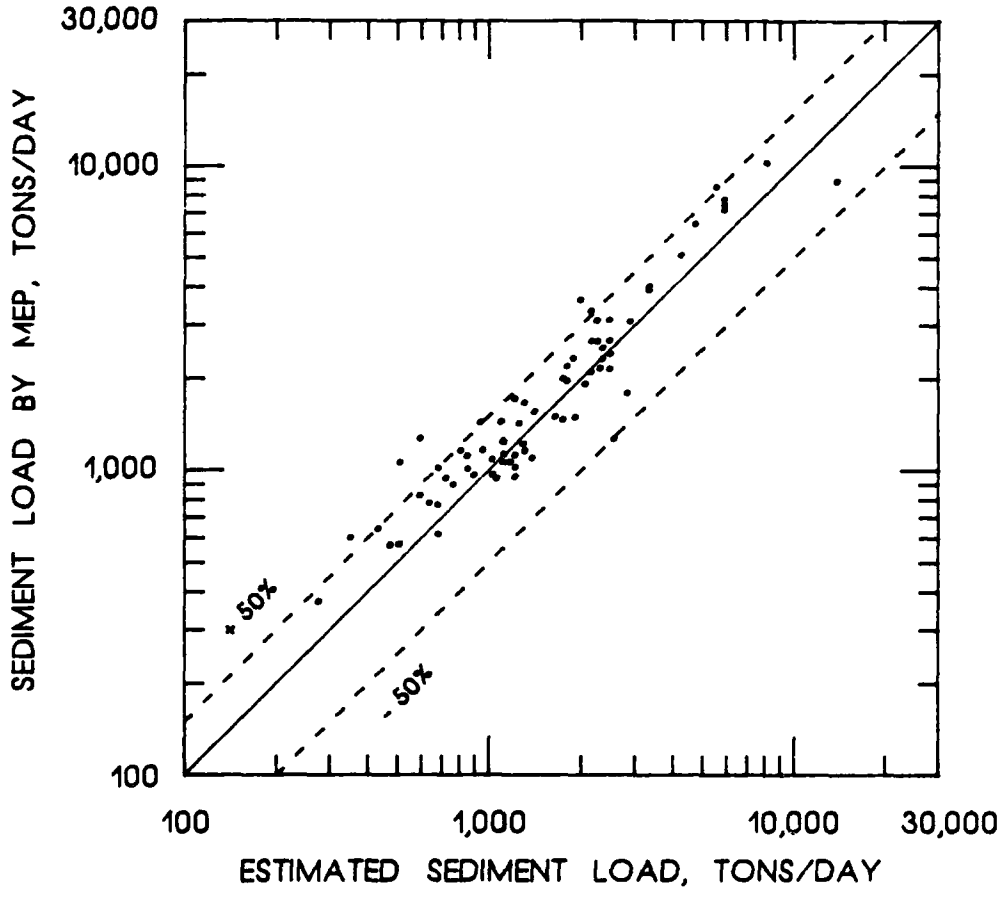

Figure 4.19. Sediment load determined by MEP versus estimated sediment load for the Niobrara River.

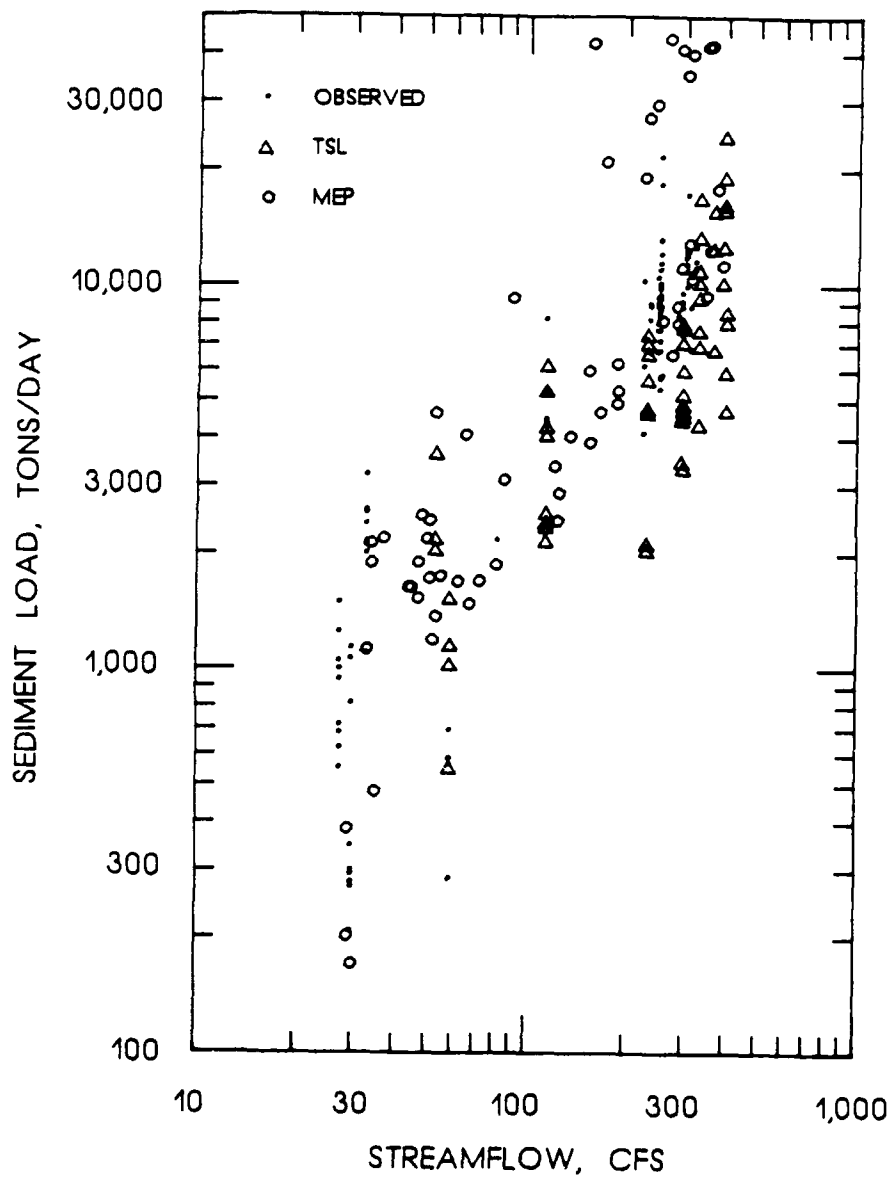

Figure 4.20. Total sediment load determined by MEP and TSL versus streamflow for Fivemile Creek.

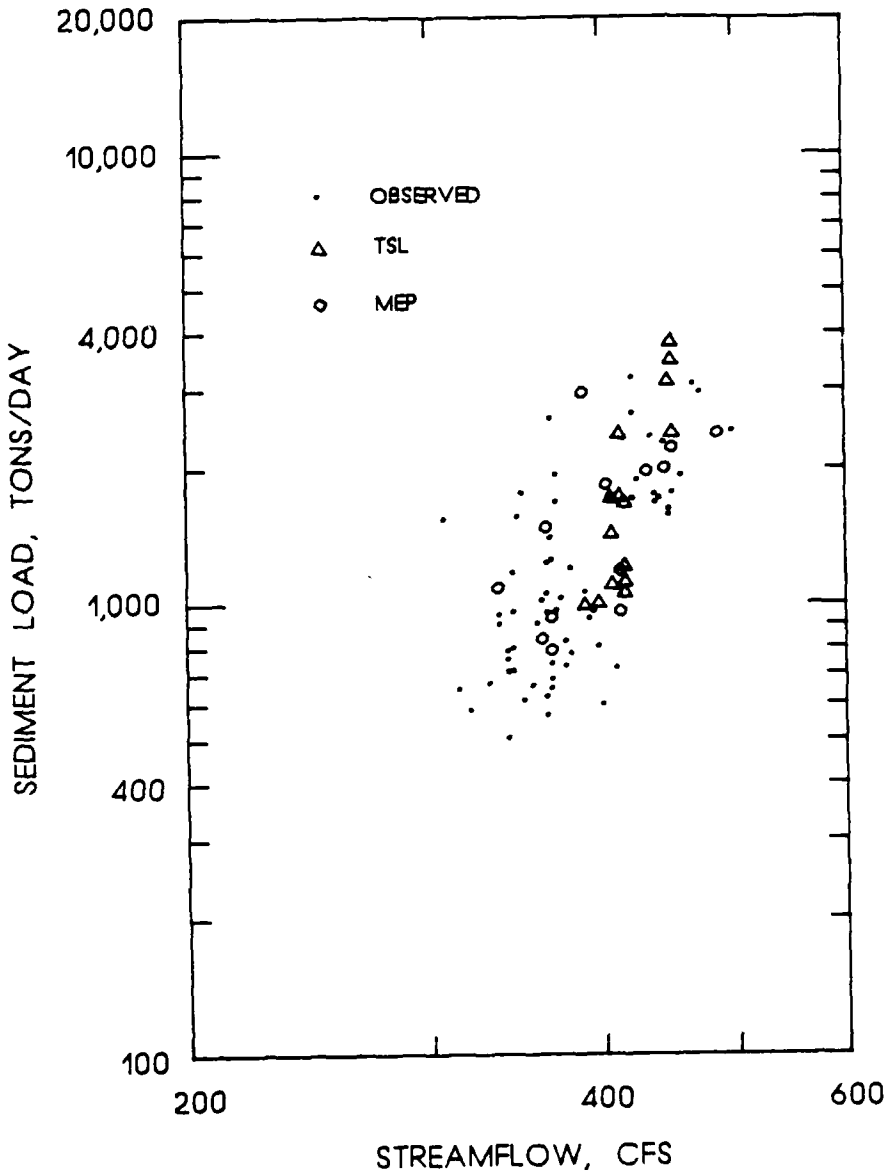

Figure 4.21. Total sediment load determined by MEP and TSL versus streamflow for section C of the Middle Loup River.

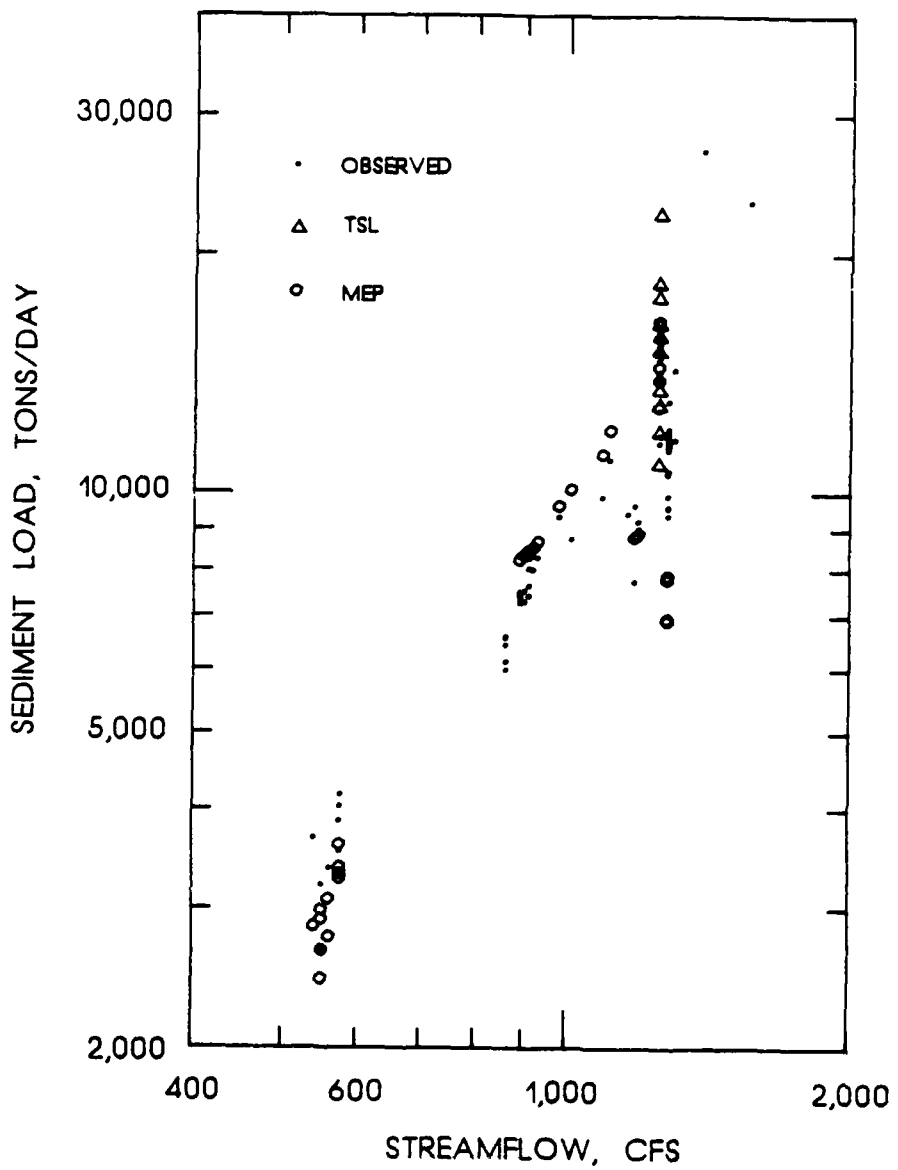

Figure 4.22. Total sediment load determined by MEP and TSL versus streamflow for the Rio Grande conveyance channel.

Niobrara River, Fivemile Creek, the Middle Loup River, and the Rio Grande conveyance channel, respectively.

The MEP and the observed sediment loads versus streamflow are shown in Figure 4.18 for the Niobrara River. Comparison of Figure 4.18 to Figure 4.4 indicates that single MEP measurements provide less data scatter than single TSL measurements. However, comparison of Figure 4.18 to Figure 4.6 indicates that the use of the TSL procedure along with time integration will provide equally reliable sediment load measurements.

Another comparison between the MEP and the TSL procedure using the Niobrara River data is made using Figures 4.5, 4.6, and 4.19. Figure 4.19 provides a comparison of the MEP sediment load measurements to Equation 4.1 (the regressed function selected to represent the observed sediment loads). In Figure 4.19, 89 percent of the MEP sediment loads are within ±50 percent of the loads determined by Equation 4.1. Figure 4.5 shows 73 percent of the TSL sediment loads to be within ±50 percent of Equation 4.1. In Figure 4.6, 100 percent of the averaged TSL sediment loads are within ±50 percent of Equation 4.1. Comparison of these statistics indicates greater reliability for a single MEP measurement than a single TSL measurement. However, when the average of multiple TSL measurements is considered, as in Figure 4.6, greater reliability is given to the average of multiple TSL measurements than to a single MEP measurement.

The MEP, the TSL, and the observed sediment loads versus streamflow are directly compared for Fivemile Creek in Figure 4.20. Figure 4.20 indicates good agreement between the measurements in the lower discharge range and the majority of the measurements in the higher discharge

range. However, in the higher discharge range, selected MEP measurements are larger and selected TSL measurements are smaller than the observed sediment loads. The variation in the TSL measurements from the observed measurements were discussed in Section 4.3.2. Burkham and Dawdy (1980) suggest that the overestimates of sediment load by the MEP may be related to an underestimate of the roughness element height k_s. However, no information on the type of bedforms present during sampling is available to further assess this explanation for the overestimates. Underestimates of k_s will lead to an improper calculation of bed load, suspended-sediment concentration distribution, and velocity profile. Further assessment between the MEP and the TSL measurements for Fivemile Creek is not possible since concurrent depth-integrated and point samples were not recorded.

The MEP, the TSL, and the observed sediment loads versus streamflow are directly compared for the Middle Loup River in Figure 4.21. Figure 4.21 indicates good agreement between all of the measurements. Additional comparisons between the MEP and the TSL measurements for the Middle Loup River were not assessed since depth-integrated and point-source suspended-sediment samples were not concurrently collected.

The MEP, the TSL, and the observed sediment loads versus streamflow are directly compared for the Rio Grande conveyance channel in Figure 4.22. Figure 4.22 indicates good agreement for the majority of the measurements. Some of the MEP sediment loads are lower than the observed sediment loads for the larger sampled streamflow. Assuming these measurements to be correct, greater reliability may be placed upon the lower TSL measurements plotted in Figure 4.16.

Overall, comparisons of the MEP, the TSL procedure, and the observed sediment load data show similar results. The Niobrara River data indicate that the MEP may provide greater reliability with a single depth-integrated suspended-sediment sample than the TSL procedure with a single point suspended-sediment sample. However, the Fivemile Creek, the Middle Loup River, and the Rio Grande conveyance channel data indicate a single TSL measurement to be as reliable as a single MEP measurement. The reliability of the TSL procedure is improved when multiple-point samples can be collected and integrated into the analysis. The similarity of the TSL, the MEP, and the observed sediment loads shows promise for use of the TSL procedure to measure total sediment load.

4.5 APPLICATION TO THE NEWLY ACQUIRED GOODWIN CREEK DATA

The final objective of this study was to apply the TSL procedure to newly acquired data. The new data was provided by the US Department of Agriculture-Agricultural Research Service (USDA-ARS), Sedimentation Laboratory, Oxford, Mississippi, and was collected at the Goodwin Creek, Mississippi, research catchment (Seely, Grissinger, and Little 1981, US Army Corps of Engineers 1981, and Bowie and Sansom 1986). The Goodwin Creek research catchment has 14 gaging stations within an 8.2-square-mile drainage area. The gaging stations have supercritical-flow flumes with instrumentation to record water level, water temperature, and precipitation. Each gaging station has an automatic pumping-type suspended-sediment sampler. The outlet of the flumes is designed with a flow overfall which permits total sediment load measurements with the absence of an unmeasured zone in the measured vertical. The total load measurements are made with a depth-integrated sampler.

The USDA-ARS Sedimentation Laboratory provided detailed data from Goodwin Creek, Station 2, for the assessment of the TSL procedure for a storm event occurring on August 27, 1986. Unlike other sediment data, the August 27, 1986, data set for Goodwin Creek provides concurrent and consecutive point-source suspended-sediment samples and total sediment load measurements for a streamflow event. The data from the streamflow event that was used with the TSL procedure are provided in Appendix D. The assessment of TSL with these data is accomplished using Figures 4.23-4.27. Total sand load is assessed in these figures rather than total sediment load, because Goodwin Creek's bed material is approximately 80 percent gravel, which is not measured by the depth-integrated and automatic pumping-type suspended sediment samplers.

Figure 4.23 shows the hydrograph for the August 27, 1986, streamflow event. Figure 4.24 presents both the total sand load observed at the flume's outlet using a depth-integrated sampler and the total sand load determined by the TSL procedure versus the streamflow. Figure 4.24 does not indicate a smooth function to describe the relation between sediment transport and streamflow; therefore, data plots which show the sediment load through time for the streamflow event are presented in Figures 4.25, 4.26, and 4.27. In these figures, greater fluctuations exist between consecutively observed sand loads than between consecutive TSL procedure sand loads. Figure 4.27 shows the magnitude of the fluctuations for the TSL procedure sand loads to be similar to or to occur within the fluctuations of the observed sand loads. This observation may be attributed to differences in the two sampling techniques. Samples for the observed total sand loads are collected with a depth-integrated sampler being lowered and raised through the entire vertical

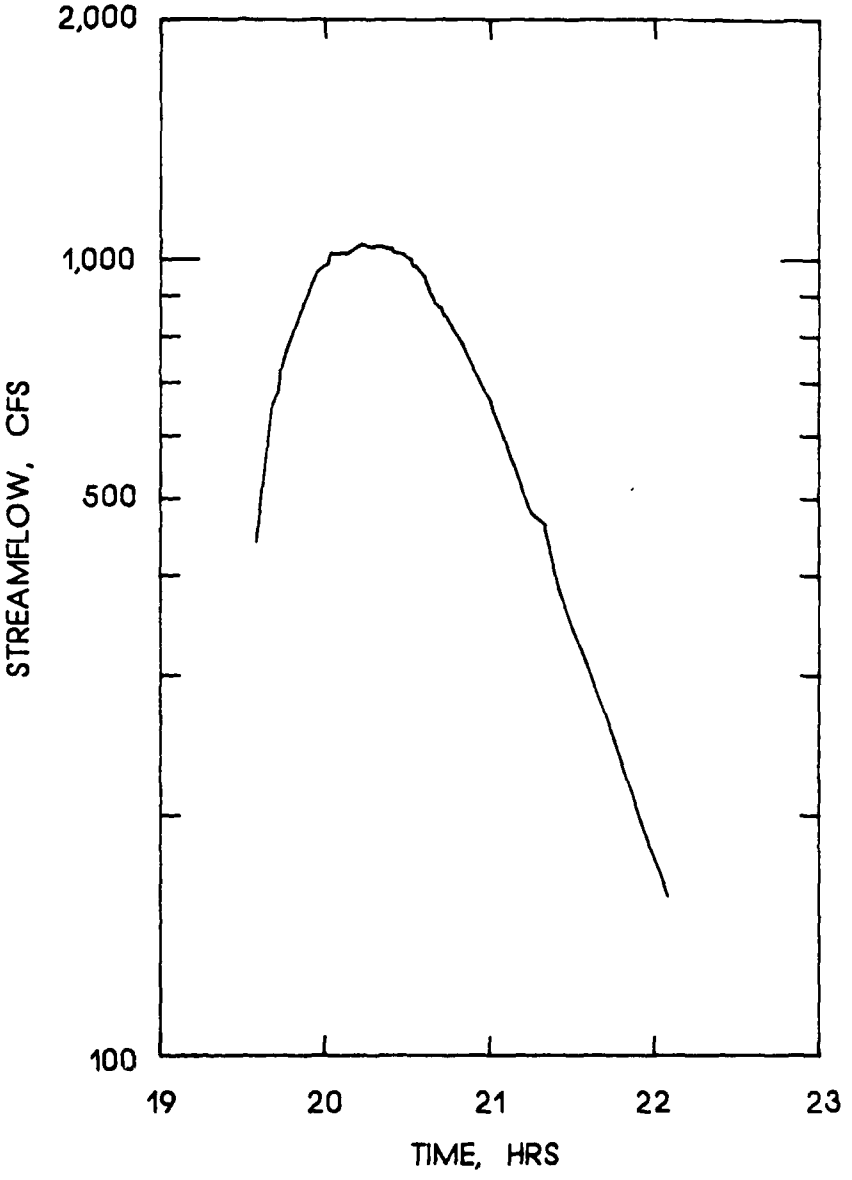

Figure 4.23. Hydrograph for the August 27, 1986, streamflow event at Goodwin Creek, Mississippi, Station 2.

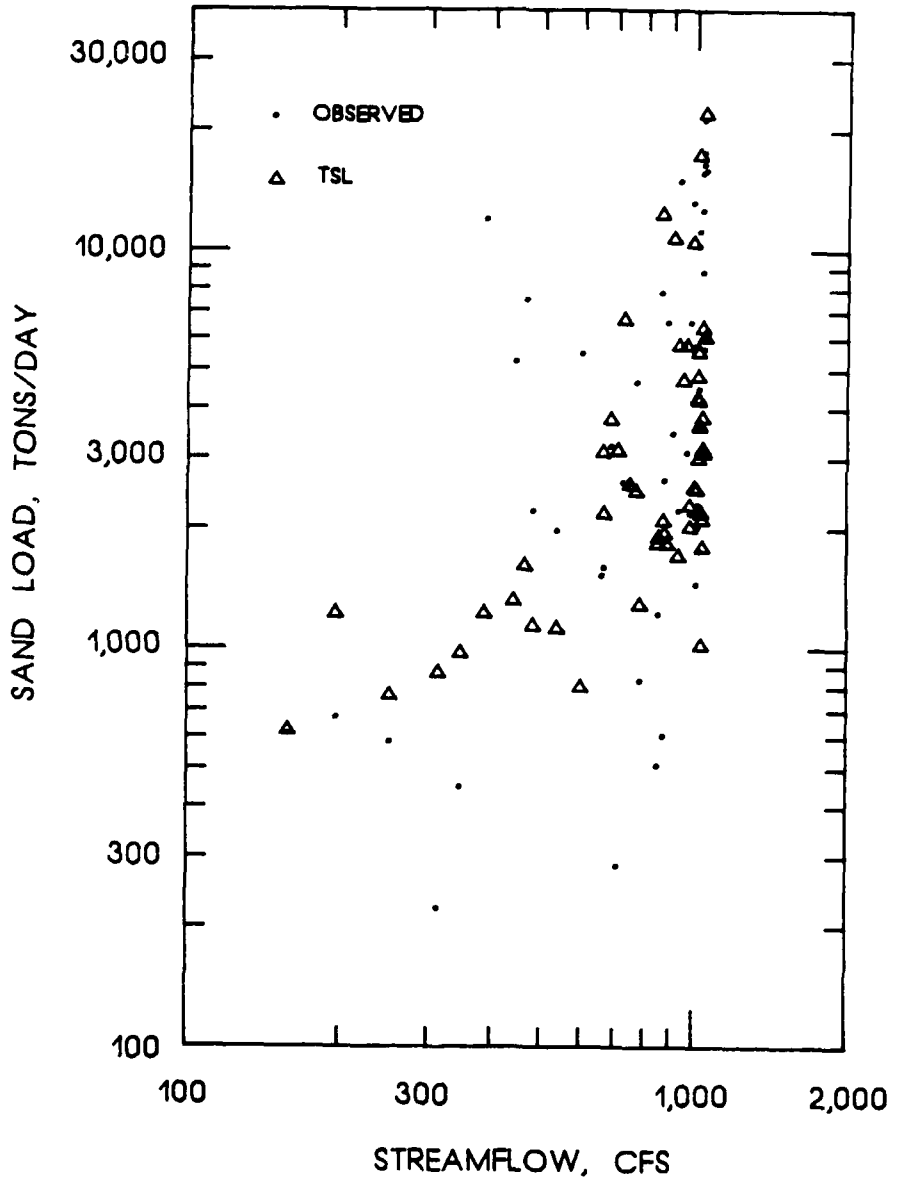

Figure 4.24. Total sand load versus streamflow for the August 27, 1986, streamflow event at Goodwin Creek, Mississippi, Station 2.

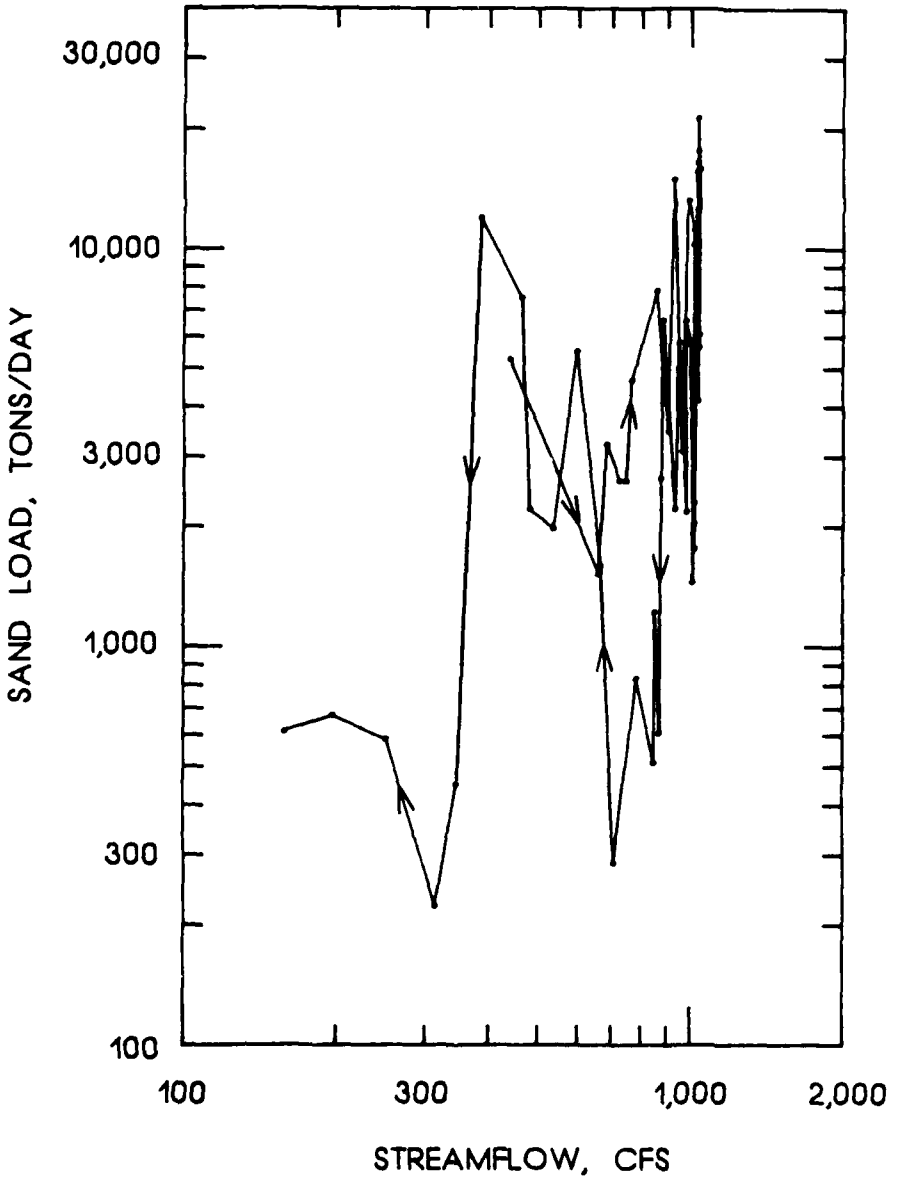

Figure 4.25. Total sand load observed versus streamflow for the August 27, 1986, streamflow event at Goodwin Creek, Mississippi, Station 2.

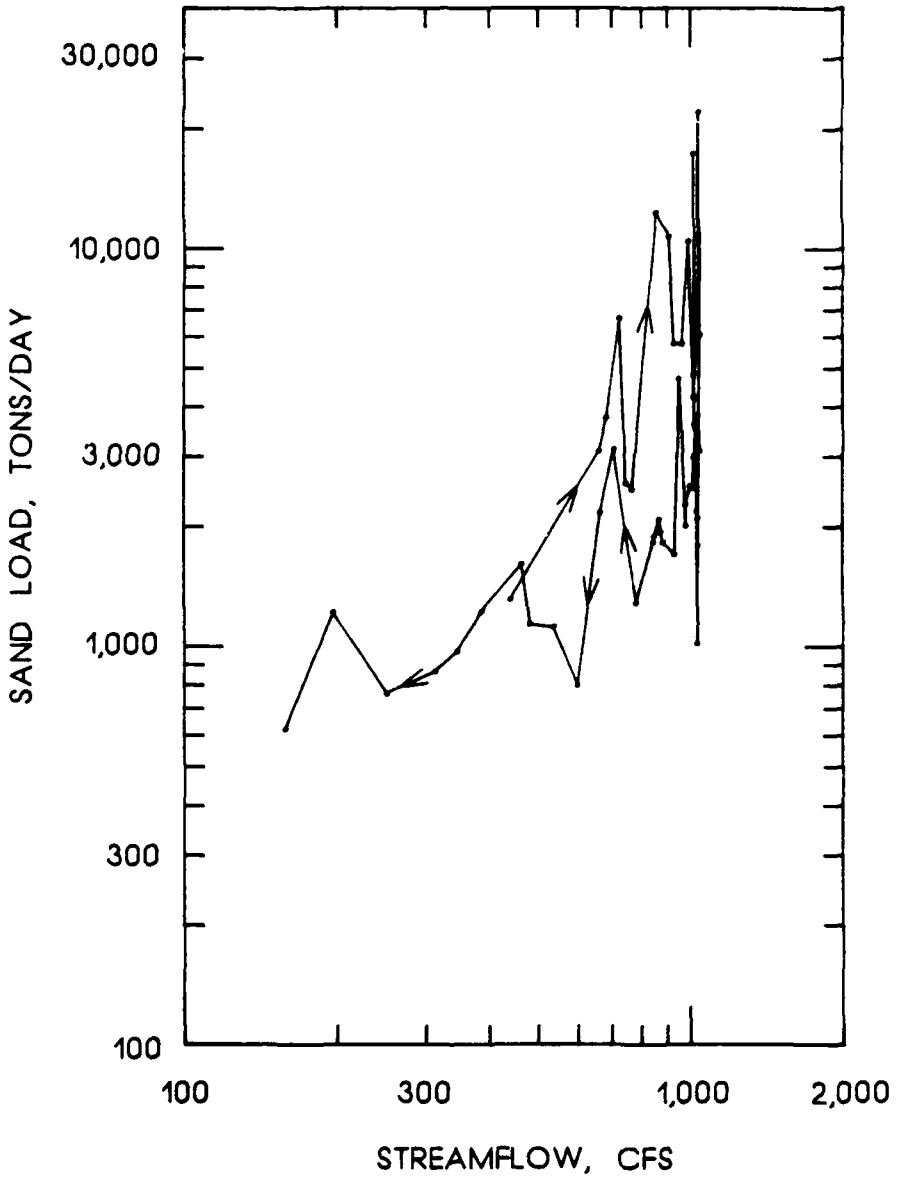

Figure 4.26. Total sand load measured by the TSL procedure versus streamflow for the August 27, 1986, streamflow event at Goodwin Creek, Mississippi, Station 2.

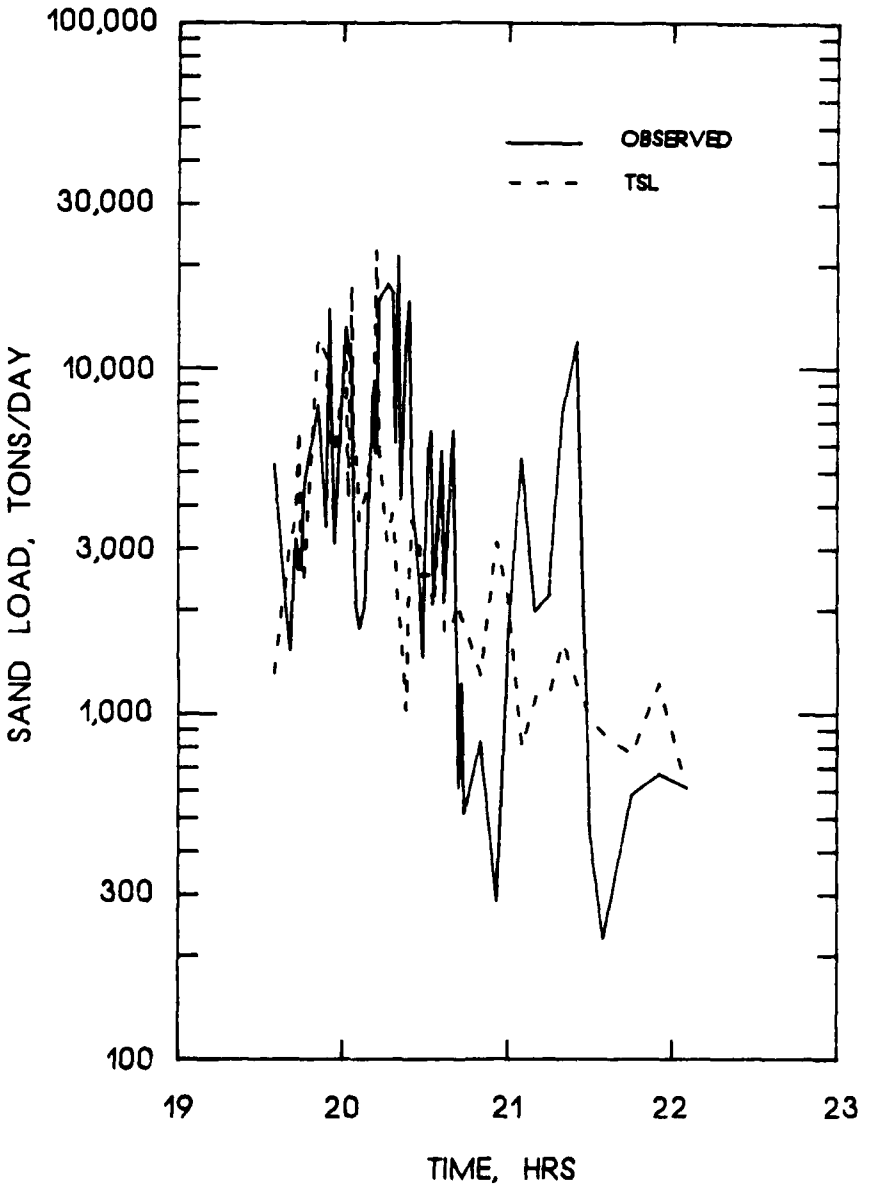

Figure 4.27. Total sand load versus time for the August 27, 1986, streamflow event at Goodwin Creek, Mississippi, Station 2. Suspended-sediment point samples are from 20 to 45 percent of the flow depth above the channel bed.

flow field. The TSL suspended-sediment samples are collected at one point.

4.6 DISCUSSION

The TSL procedure was compared to total sediment load field data and the MEP. The assessed data were collected in small streams with flow depths of less than 5 ft. Four of the assessed data sets were for the Niobrara River at Cody, Nebraska; Fivemile Creek at Shoshoni, Wyoming; the Middle Loup River near Dunning, Nebraska; and the Rio Grande conveyance channel near Bernardo, New Mexico. These data sets had previously been used in the development and evaluation of the MEP. A newly acquired data set collected at Goodwin Creek, Mississippi, was also assessed.

Comparison of the TSL procedure to field data and the MEP highlight the use of the TSL procedure as an alternative to depth-integrated suspended-sediment sampling. Statistics for the Niobrara River data indicate that the MEP procedure may provide greater reliability with a single depth-integrated suspended-sediment sample than the TSL procedure with a single point suspended-sediment sample. The Niobrara River data showed 89 percent of the the MEP measurements and 76 percent of the TSL procedure measurements to be less than a 50 percent deviation from sediment load estimated by Equation 4.1. Further assessment of the Niobrara River data indicates that the average of multiple TSL measurements, as in Figure 4.6, is as reliable as a single MEP measurement.

The Fivemile Creek, the Middle Loup River, and the Rio Grande conveyance channel data indicate a single TSL measurement is as reliable as a single MEP measurement. Comparisons on the percent differences between the MEP and the TSL procedure for these data were not assessed

since concurrent measurements of depth-integrated and point suspended-sediment samples were not reported.

The tested data show that the [illegible] measurement procedure is improved when point suspended-sediment samples are obtained in the lower flow depth but not too close to the channel bed. Lane and Kalinske (1941) recommended that point samples should be collected in the lower half-depth. The TSL procedure was tested and found to be reliable using point samples collected in the lower 20 to 45 percent flow depth. Point samples collected at locations further from the channel bed may provide less reliable measurements due to deviations in the theoretical sediment concentration and flow velocity profiles. These deviations may result from macroturbulence and are not numerically significant to the TSL procedure when the point samples are collected in the lower flow depth. Point samples collected close to the channel bed may exhibit greater variance than other point samples due to the same processes that influence the stochastic nature of bed load transport. In particular, point samples may not be representative if they are collected near bed forms of a significant height.

The Goodwin Creek data provided consecutive and concurrent depth-integrated and point suspended-sediment samples. These data demonstrate that both depth-integrated measurements and TSL procedure measurements can yield scatter in sediment load through time. Comparison of the total sand load observed with the depth-integrated sampler to the total sand load measured using the TSL procedure demonstrates that the TSL procedure provides a reliable measurement of sediment load.

The assessments of the reviewed data sets highlight advantages for selecting the TSL procedure over the MEP. Advantages of the TSL

procedure include realistic sediment load measurements, greater control in obtaining suspended-sediment samples, automatic sampling, the collection of near-continuous measurements, and time integration for determining the true sediment transport. Also, the use of point-source suspended-sediment samples requires less time in the field and lower sediment sampling costs.

CHAPTER 5

SUMMARY, CONCLUSION, AND RECOMMENDATIONS

5.1 SUMMARY

The main objective of this study was to develop a procedure for total sediment load measurement using a point-source suspended-sediment sample. The procedure was developed and compared to field data and the modified Einstein procedure (MEP). The computational step solution and computer code listing for the proposed procedure are provided in Appendices A and B, respectively. The proposed procedure and computer code are identified as TSL (Total Sediment Load).

The TSL procedure applies Einstein's (1950) modification to Keulegan's (1938) mean and point velocity relations, the suspended-sediment concentration distribution equation developed by Rouse (1937), and Burkham and Dawdy's (1980) modified form of Einstein's bed load function. The data required for application of the TSL procedure include descriptors of the streamflow, the channel geometry, the bed material, and the point-source suspended-sediment sample.

The TSL procedure was evaluated using field data from the Niobrara River at Cody, Nebraska; Fivemile Creek at Shoshoni, Wyoming; the Middle Loup River near Dunning, Nebraska; the Rio Grande conveyance channel near Bernardo, New Mexico; and Goodwin Creek near Oxford, Mississippi. The field data enabled comparisons of the TSL procedure, the MEP, and field measurements of total sediment load. The similarity in the

results of the comparisons highlights the use of the TSL procedure as an alternative to depth-integrated suspended-sediment sampling.

5.2 CONCLUSIONS

The TSL procedure provides total sediment load measurements that are similar in magnitude to both field and MEP measurements. The Niobrara River data indicate that the MEP procedure may provide greater reliability with a single depth-integrated suspended-sediment sample than the TSL procedure with a single point suspended-sediment sample. However, further assessment of the Niobrara River data indicates that the average of multiple TSL measurements is as reliable as a single MEP measurement. The Fivemile Creek, the Middle Loup River, and the Rio Grande conveyance channel data indicate a single TSL measurement is as reliable as a single MEP measurement.

The tested data show that the TSL measurement procedure is improved when point suspended-sediment samples are obtained in the lower flow depth. Lane and Kalinske (1941) recommended that point samples should be collected in the lower half-depth. The TSL procedure was tested and found to be reliable using point samples collected in the lower 20 to 45 percent flow depth.

The Goodwin Creek data provided consecutive and concurrent depth-integrated and point suspended-sediment samples. These data demonstrate that both depth-integrated measurements and TSL procedure measurements can yield scatter in sediment load through time. Comparison of the total sand load observed with the depth-integrated sampler to the total sand load measured using the TSL procedure demonstrates that the TSL procedure provides a reliable measurement of sediment load.

The assessments of the reviewed data sets highlight advantages for selecting the TSL procedure over the MEP. Advantages of the TSL procedure include realistic sediment load measurements, greater control in obtaining suspended-sediment samples, automatic sampling, the collection of near-continuous measurements, and time integration for determining the true sediment transport. Also, the use of point-source suspended-sediment samples requires less time in the field and lower sediment sampling costs.

5.3 RECOMMENDATIONS FOR FURTHER STUDIES

The data used to compare the TSL procedure to turbulence flume total sediment load measurements and the MEP were not from concurrently collected data sets. The exception was concurrently collected data at the Goodwin Creek research catchment. Additional data sets which provide concurrent sampling of point-source suspended-sediment samples should be collected and assessed. The additional data sets will assist in learning more about field procedures for sediment measurement and the sediment transport processes that each sediment sampling procedure is measuring. For example, a depth-integrated sample measures a flow column over time while a point sample can measure a point over time. Further studies may confirm that point sampling with application of the TSL procedure and time integration will provide more realistic measurements of sediment transport.

The TSL procedure now permits researchers to consider continuous sampling. The research community is now encouraged to develop a point sampler which can continuously collect or record data representing suspended-sediment size analyses and concentrations at a point. The

proposed sampling device along with the TSL procedure will permit continuous measurement of total sediment load through time.

Further assessment should be made on the location of the sediment sampler in the vertical and in the cross section. The assessment will require continuous total sediment load sampling and a near-constant sediment load and streamflow. The present recommendation is to collect a suspended-sediment sample in the lower flow depths (the lower 20 to 45 percent flow depth was assessed in this study) in a vertical section representing the cross section. Additional studies may consider multiple point samples across a cross section with one sampler per vertical section.

Studies designed to assess and improve the determination of the vertical velocity distribution, the sediment concentration distribution, and the bed load discharge will be useful for further modifications to the TSL procedure and the general understanding of sediment transport.

REFERENCES

Allen, P. B., and Barnes, B. B. (1975). "Total sediment load by the extrapolated data procedure." Present and Prospective Technology for Predicting Sediment Yields and Sources, Proceedings of the Sediment-Yield Workshop, US Department of Agriculture, Sedimentation Laboratory, Oxford, Mississippi, November 28-30, 1972, ARS-S-40, 100-108.

Barnes, H. H. (1967). "Roughness characteristics of natural streams." Water-Supply Paper 1849, US Geological Survey, Washington, D.C.

Bazin, H. E. (1865). "Researches experimentales sur l'ecoulement de l'eau dans les canaux decouverts (Experimental researches on the flow of water in open channels)." Momoires Presentes par Divers Savants a l'Academie des Sciences, Paris, 19.

Bowie, A. J., Bolton, G. C., and Murphree, C. E. (1972). "Direct measurements and computations of total sediment discharge." Transactions, American Society of Agricultural Engineers, 15(1), 91-93,98.

Bowie, A. J., and Sansom, O. W. (1986). "Innovative techniques for collecting hydrologic data." Proceedings, Fourth Federal Interagency Sedimentation Conference, Subcommittee on Sedimentation of the Interagency Advisory Committee on Water Data, 1-59 - 1-69.

Brooks, N. H. (1963). "Calculation of suspended load discharge from velocity and concentration parameters." Proceedings, Federal Interagency Sedimentation Conference, US Department of Agriculture, Agricultural Research Service, Miscellaneous Publication No. 970, 229-237.

Brownlie, W. R. (1981). "Prediction of flow depth and sediment discharge in open channels." Report No. KH-R-43A, W. M. Keck Laboratory of Hydraulics and Water Resources, California Institute of Technology, Pasadena, Calif.

_____. (1983). "Flow depth in sand-bed channels." Journal, Hydraulics Division, American Society of Civil Engineers, 109(HY7), 959-990.

Burkham, D. E., and Dawdy, D. R. (1976). "Resistance equation for alluvial channel flow." Journal, Hydraulics Division, American Society of Civil Engineers, 102(HY10), 1479-1489.

Burkham, D. E., and Dawdy, D. R. (1980). "General study of the modified Einstein method of computing total sediment discharge." Water-Supply Paper 2066, US Geological Survey, Washington, D.C.

Christiansen, J. E. (1935). "Distribution of silt in open channels." Transactions, American Geophysical Union, Part II, 16, 478.

Colby, B. R. (1957). "Relationship of unmeasured sediment discharge to mean velocity." Transactions, American Geophysical Union, 38(5), 708-717.

Colby, B. R., and Hembree, C. H. (1955). "Computations of total sediment discharge, Niobrara River near Cody, Nebraska." Water-Supply Paper 1357, US Geological Survey, Washington, D.C.

Colby, B. R., Hembree, C. H., and Rainwater, F. H. (1956). "Sedimentation and chemical quality of surface waters in the Wind River Basin, Wyoming." Water-Supply Paper 1373, US Geological Survey, Washington, D.C.

Colby, B. R., and Hubbell, D. W. (1961). "Simplified methods for computing total sediment discharge with the modified Einstein procedure." Water-Supply Paper 1593, US Geological Survey, Washington, D.C.

Culbertson, J. K., Scott, C. H., and Bennett, J. P. (1972). "Summary of alluvial channel data from Rio Grande Conveyance Channel, New Mexico, 1965-69." Professional Paper 562-J, US Geological Survey, Washington, D.C.

Einstein, H. A. (1950). "The bed-load function for sediment transportation in open channel flows." Technical Bulletin No. 1026, US Department of Agriculture, Soil Conservation Service, Washington, D.C.

Hubbell, D. W., and Matejka, D. Q. (1959). "Investigations of sediment transportation, Middle Loup River at Dunning, Nebraska." Water Supply Paper 1476, US Geological Survey, Washington, D.C.

Keulegan, G. H. (1938). "Laws of turbulent flow in open channels." Journal of Research of the National Bureau of Standards, 21, 707-741.

Lane, E. W., and Kalinske, A. A. (1941). "Engineering calculations of suspended sediment." Transactions, American Geophysical Union, 22, 603-607.

Lara, J. M. (1966). "Change in the modified Einstein procedure to compute z ." US Bureau of Reclamation, Denver, Colo.

Limerinos, J. T. (1970). "Determination of the Manning coefficient from measured bed roughness in natural channels." Water-Supply Paper 1898-B, US Geological Survey, Washington, D.C.

Meyer-Peter, E., and Muller, R. (1948). "Formulas for bed-load transport." International Association for Hydraulic Structures Research, Second Meeting, Stockholm, Appendix 2, 39-65.

Nikuradse, J. (1932). "Gesetzmassigkeiten der turbulenten stromung in glatten Rohren (Laws to turbulent flow in smooth pipes)." Gorschungsheft des Vereins deutscher Ingenieure, 356.

_____. (1933). "Stromungsgesetze in Rauhen Rohren." Forschungsheft des Vereins deutscher Ingenieure, 361.

Nordin, C. F., Jr., and Dempster, G. R. Jr. (1963). "Vertical distribution of velocity and suspended sediment in Middle Rio Grande, New Mexico." US Geological Survey Professional Paper 462-B, Washington, D.C.

O'Brien, M. P. (1933). "Review of the theory of turbulent flow and its relation to sediment-transportation." Transactions, American Geophysical Union, 487-491.

Prandtl, L. (1926). "Ueber die ausgelbildeter turbulenz (On fully developed turbulence)." Proceedings, Second International Congress on Applied Mechanics, Zurich, 62-74.

Richardson, E. G. (1937). "Suspension of solids in a turbulent stream." Proceedings, Royal Society of London, 162, 583-597.

Rouse, H. (1937). "Modern conceptions of the mechanics of fluid turbulence." Transactions, American Society of Civil Engineers, Paper No. 1965, 102, 463-543.

Rubey, W. W. (1933). "Settling velocities of gravel, sand and silt particles." American Journal of Science, 5th series, 25(148), 325-338.

Schroeder, K. B., and Hembree, C. H. (1956). "Application of the modified Einstein procedure for computation of total sediment load." Transactions, American Geophysical Union, 37(2), 197-212.

Seely, E. H., Grissinger, E. H., and Little, W. C. (1981). "Stream channel stability; Appendix F, Goodwin Creek: catchment, data collection and data management." US Department of Agriculture, Sedimentation Laboratory, Oxford, Miss.

Shen, H. W., and Hung, C. S. (1983). "Remodified Einstein procedure for sediment load." Journal, Hydraulics Division, American Society of Civil Engineers, 109(4), 565-578.

Toffaleti, F. B. (1969). "Definitive computations of sand discharge in rivers." Journal, Hydraulics Division, American Society of Civil Engineers, 95(HY1), 225-248.

US Army Corps of Engineers. (1981). "Final report to Congress, the Streambank Erosion Control Evaluation and Demonstration Act of 1974, Section 32, Public Law 93-251; Appendix F, Yazoo River Basin demonstration projects."

US Interagency Committee on Water Resources, Subcommittee on Sedimentation. (1940). "Field Practice and Equipment used in Sampling Suspended Sediment," Report 1, Iowa City, Iowa.

van Rijn, L. C. (1982). "Equivalent roughness of alluvial bed." Journal, Hydraulics Division, American Society of Civil Engineers, Technical Note, 108(HY10), 1215-1218.

Vanoni, V. A., and Brooks, N. H. (1957). "Laboratory studies of the roughness and suspended load of alluvial streams." Report No. E-68, Sedimentation Laboratory, California Institute of Technology, Pasadena, Calif.

Vanoni, V. A., ed. (1975). "Sedimentation engineering." American Society of Civil Engineers Manuals and Reports on Engineering Practice - No. 54, New York.

von Karman, T. (1930). "Mechanische aehnlichkeit und turbulenz (Mechanical similarity and turbulence)." Proceedings, Third International Congress on Applied Mechanics, Stockholm, 1, 85-92.

APPENDIX A

STEP SOLUTION

The following computational procedure may be used to determine the total sediment load using a point-source suspended-sediment sample.

Step 1. Identify the basic data: Q, streamflow for the sampled cross section; W, width of the cross section; A_c, cross-sectional area; R, hydraulic radius; d_s, flow depth of the sampled vertical; y_p, sample height above the channel bed; C_p, concentration of the suspended-sediment sample, mg/liter; i_b, fraction of bed material in each size range; i_s, fraction of suspended material in each size range; D_{35}, D_{65}, and D_{84}, particle sizes at which 35, 65, and 84 percent by weight, respectively, of the bed material is finer, mm; and ν, the kinematic viscosity of the water. (Except when noted otherwise, the English system of units is used throughout the computation.)

Step 2. Compute the mean flow depth d and the average flow velocity $\overline{V}$ using

$$d = \frac{Q}{W} \qquad \text{A.1}$$

and

$$\overline{V} = \frac{Q}{A_c} \qquad \text{A.2}$$

Step 3. Determine the effective grain roughness height k_s' . The computer program TSL (Total Sediment Load) provides a default of $k_s' = 3.3D_{84}$ as proposed by Limerinos (1970). Otherwise, the program user may supply a D_{84} multiplier for k_s' .

Step 4. Compute the shear velocity due to grain roughness U_*' using the modified form of Equation 3.3,

$$U_*' = \frac{\bar{V}}{5.75 \log \left(12.27 \frac{Rx'}{k_s'}\right)} \qquad A.3$$

where x' is a function of k_s'/δ' which is presented in Figure 4 of Einstein (1950) and $\delta' = (11.6\nu)/U_*'$.

Step 5. Compute the RS' product from

$$RS' = \frac{U_*'^2}{g} \qquad A.4$$

where S' is the energy grade line slope due to grain roughness and g is the acceleration due to gravity.

Step 6. Determine the effective roughness height k_s due to grain and form roughness. The computer program TSL provides a default of $k_s = 3.3D_{84}$ as proposed by Limerinos (1970). Other available user options include the procedures of Einstein (1950), Brownlie (1981, 1983), or a user-supplied D_{84} multiplier. When either the Brownlie or the Einstein procedure is applied, the friction factor f is determined and the relation

$$\frac{\bar{V}}{U_*} = \sqrt{8/f} \qquad \text{A.5}$$

where U_* is the shear velocity, is applied with Equation 2.19 for the determination of k_s .

Step 7. Compute the shear velocity due to grain and form roughness using Equation 2.19 modified as

$$U_* = \frac{\bar{V}}{5.75 \log \left(12.27 \frac{Rx}{k_s}\right)} \qquad \text{A.6}$$

where x is a function of k_s/δ which is presented in Figure 4 of Einstein (1950) and $\delta = 11.6\nu/U_*$.

Step 8. Compute the intensity of shear ψ_* for each bed material size interval, where

$$\psi_* = 1.65(\xi Y)_{RM} \left(\frac{\beta_1}{\beta_{x1}}\right)^2 \frac{k_s}{RS'} \qquad \text{A.7}$$

in which

$$\beta_1 = \log 10.6$$

$$\beta_{x1} = \log (10.6x)$$

$$(\xi Y)_{RM} = \frac{\delta + C_s D}{k_s} \quad \text{when} \quad D < \delta + C_s D \quad \text{and}$$

$$= \frac{D}{k_s} \quad \text{when} \quad D \geq \delta + C_s D$$

and

$$C_s = -0.62 + 3.12(D_{65}D_{35})^{1/2}$$

(The representative grain size D for each sediment size interval is the geometric mean of the interval limits.)

Step 9. Determine the transport intensity ϕ_* for each bed material size interval using Figure 10 from Einstein (1950) and ψ_* from step 8.

Step 10. Compute the bed load discharge $i_B q_B$ for a unit width of flow for each bed material size interval using Equation 2.28. With $g = 32.2$ ft/sec^2, the density of solids $\rho_s = 5.17$ slugs/ft^3, and the specific gravity of the sediment $S_s = 2.65$, Equation 2.28 becomes

$$i_B q_B = 1200 i_b D^{3/2} \phi_* \qquad \text{A.8}$$

where i_b is the fraction of bed material in a given size range.

Step 11. Compute the bed load concentration, C_b, for each bed material size fraction using

$$C_b = \frac{1}{11.6} \frac{i_B q_B}{2DU'_*} \qquad A.9$$

where $11.6U'_*$ is equivalent to the rate of sediment transport in the bed layer as proposed by Einstein (1950).

Step 12. Compare the concentration of the suspended sediment sample C_p to the bed load concentration C_b. If $C_p > C_b$, set $C_b = C_p$ and recompute $i_B q_B$. This limits the suspended-sediment concentration at less than or equal to the bed load concentration.

Step 13. Determine the lower limit of the suspended load zone. This limit is set at the largest of two possible heights above the channel bed. The first limiting height is $y_b = 2D$ (Einstein's suggestion for the height of the bed load zone) and the second limiting height is where $V_y = 0$ according to Equation 2.18, where V_y is the average flow velocity at a distance y from the channel bed or

$$y_b = \frac{k_s}{30.2x} \qquad A.10$$

Step 14. Determine z for each measured suspended sediment size interval using Equation 2.26 from which

$$z = \frac{\log\left(\frac{C_b}{C_p}\right)}{\log\left(\frac{d - y_b}{y_b} \frac{y_p}{d - y_p}\right)} \qquad A.11$$

Step 15. Develop a linear regressed relationship for z

$$z = \alpha_1 w^{\alpha_2} \qquad \text{A.12}$$

where α_1 and α_1 are regression coefficients and w is the particle fall velocity for the geometric mean of each sampled sediment size interval as determined using Ruby's equation (Ruby 1933)

$$w = \left\{ \left[\frac{2}{3} + \frac{36\nu^2}{g(S_s - 1)D^3} \right]^{1/2} - \left[\frac{36\nu^2}{g(S_s - 1)D^3} \right]^{1/2} \right\} [g(S_s - 1)D]^{1/2} \qquad \text{A.13}$$

Step 16. Recompute C_b for each sampled suspended sediment size fraction with Equation 2.26 modified as

$$C_b = \frac{C_p}{\left(\frac{d - y_p}{y_p} \frac{y_b}{d - y_b} \right)^z} \qquad \text{A.14}$$

wherein y_b is set for each sediment size interval according to step 13 and z is determined using Equation A.12.

Step 17. Recomputed $i_B q_B$ for each sampled suspended sediment size fraction, where

$$i_B q_B = C_b 11.6(2D)U'_* \qquad \text{A.15}$$

The height of the bed load zone is set at $2D$ for all sediment size fractions for the numerical calculations to agree with Einstein's (1950) formulation of bed load transport.

Step 18. Compute the suspended sediment transport $i_s q_s$ for each sampled size fraction using

$$i_s q_s = i_B q_B (PI_1 + I_2) \qquad \text{A.16}$$

with P given by Equation 2.52 I_1 given by Equation 2.48, and I_2 given by Equation 2.49.

Step 19. Compute the total sediment load through a cross section Q_T using

$$i_T q_T = i_B q_B + i_s q_s \qquad \text{A.17}$$

and

$$Q_T = 43.2W \sum i_T q_T \qquad \text{A.18}$$

where $43.2W$ is the stream width multiplied by a constant for converting pounds per second to tons per day.

APPENDIX B

COMPUTER PROGRAM LISTING

The following computer program was written for use on a personal computer. The program is written in Fortran 77 and can be run in executible form on an IBM compatible personal computer with 128K and a single floppy disk drive. During program execution, the user is prompted for input and output data file names.

```
      PROGRAM TSL
C  VERSION:  9-29-87
      CHARACTER*8 FL
      REAL IBQB(15),ISQS(15),ITQT(15),KS,KSP
      DIMENSION D(15),FB(15),FS(15),PB(15),PS(15),CA(15),
     1CB(15),PSI(15),PHI(15),GM(15),Z(15),Z1(15),W(15),
     2A(15)
C
C
C*****************************************************************
C    INPUT VARIABLES
C*****************************************************************
C
C   AREA - FLOW AREA OF MEASURED CROSS SECTION, FT**2
C   CON  - CONCENTRATION OF SUSPENDED SEDIMENT SAMPLE,
C          MG/LITER
C   CS   - COEFFICIENT USED TO COMPUTE BED LOAD WHICH IS A
C          FUNCTION OF MEDIAN DIAMETER
C          IF CS=0, CS WILL BE COMPUTED
C   D    - SEDIMENT SIZE FRACTION DIVISIONS, MM
C   DKS  - EFFECTIVE FLOW ROUGHNESS HEIGHT MULTIPLIER
C          (KS=DKS*D84) IF DKS=0, KS WILL BE COMPUTED (USE
C          OF THIS PARAMETER OVERRIDES THE USE OF IKS)
C   DKSP - EFFECTIVE GRAIN ROUGHNESS HEIGHT MULTIPLIER
C          (KSP=DKSP*D84)
C          IF DKSP=0, DKSP DEFAULTS TO 3.3
C   DSV  - DEPTH OF SAMPLING VERTICAL, FT
C   IKS  - IDENTIFIER FOR FRICTION FACTOR COMPUTATION
C          METHOD
```

```
C          IKS=0  FOR LIMERINOS
C          IKS=1  FOR BROWNLIE
C          IKS=2  FOR EINSTEIN
C   ISTA - STATION OR SAMPLE NUMBER
C   ND   - NUMBER OF SIZE FRACTIONS (MAXIMUM = 12)
C   NST  - NUMBER OF TOTAL LOAD SAMPLES
C   PB   - PERCENT OF BED MATERIAL FINER THAN D
C   PS   - PERCENT OF SUSPENDED MATERIAL FINER THAN D
C   Q    - STREAMFLOW, CFS
C   R    - HYDRAULIC RADIUS OF MEASURED CROSS SECTION, FT
C   T    - WATER TEMPERATURE, DEGREES FAHRENHEIT
C   WD   - CROSS SECTION WIDTH, FT
C   YS   - SAMPLE HEIGHT ABOVE CHANNEL BED, FT
C
C
C*****************************************************************
C*  INPUT DATA FILE FORMAT REQUIREMENTS
C*****************************************************************
C
C     READ(11,230) ND
C
C     DO 5 I=1,ND+1
C   5 READ(11,210) D(I)
C
C     READ(11,230) NST,IKS
C
C     DO 900 IST=1,NST
C     READ(11,240) Q,WD,AREA,R,DSV,YS,T,ISTA
C     READ(11,255) (PB(J),J=1,ND+1)
C     READ(11,255) (PS(J),J=1,ND+1)
C     READ(11,260) CON,CS,DKS,DKSP
C 900 CONTINUE
C
C 210 FORMAT(F10.4)
C 230 FORMAT(2I5)
C 240 FORMAT(7F10.2,I5)
C 255 FORMAT(15F5.0)
C 260 FORMAT(4F10.0)
C
C*****************************************************************
C
      WRITE(*,*)'ENTER INPUT DATA FILE NAME'
      READ(*,200) FL
  200 FORMAT(A8)
      OPEN(11,FILE=FL)
      WRITE(*,*)'ENTER OUTPUT FILE NAME'
      READ(*,200) FL
      OPEN(12,FILE=FL,STATUS='NEW')
      WRITE(*,*) 'ENTER GRAPHICS OUTPUT FILE NAME'
      READ(*,200) FL
      OPEN(13,FILE=FL,STATUS='NEW')
```

```
C
C*****************************************************************
C*  READ INPUT DATA FILE / SIZE FRACTION DIVISIONS
C*****************************************************************
C
      READ(11,230) ND
      DO 5 I=1,ND+1
      READ(11,210) D(I)
  210 FORMAT(F10.4)
    5 CONTINUE
C
C*****************************************************************
C*  DETERMINE EACH SIZE RANGE'S GEOMETRIC MEAN, FT
C*****************************************************************
C
      DO 10 I=1,ND
   10 GM(I)=(D(I)*D(I+1))**0.5/304.8
C
C*****************************************************************
C*  READ AND ANALYZE EACH DATA SET
C*****************************************************************
C
      READ(11,230) NST,IKS
  230 FORMAT(2I5)
      WRITE(13,205)IKS
  205 FORMAT('IKS = ',I5,/,11X,'Q',7X,'TL',8X,'TF',8X,'TS',
     19X,'TG' ,7X,'TFS',3X,'YS/DSV',1X,'DSV/D',1X,'STA',3X,
     2'D50G',7X,'CS',/)
      DO 900 IST=1,NST
      DO 15 J=1,ND
      Z(J)=0.0
   15 Z1(J)=0.0
      WRITE(*,235) IST,NST
  235 FORMAT(////,' DATA SET ',I3,' OF ',I3,//)
      READ(11,240) Q,WD,AREA,R,DSV,YS,T,ISTA
  240 FORMAT(7F10.2,I5)
      DEPTH=AREA/WD
      V=Q/AREA
      X1=YS/DSV
      X2=DSV/DEPTH
      WRITE(12,250) Q,V,WD,DEPTH,DSV,YS,T,IKS
  250 FORMAT(////,'TSL VERSION 9-29-87',///,
     1'STREAMFLOW,CFS = ',E10.3,/,'MEAN VELOCITY, FPS = ',
     2E10.3,/,'CHANNEL WIDTH, FT = ',E10.3,/,
     3'MEAN FLOW DEPTH, FT = 'E10.3,/,
     4'DEPTH OF SAMPLING VERTICAL, FT = ',E10.3,/,
     5'SAMPLE HEIGHT ABOVE CHANNEL BED, FT = ',E10.3,/,
     6'WATER TEMPERATURE, DEGREES FAHRENHEIT = ',E10.3,/,
     7'IKS = ',I5)
      READ(11,255) (PB(J),J=1,ND+1)
      READ(11,255) (PS(J),J=1,ND+1)
      READ(11,260) CON,CS,DKS,DKSP
  255 FORMAT(15F5.0)
  260 FORMAT(4F10.0)
```

```
C
C*****************************************************************
C   DETERMINE D16,D35,D50,D65, AND D84; MM
C*****************************************************************
C
      DO 20 J=1,ND
      FB(J)=(PB(J+1)-PB(J))/100.0
      FS(J)=(PS(J+1)-PS(J))/100.0
      IF(FB(J).LE.0.0) FB(J)=0.0
      IF(FS(J).LE.0.0) FS(J)=0.0
   20 CONTINUE
      P16L=0.0
      DO 25 J=1,ND+1
      IF(P16L.GT.0.0.AND.PB(J).LE.0.0)GO TO 25
      IF(PB(J).LE.16.0) THEN
      P16L=PB(J)
      D16L=D(J)
      ENDIF
      IF(PB(J).LE.35.0) THEN
      P35L=PB(J)
      D35L=D(J)
      ENDIF
      IF(PB(J).LE.50.0) THEN
      P50L=PB(J)
      D50L=D(J)
      ENDIF
      IF(PB(J).LE.65.0) THEN
      P65L=PB(J)
      D65L=D(J)
      ENDIF
      IF(PB(J).LE.84.0) THEN
      P84L=PB(J)
      D84L=D(J)
      ENDIF
   25 CONTINUE
      DO 30 J=ND+1,1,-1
      IF(PB(J).GT.16.0) THEN
      P16H=PB(J)
      D16H=D(J)
      ENDIF
      IF(PB(J).GT.35.0) THEN
      P35H=PB(J)
      D35H=D(J)
      ENDIF
      IF(PB(J).GT.50.0) THEN
      P50H=PB(J)
      D50H=D(J)
      ENDIF
      IF(PB(J).GT.65.0) THEN
      P65H=PB(J)
      D65H=D(J)
      ENDIF
      IF(PB(J).GT.84.0) THEN
      P84H=PB(J)
```

```
      D84H=D(J)
      ENDIF
   30 CONTINUE
      AB=P16H-P16L
      B=ALOG10(D16H)-ALOG10(D16L)
      SM=AB/B
      AB=(16.0-P16L)/SM+ALOG10(D16L)
      D16=10.0**AB
      AB=P35H-P35L
      B=ALOG10(D35H)-ALOG10(D35L)
      SM=AB/B
      AB=(35.0-P35L)/SM+ALOG10(D35L)
      D35=10.0**AB
      AB=P50H-P50L
      B=ALOG10(D50H)-ALOG10(D50L)
      SM=AB/B
      AB=(50.0-P50L)/SM+ALOG10(D50L)
      D50=10.0**AB
      AB=P65H-P65L
      B=ALOG10(D65H)-ALOG10(D65L)
      SM=AB/B
      AB=(65.0-P65L)/SM+ALOG10(D65L)
      D65=10.0**AB
      AB=P84H-P84L
      B=ALOG10(D84H)-ALOG10(D84L)
      SM=AB/B
      AB=(84.0-P84L)/SM+ALOG10(D84L)
      D84=10.0**AB
      WRITE(12,*)'D16 = ',D16
      WRITE(12,*)'D35 = ',D35
      WRITE(12,*)'D50 = ',D50
      WRITE(12,*)'D65 = ',D65
      WRITE(12,*)'D84 = ',D84
C
C*****************************************************************
C*  DETERMINE THE SHEAR VELOCITY FOR GRAIN ROUGHNESS,
C*  FT/SEC
C*****************************************************************
C
      VIS=VISCOS(T)
      IF(DKSP)85,85,90
   85 DKSP=3.3
   90 KSP=DKSP*D84/304.8
      RKS=KSP
      CALL SHEAR(V,R,RKS,VIS,XP,USP)
      SP=USP**2.0/(32.2*R)
      DKSP=KSP*304.8/D84
      DKSPA=KSP*304.8/D65
      WRITE(12,*)'KSP = ',KSP,' KSP/D84 = ',DKSP,
     1' KSP/D65 = ',DKSPA
      WRITE(12,*)'SP = ',SP,' XP = ',XP
```

```
C
C*****************************************************************
C*  DETERMINE KS, FT, EFFECTIVE FLOW ROUGHNESS HEIGHT
C*****************************************************************
C
      I=0
      FG=V/SQRT(1.65*32.2*D50/304.8)
      IF(DKS)35,35,33

C
C*****************************************************************
C   DETERMINE FRICTION FACTOR USING THE ENTERED DKS
C*****************************************************************
C
   33 RKS=DKS*D84/304.8
      KS=RKS
      CALL SHEAR(V,R,RKS,VIS,X,US)
      F=8.0*(US/V)**2.0
      GO TO 80
   35 GO TO(36,37,42)IKS+1
C
C*****************************************************************
C   DETERMINE FRICTION FACTOR USING LIMERINOS (1970)
C*****************************************************************
C
   36 DKS=3.3
      GO TO 33
C
C*****************************************************************
C   DETERMINE FRICTION FACTOR USING BROWNLIE (1981)
C*****************************************************************
C
   37 D50=D50/304.8
      SIG=SQRT(D84/D16)
      S=0.038805*FG**2.572*SIG**0.413/(R/D50)**1.361
      IF(S.LE.0.006)GO TO 39
   38 S=0.021425*FG**2.172*SIG**0.2785/(R/D50)**1.304
      GO TO 41
   39 FGP=1.74/S**.3333
      IF(FGP/FG-1.0)41,41,40
   40 F=0.188925*FG**0.572*SIG**0.413/(R/D50)**0.361
      GO TO 65
   41 I=I+1
      IF(I.LE.1)GO TO 38
      F=0.104346*FG**0.172*SIG**0.279/(R/D50)**0.304
      GO TO 65
C
C*****************************************************************
C   DETERMINE FRICTION FACTOR USING EINSTEIN (1950)
C*****************************************************************
C
   42 RSP=USP**2.0/32.2
      CHI=1.65*D35/(304.8*RSP)
      CALL FIG5(CHI,USPP)
```

```
      USPP=V/USPP
      US=SQRT(USP**2.0+USPP**2.0)
      F=8.0/(V/US)**2.0
C
   65 DEL=12.27*R/10.0**(SQRT(8.0/F)/5.75)
      US=SQRT(F/8.0)*V
      DELTA=11.6*VIS/US
      X=1.0
      KS=DEL*X
      SIN=KS/DELTA
      XP=FX(SIN)
      IF(XP-X)70,80,70
   70 KS=20.0*DELTA
   75 SIN=KS/DELTA
      X=FX(SIN)
      KSP=X*DEL
      TEST=ABS(KSP-KS)/KS
      IF(TEST.LE.0.001)GO TO 80
      KS=KSP
      GO TO 75
   80 DKS=KS/D84*304.8
      DKSA=KS/D65*304.8
      S=US**2.0/(32.2*R)
      FGP=1.74/S**.3333
      WRITE(12,*)'KS = ',KS,' KS/D84 = ',DKS,
     1' KS/D65 = ',DKSA
      WRITE(12,*)'FG = ',FG,' FGP = ',FGP,'      S = ',S,
     1' F = ',F,' X = ',X
C
C*****************************************************************
C*  COMPUTE CS FOR PSI COMPUTATIONS
C*****************************************************************
C
      D50G=(D65*D35)**0.5
      IF(CS)125,120,125
  120 CS=D50G*3.12-0.62
      IF(D50G.LT.0.20) CS=0.0
      IF(D50G.GT.0.52) CS=1.0
      WRITE(12,*)'(D65*D35)**0.5 =',D50G,' CS =',CS
C
C*****************************************************************
C*   DETERMINE PSI FOR EACH BED MATERIAL GRAIN SIZE
C*   FRACTION
C*****************************************************************
C
  125 BETA=ALOG10(10.6)
      BETAX1=ALOG10(10.6*X)
      RS=(USP**2)/32.2
      DELTA=11.6*VIS/US
      F1=1.65*(BETA/BETAX1)**2/RS
      DO 135 I=2,ND
      F2=DELTA+CS*GM(I)
      IF(GM(I).GT.F2) GO TO 130
```

```
      PSI(I)=F1*F2
      GO TO 135
  130 PSI(I)=F1*GM(I)
  135 CONTINUE
      WRITE(12,270) (PSI(I),I=2,7)
      WRITE(12,275) (PSI(I),I=8,ND)
  270 FORMAT('PSI(I),I=2,7  = ',6E10.3)
  275 FORMAT('PSI(I),I=8,14 = ',7E10.3)
C
C*****************************************************************
C*  DETERMINE THE INTENSITY OF TRANSPORT FOR EACH GRAIN
C*  SIZE
C*****************************************************************
C
      DO 140 I=2,ND
      PHI(I)=FIG10(PSI(I))
  140 CONTINUE
      WRITE(12,285) (PHI(I),I=2,7)
      WRITE(12,290) (PHI(I),I=8,ND)
  285 FORMAT('PHI(I),I=2,7  = ',6E10.3)
  290 FORMAT('PHI(I),I=8,ND = ',7E10.3)
C
C*****************************************************************
C*  COMPUTE THE BEDLOAD DISCHARGE FOR EACH GRAIN SIZE RANGE
C*****************************************************************
C
      DO 145 I=2,ND
  145 IBQB(I)=1200.0*FB(I)*GM(I)**(3.0/2.0)*PHI(I)
      WRITE(12,295) (IBQB(I),I=2,7)
      WRITE(12,300) (IBQB(I),I=8,ND)
  295 FORMAT('IBQB(I),I=2,7  = ',6E10.3)
  300 FORMAT('IBQB(I),I=8,ND = ',7E10.3)
C
C*****************************************************************
C*  DETERMINE THE CONCENTRATION IN THE BEDLOAD ZONE
C*****************************************************************
C
      DO 150 I=2,ND
      CB(I)=IBQB(I)/(11.6*2.0*GM(I)*USP)
      WRITE(12,305) I,CB(I)
  305 FORMAT('CB(',I2,') = ',E10.3)
C
C*****************************************************************
C*  COMPARE CA TO CB
C*****************************************************************
C
      CA(I)=FS(I)*CON*6.24E-5
      IF(CA(I).LE.CB(I)) GO TO 150
      CB(I)=1.001*CA(I)
      IBQB(I)=CB(I)*11.6*2.0*GM(I)*USP
  150 CONTINUE
      WRITE(12,310) (CA(I),I=2,7)
      WRITE(12,315) (CA(I),I=8,ND)
  310 FORMAT('CA(I),I=2,7  = ',6E10.3)
```

```
  315 FORMAT('CA(I),I=8,ND = ',7E10.3)
      WRITE(12,320) (CB(I),I=2,7)
      WRITE(12,325) (CB(I),I=8,ND)
  320 FORMAT('CB(I),I=2,7  = ',6E10.3)
  325 FORMAT('CB(I),I=8,ND = ',7E10.3)
      WRITE(12,330) (IBQB(I),I=2,7)
      WRITE(12,335) (IBQB(I),I=8,ND)
  330 FORMAT('IBQB(I),I=2,7  = ',6E10.3)
  335 FORMAT('IBQB(I),I=8,14 = ',7E10.3)
C
C*****************************************************************
C*  DETERMINE Z FOR EACH SAMPLED SUSPENDED SEDIMENT GRAIN
C*  SIZE
C*****************************************************************
C
      DO 155 I=2,ND
      F1=0.0
      F2=1.0
      IF(CA(I).LE.0.0) GO TO 155
      IF(CB(I).LE.0.0) GO TO 155
      IF(FS(I).LE.0.001) GO TO 155
      F1=ALOG10(CB(I)/CA(I))
      F2=2.0*GM(I)
      T=KS/(30.2*X)
      IF(F2.LT.T)F2=T
      F2=DSV/F2-1.0
      F2=ALOG10(F2/(DSV/YS-1.0))
      Z(I)=F1/F2
  155 Z1(I)=Z(I)
      WRITE(12,340) (Z(I),I=2,7)
      WRITE(12,345) (Z(I),I=8,ND)
  340 FORMAT('Z(I),I=2,7  = ',6E10.3)
  345 FORMAT('Z(I),I=8,14 = ',7E10.3)
C
C*****************************************************************
C*  COMPUTE THE REGRESSED RELATION     Z=A*W**B
C*****************************************************************
C
      DO 160 I=1,ND
      F1=36.0*VIS**2/(53.13*GM(I)**3.0)
  160 W(I)=((2.0/3.0+F1)**0.5-F1**0.5)*(53.13*GM(I))**0.5
      WRITE(12,350) (W(I),I=1,7)
      WRITE(12,355) (W(I),I=8,ND)
  350 FORMAT('W(I),I=1,7  = ',7E10.3)
  355 FORMAT('W(I),I=8,14 = ',7E10.3)
      Z(1)=0.0
      CALL RGRS(ND,W,Z,FS,AL,B,RSQ,STD)
C
C*****************************************************************
C*  RECOMPUTE Z FOR EACH SIZE FRACTION
C*****************************************************************
C
      DO 165 I=1,ND
      Z(I)=AL*W(I)**B
```

```
  165 CONTINUE
      WRITE(12,365) AL,B,(W(I),I=1,ND)
  365 FORMAT('AL = ',E10.3,/,'B = ',E10.3,/,
     1'W(I),I=1,7  = ',7E10.3,/,'W(I),I=8,14 = ',7E10.3)
      WRITE(12,366)(Z(I),I=1,ND)
  366 FORMAT('Z(I),I=1,7  = ',7E10.3,/,
     1'Z(I),I=8,14 = ',7E10.3)
C
C*************************************************************
C*  RECOMPUTE CB USING THE NEW Z VALUES FOR THE SAMPLED
C*  SUSPENDED SEDIMENT GRAIN SIZES
C*************************************************************
C
      CA(1)=FS(1)*CON*6.24E-5
      DO 170 I=1,ND
      IF(FS(I).LE.0.0) GO TO 170
      F1=2.0*GM(I)
      IF(F1.LT.T)F1=T
      F1=DSV/F1-1.0
      F2=YS/(DSV-YS)
      CB(I)=CA(I)*(F1*F2)**Z(I)
  170 CONTINUE
C
C*************************************************************
C*  RECOMPUTE IBQB FOR EACH SAMPLED SIZE FRACTION
C*************************************************************
C
      DO 175 I=1,ND
  175 IBQB(I)=CB(I)*11.6*2.0*GM(I)*USP
      WRITE(12,370) (CB(I),I=1,ND)
  370 FORMAT('CB(I),I=1,7  = ',7E10.3,/,
     1'CB(I),I=8,14 = ',7E10.3)
      WRITE(12,371) (IBQB(I),I=1,ND)
  371 FORMAT('IBQB(I),I=1,7  = ',7E10.3,/,
     1'IBQB(I),I=8,14 = ',7E10.3)
C
C*************************************************************
C*  COMPUTE ISQS AND ITQT FOR EACH SIZE FRACTION
C*************************************************************
C
      P=2.303*ALOG10(30.2*DSV*X/KS)
      WRITE(12,375) P
  375 FORMAT('P = ',E10.3,//,3X,'I',5X,'Z(I)',6X,'A',9X,
     1'XI1',7X,'XI2',5X,'ISQS(I)',3X,'IBQB(I)',3X,'ITQT(I)')
      WRITE(*,*)'COMPUTING CONCENTRATION PROFILE INTEGRALS'
      CONV=1.0E-3
      WRITE(*,*) 'CONV = ',CONV
      DO 180 I=1,ND
      ZI=Z(I)
      AI=2.0*GM(I)
      IF(AI.LT.T)AI=T
      A(I)=AI/DSV
      AI=A(I)
      WRITE(*,*) 'I = ',I
```

```
C
C   TEST TO AVOID - REAL math overflow error
C
      ZMAX=1.0/(.8587E-2-.1395E-1*ALOG(AI))
      XI1=0.0
      XI2=0.0
      IF(ZI.LT.ZMAX) CALL I1I2(ZI,AI,CONV,XI1,XI2)
      ISQS(I)=IBQB(I)*(P*XI1+XI2)
      ITQT(I)=ISQS(I)+IBQB(I)
  180 WRITE(12,380) I,Z(I),A(I),XI1,XI2,ISQS(I),IBQB(I),
     &ITQT(I)
  380 FORMAT(I4,7E10.3)
C
C*************************************************************
C*  COMPUTE THE TOTAL LOAD FOR THE SAMPLING STATION
C*************************************************************
C
      TL=0.0
      TG=0.0
      TF=0.0
      TS=0.0
      TFS=0.0
      DO 185 I=1,ND
      ITQT(I)=ITQT(I)*43.2*WD
      TL=TL+ITQT(I)
      F1=GM(I)*304.8
      IF(F1.LT.0.0625)TF=TF+ITQT(I)
      IF(F1.GE.0.0625.AND.F1.LE.2.0)TS=TS+ITQT(I)
      IF(F1.GT.2.0)TG=TG+ITQT(I)
  185 CONTINUE
      TFS=TS+TF
      WRITE(12,390) (ITQT(I),I=1,ND)
  390 FORMAT(/,'ITQT(I),I=1,7  = ',7E10.3,/,
     1'ITQT(I),I=8,14 = ',7E10.3)
      WRITE(12,391)TL
  391 FORMAT(/,'TL = ',E10.3,' TONS/DAY')
      WRITE(13,395) IST,Q,TL,TF,TS,TG,TFS,X1,X2,ISTA,D50G,GS
  395 FORMAT(1X,I3,6F10.2,2F6.2,I4,2E10.3)
  900 CONTINUE
      CLOSE(11)
      CLOSE(12)
      CLOSE(13)
      STOP
      END
C
C
      FUNCTION FX(SIN)
      IF(SIN.GE.10.) THEN
      FX=1.
      ELSEIF(SIN.LT.0.16) THEN
      FX=3.47*SIN
      ELSEIF(SIN.LT.0.35) THEN
      FX=0.5506*ALOG10(SIN)**2+2.42708*ALOG10(SIN)+2.13114
      ELSEIF(SIN.LT.0.76) THEN
```

```
      FX=1.66704+0.40926*ALOG10(SIN)-1.64269*ALOG10(SIN)**2
      ELSEIF(SIN.LT.0.87) THEN
      FX=1.58819-0.90491*ALOG10(SIN)-7.11837*ALOG10(SIN)**2
      ELSEIF(SIN.LT.1.20) THEN
      FX=1.61092-0.14721*ALOG10(SIN)-0.80425*ALOG10(SIN)**2
      ELSEIF(SIN.LT.1.38) THEN
      FX=1.56414+1.02233*ALOG10(SIN)-8.11388*ALOG10(SIN)**2
      ELSEIF(SIN.LT.2.88) THEN
      FX=1.72783-1.31612*ALOG10(SIN)+0.23774*ALOG10(SIN)**2
      ELSEIF(SIN.LT.3.31) THEN
      FX=2.83698-6.13852*ALOG10(SIN)+5.47947*ALOG10(SIN)**2
      ELSEIF(SIN.LT.6.92) THEN
      FX=1.41244-0.65949*ALOG10(SIN)+0.21118*ALOG10(SIN)**2
      ELSEIF(SIN.LT.8.32) THEN
      FX=3.45772-5.52922*ALOG10(SIN)+3.10983*ALOG10(SIN)**2
      ELSE
      FX=5.49124*ALOG10(SIN)-2.87955*ALOG10(SIN)**2-1.61169
      ENDIF
      RETURN
      END
C
C
      SUBROUTINE FIG5 (X,Y)
C*****************************************************************
C THIS SUBROUTINE APPROXIMATES EINSTEINS FIG 5 BY A SERIES
C OF EQNS.
C*****************************************************************
      IF (X.LE.1.0) THEN
      Y=40.0*X**(-1.288)
      ELSEIF(X.LE.2.0) THEN
      Y=40.0*X**(-0.982)
      ELSEIF(X.LE.4.0) THEN
      Y=31.1*X**(-0.618)
      ELSEIF(X.LE.8.0) THEN
      Y=26.0*X**(-0.486)
      ELSE
      Y=21.4*X**(-0.394)
      ENDIF
      RETURN
      END
C
C
      FUNCTION FIG10(X)
C*****************************************************************
C THIS FUNCTION APPROXIMATES EINSTEINS FIG 10 BY A SERIES
C OF EQNS.
C*****************************************************************
      IF(X.LT.0.4) THEN
      FIG10=8.106078*X**(-0.989002)
      ELSEIF(X.LT.1.0) THEN
      FIG10=7.473444*X**(-1.067367)
      ELSEIF(X.LT.2.0) THEN
      FIG10=7.512081*X**(-1.182832)
      ELSEIF(X.LT.3.0) THEN
```

```
      FIG10=9.151968*X**(-1.472483)
      ELSEIF(X.LT.5.0) THEN
      FIG10=16.025332*X**(-1.972806)
      ELSEIF(X.LT.7.0) THEN
      FIG10=41.421873*X**(-2.578713)
      ELSEIF(X.LT.10.0) THEN
      FIG10=130.2209*X**(-3.165102)
      ELSEIF(X.LT.13.0) THEN
      FIG10=584.560594*X**(-3.818249)
      ELSEIF(X.LT.17.0) THEN
      FIG10=3543.989886*X**(-4.522935)
      ELSEIF(X.LT.20.0) THEN
      FIG10=1690645.945*X**(-6.703904)
      ELSEIF(X.LT.23.0) THEN
      FIG10=5188257832.0*X**(-9.381815)
      ELSE
      FIG10=3.134987996E15*X**(-13.597547)
      ENDIF
      RETURN
      END
C
C
      FUNCTION VISCOS(TEMP)
      DIMENSION V(13)
      DATA V/2.22E-5,1.922E-5,1.686E-5,1.491E-5,
     11.33E-5,1.194E-5,1.08E-5,9.829E-6,8.993E-6,
     28.269E-6,7.636E-6,7.08E-6,6.589E-6/
      TEP=(TEMP-32.0)*5.0/9.0
      NPOS=TEP/4.0+2
      TO=FLOAT(NPOS)*4.0-8.0
      IF(TO-TEP) 570,560,560
  560 VISCOS=V(NPOS)
      RETURN
  570 P=(TEP-TO)/4.0
      F1=V(NPOS-1)*(P-P*P)*(P-2.0)/6.0
      F2=V(NPOS)*(P*P-1.0)*(P-2.0)/2.0
      F3=V(NPOS+1)*(2.0*P-P*P)*(P+1.0)/2.0
      F4=V(NPOS+2)*(P*P*P-P)/6.0
      VISCOS=F1+F2+F3+F4
      RETURN
      END
C
C
      SUBROUTINE SHEAR(U,R,RKS,VIS,XF,UST)
      SL=2.0
      SLH=SL
      SLL=0.0
  105 SL=(SLH+SLL)/2.0
      UST=SQRT(R*SL*32.2)
      DELTA=11.6*VIS/UST
      SIN=RKS/DELTA
      XF=FX(SIN)
      UB=5.75*ALOG10(12.27*R*XF/RKS)*UST
      CNV=ABS(UB-U)/U
```

```
      IF(CNV.LE.0.001)GO TO 110
      IF(UB.GT.U)SLH=SL
      IF(UB.LT.U)SLL=SL
      IF(SLL.GE.SLH)SLH=SLH+2.0
      GO TO 105
  110 RETURN
      END
C
C
      SUBROUTINE RGRS(ND,X,Y,F,A,B,RSQ,STD)
      DIMENSION X(15),Y(15),F(15)
      A=1.0
      B=0.0
      RSQ=1.0
      NP=ND-1
      NP1=NP
      SLNXY = 0.0
      SLNX = 0.0
      SLNY = 0.0
      SLNXS = 0.0
      SLNYS = 0.0
      AY = 0.0
      DO 15 I=2,ND
      IF(X(I).LE.0.0) GO TO 10
      IF(Y(I).LE.0.0) GO TO 10
      IF(F(I).LE.0.001) GO TO 10
      IC=IFIX(1000.0*F(I))
      DO 5 IY=1,IC
      AY=AY+Y(I)
      SLNXY = SLNXY+ALOG(X(I))*ALOG(Y(I))
      SLNX = SLNX+ALOG(X(I))
      SLNY = SLNY+ALOG(Y(I))
      SLNXS = SLNXS+ALOG(X(I))**2
    5 SLNYS = SLNYS+ALOG(Y(I))**2
      NP=NP+IC-1
      GO TO 15
   10 NP=NP-1
      NP1=NP1-1
   15 CONTINUE
      IF(NP1-2) 65,40,20
C
C*****************************************************************
C*  COMPUTE A & B WITH 3 OR MORE DATA POINTS
C*****************************************************************
C
   20 B=SLNXY-SLNX*SLNY/FLOAT(NP)
      B=B/(SLNXS-(SLNX*SLNX)/FLOAT(NP))
      AY=AY/FLOAT(NP)
      SLNYA=SLNY/FLOAT(NP)
      IF(B.LE.0.0) GO TO 22
      A=EXP(SLNYA-B*SLNX/FLOAT(NP))
      RSQ=(SLNXY-SLNX*SLNY/FLOAT(NP))**2
      RSQ=RSQ/(SLNXS-SLNX**2/FLOAT(NP))
      RSQ=RSQ/(SLNYS-SLNY**2/FLOAT(NP))
```

```
   22 NP=ND-1
      DO 35 I=2,ND
      IF(X(I).LE.0.0) GO TO 30
      IF(Y(I).LE.0.0) GO TO 30
      IF(F(I).LE.0.001) GO TO 30
      IC=IFIX(1000.0*F(I))
      YI=A*X(I)**B
      DO 25 IY=1,IC
      DSLNYI = DSLNYI+(ALOG(Y(I))-ALOG(YI))**2
   25 DSLNY = DSLNY+(Y(I)-AY)**2
      NP=NP+IC-1
      GO TO 35
   30 NP=NP-1
   35 CONTINUE
      STD=(DSLNYI/FLOAT(NP))**0.5
      IF(B.GT.0.0) RETURN
      A=AY
      B=0.0
      RSQ=0.0
      STD=(DSLNY/FLOAT(NP))**0.5
      RETURN
C
C*****************************************************************
C*  COMPUTE A & B USING 2 DATA POINTS
C*****************************************************************
C
   40 Y1=0.0
      Y2=0.0
      DO 60 I=2,ND
      IF(Y(I))60,60,45
   45 IF(Y1)50,50,55
   50 Y1=Y(I)
      X1=X(I)
      GO TO 60
   55 Y2=Y(I)
      X2=X(I)
   60 CONTINUE
      B=ALOG10(Y1/Y2)/ALOG10(X1/X2)
      A=Y1/X1**B
      IF(B.GT.0.0) RETURN
      B=0.0
      A=(Y1+Y2)/2.0
      RETURN
C
C*****************************************************************
C*  COMPUTE A & B USING ONE DATA POINT ASSUMMING
C*                 Y(I) = A * X(I) ** 0.7
C*****************************************************************
C
   65 B=0.7
      DO 75 I=2,ND
      IF(Y(I))75,75,70
   70 A=Y(I)/X(I)**0.7
   75 CONTINUE
```

```
      RETURN
      END
C
C
      SUBROUTINE I1I2(Z,A,CONV,XI1,XI2)
C*****************************************************************
C*   INTEGRATION OF I1 AND I2 USING SIMPSON'S RULE
C*****************************************************************
C
      WRITE(*,*) 'Z,A = ',Z,A
      XI1=0.0
      XI2=0.0
      FI1=0.0
      FI2=0.0
C
      N=80
      C=.216*A**(Z-1.0)/(1.0-A)**Z
C
   10 XI1=((1.0-A)/A)**Z
      XI2=XI1*ALOG(A)
C
      K=1
      DO 60 I=1,N-1
      IF(K-3) 30,20,20
   20 K=1
   30 AN=A+FLOAT(I)*(1.0-A)/FLOAT(N)
      FNC=((1.0-AN)/AN)**Z
      IF(K-2) 40,50,50
   40 XI1=XI1+4.0*FNC
      XI2=XI2+4.0*FNC*ALOG(AN)
      GO TO 60
   50 XI1=XI1+2.0*FNC
      XI2=XI2+2.0*FNC*ALOG(AN)
   60 K=K+1
C
      XI1=(1.0-A)/(FLOAT(N)*3.0)*XI1
      XI2=(1.0-A)/(FLOAT(N)*3.0)*XI2
      CI1=ABS(XI1-FI1)/XI1
      CI2=ABS(XI2-FI2)/XI2
      IF(CI1.LE.CONV.AND.CI2.LE.CONV) GO TO 70
      IF(N.GE.1.0E5)GO TO 70
      N=N+N
      FI1=XI1
      FI2=XI2
      GO TO 10
   70 XI1=C*XI1
      XI2=C*XI2
      RETURN
      END
```

APPENDIX C

FIVEMILE CREEK NEAR SHOSHONI, WYOMING

This appendix presents figures used in this study to estimate the channel width and cross-sectional area for Fivemile Creek near Shoshoni, Wyoming. The data for these figures are available in the files of the US Geological Survey, Cheyenne, Wyoming. The data were collected between September, 1953 and October, 1954.

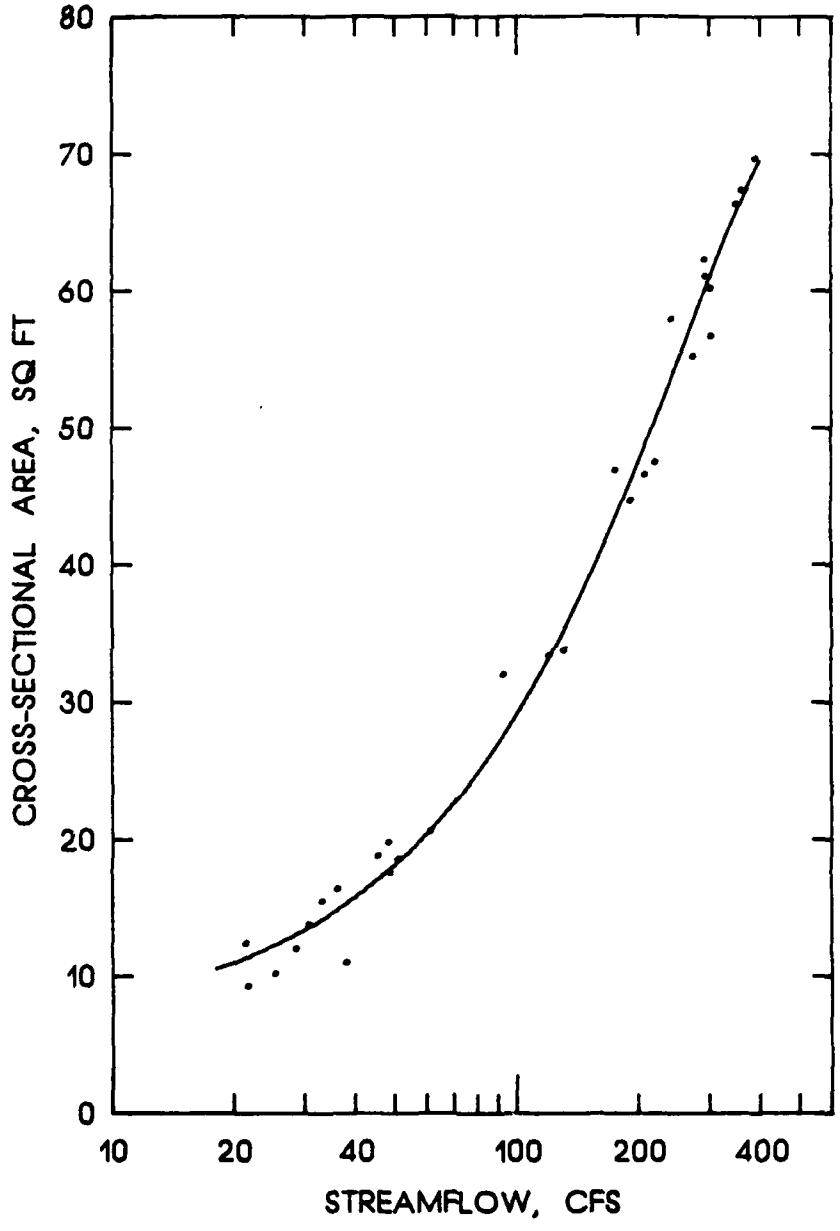

Figure C.1. Cross-sectional area versus streamflow for Fivemile Creek.

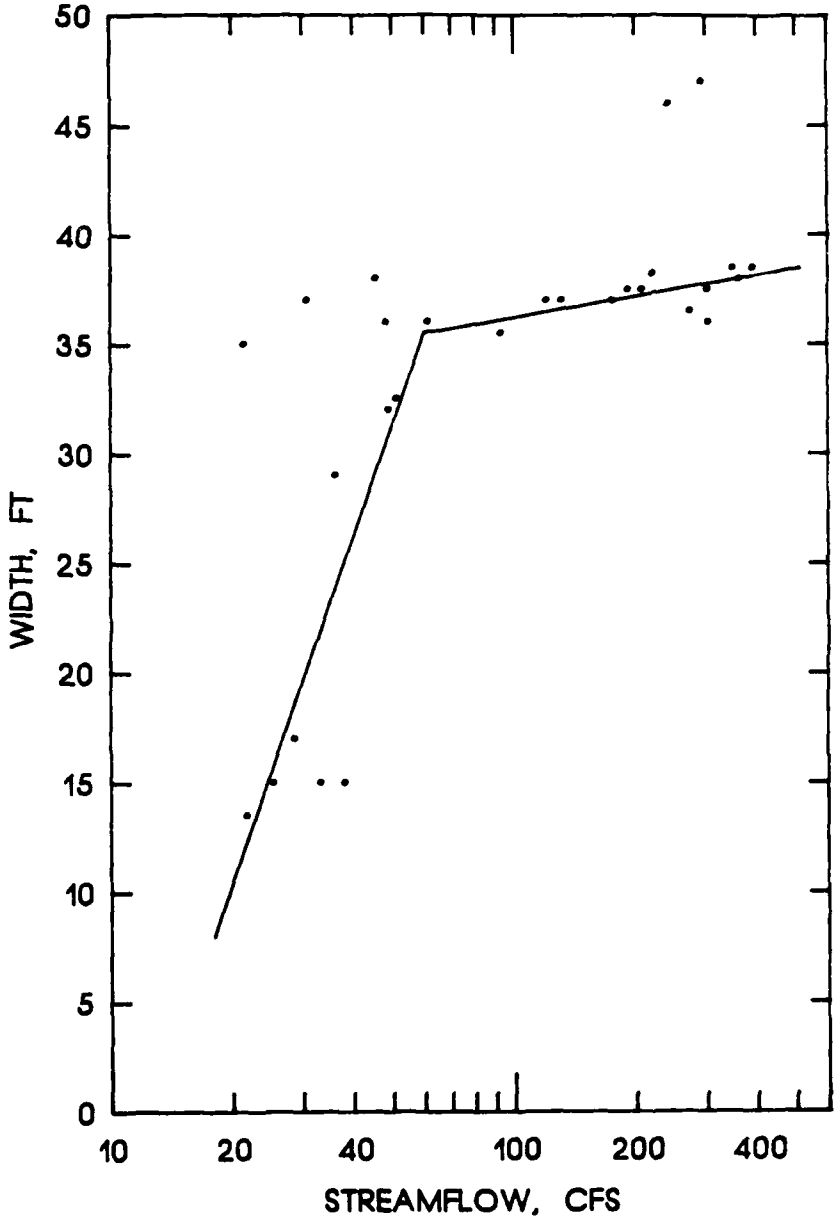

Figure C.2. Channel width versus streamflow for Fivemile Creek.

APPENDIX D

GAGING DATA FOR GOODWIN CREEK, MISSISSIPPI

The data in this appendix were collected and provided by the US Department of Agriculture-Agricultural Research Service, Sedimentation Laboratory, Oxford, Mississippi. The data were collected at the Goodwin Creek research catchment, Station 2. The streamflow and suspended-sediment data were collected on August 27, 1986. The bed material was sampled on May 9, 1986.

Table D.1. Bed Material at Station 2, Goodwin Creek, Mississippi

Size, mm	Percent Finer
0.0625	0.24
0.088	0.26
0.125	0.34
0.177	0.74
0.25	2.9
0.354	6.1
0.5	8.0
0.707	9.7
1.0	12.4
2.0	19.6
4.0	30.0
8.0	46.3
16.0	69.6
38.05	100.0

Table D.2. Streamflow Data for Goodwin Creek, Station 2
Water Temperature 72° F

Time hrs	Discharge cfs	Effective Width ft	Cross-Sectional Area ft	Hydraulic Radius ft	Depth of Sampled Vertical ft
1935	440.28	15.87	50.46	1.61	3.18
1941	659.43	18.46	69.95	2.05	3.79
1943	683.71	18.69	71.94	2.09	3.85
1944	725.28	19.06	75.30	2.16	3.95
1946	768.25	19.43	78.71	2.23	4.05
1951	858.40	20.15	85.62	2.37	4.25
1954	905.61	20.49	89.14	2.43	4.35
1955	929.75	20.66	90.92	2.47	4.40
1957	964.15	20.90	93.42	2.51	4.47
2001	989.16	21.07	95.22	2.55	4.52
2002	1019.65	21.26	97.39	2.59	4.58
2003	1014.53	21.23	97.03	2.58	4.57
2004	1014.53	21.23	97.03	2.58	4.57
2005	1014.53	21.23	97.03	2.58	4.57
2006	1019.65	21.26	97.39	2.59	4.58
2008	1014.53	21.33	98.12	2.60	4.60
2011	1035.09	21.36	98.48	2.61	4.61
2012	1040.27	21.40	98.85	2.61	4.62
2013	1045.46	21.43	99.21	2.62	4.63
2016	1035.09	21.36	98.48	2.61	4.61
2018	1035.09	21.36	98.48	2.61	4.61
2019	1040.27	21.40	98.85	2.61	4.62
2020	1035.09	21.36	98.48	2.61	4.61
2021	1035.09	21.36	98.48	2.61	4.61
2023	1029.93	21.33	98.12	2.60	4.60
2024	1029.93	21.33	98.12	2.60	4.60
2025	1019.65	21.26	97.39	2.59	4.58
2028	1014.53	21.23	97.03	2.58	4.57
2029	1009.43	21.20	96.67	2.57	4.56
2031	999.27	21.13	95.94	2.56	4.54
2032	979.11	21.00	94.50	2.53	4.50
2033	979.11	21.00	94.50	2.53	4.50
2036	949.32	20.80	92.35	2.49	4.44
2037	929.75	20.66	90.92	2.47	4.40
2040	881.83	20.32	87.38	2.40	4.30
2041	872.41	20.25	86.68	2.39	4.28
2042	867.72	20.22	86.33	2.38	4.27
2043	849.13	20.08	84.93	2.35	4.23
2044	844.52	20.04	84.58	2.35	4.22
2050	781.41	19.54	79.73	2.25	4.08
2056	704.32	18.88	73.62	2.13	3.90
2100	663.44	18.49	70.28	2.06	3.80

(Continued)

Table D.2 (Concluded)

Time hrs	Discharge cfs	Effective Width ft	Cross-Sectional Area ft	Hydraulic Radius ft	Depth of Sampled Vertical ft
2105	597.10	17.82	64.69	1.94	3.63
2110	534.68	17.12	59.22	1.81	3.46
2115	479.47	16.42	54.18	1.70	3.30
2110	462.91	16.19	52.62	1.66	3.25
2125	385.01	15.00	45.00	1.47	3.00
2130	344.90	14.30	40.90	1.40	2.86
2135	312.49	13.70	37.54	1.34	2.74
2145	250.72	12.45	31.00	1.22	2.49
2155	196.52	11.20	25.09	1.10	2.24
2205	158.46	10.20	20.81	1.00	2.04

Table D.3. Point Sampler Data for Goodwin Creek, Station 2

The point sampler is located 0.92 ft above the channel invert.

Time	Percent Finer than Indicated Size, mm												Sample Concentration
hrs	0.002	0.0625	0.088	0.125	0.177	0.25	0.354	0.5	0.707	1.0	2.0	4.0	ppm
1935	12.9	74.6	74.6	75	76	80	88.4	96	97.9	98.7	99.6	100	9450
1941	13	71	71	72.3	73.5	78.8	86.8	93.7	97.4	100			8120
1943	12	65	65	66	67	73	83.6	92.8	97.5	99.7	99.7	100	8600
1944	10	53.6	53.6	53.8	54.8	65.6	86.7	96	100				10100
1946	2.5	62.4	62.4	62.4	63.4	66.9	71.6	83	94	98	100		8000
1951	4.2	20.3	20.3	20.3	20.7	25.7	38.6	52.6	74.6	87.5	99	100	19400
1954	5.4	26.1	26.1	26.1	26.2	27.7	34	43.6	66.6	89	98.9	100	15600
1955	7.2	35.8	35.8	35.8	37	41.9	53.7	68.6	87.5	94.7	99.3	100	11500
1957	6	30.8	30.8	30.8	30.8	36	55	79.5	94.8	99	100		13000
2001	5	25.4	25.4	25.4	25.4	28.8	37.3	47.8	62.4	85.7	98.4	100	13500
2002	8	39	39	39	39	44	59.7	75.1	90.5	96	99.4	100	8270
2003	3.4	16	16	16	16	17.5	24.2	40.4	59.9	84	98	100	20600
2004	8	40	40	40	40.1	41.7	53	72.3	89.6	95.6	100		9400
2005	6.4	31.4	31.4	31.4	31.4	36	48.6	73.4	92	98	99	100	11400
2006	10.8	52	52	52	52	54.8	61.9	73.5	87.3	96.3	100		6930
2008	9.25	45.8	45.8	45.8	45.8	52.2	62.8	75	80.9	88.2	99	100	5970
2011	8.8	50.2	50.2	51.2	51.3	54.3	70.6	87.2	99	100			6940
2012	3.6	18.4	18.4	18.4	18.4	22.4	57.7	84.5	99	100			17300
2013	5.9	31.4	31.4	31.4	31.4	34.1	45.5	60.6	81.7	96.5	98	100	10400
2016	9.8	50.4	50.4	50.4	50.4	53.8	64.4	80	91.8	95.2	100		6280
2018	2.3	65.6	65.6	65.6	66.5	70.1	79.6	94	95.5	100			4690
2019	16.4	74	74	74	74	74	86.2	93.4	98.7	100			4200
2020	17.2	78.8	78.8	78.8	78.8	80.3	90.2	96.6	96.6	96.6	100		3890
2021	17.5	80.6	80.6	80.6	80.6	82.8	86.5	93.4	94.4	96.6	100		3640

(Continued)

Table D.3. (Concluded)

Time	Percent Finer than Indicated Size, mm												Sample Concentration
hrs	0.002	0.0625	0.088	0.125	0.177	0.25	0.354	0.5	0.707	1.0	2.0	4.0	ppm
2023	19.7	85.7	85.7	85.9	86	87	92.2	97.8	98.5	99.1	100		3630
2024	20.3	85.4	85.4	85.4	86	88.3	94.2	98	98.4	100			3620
2025	9.3	42.7	42.7	42.7	43.4	48.9	64.1	80.7	92.4	97.4	100		7770
2028	10.2	45.4	45.4	45.4	45.6	48.9	62.8	84.4	92.7	97.4	100		6660
2029	12.1	53.2	53.2	53.2	54.3	55.9	63.4	79.9	93.1	96.8	100		5170
2031	11.5	53.6	53.6	53.6	53.8	56.9	62.4	78	90.9	97.2	100		4990
2032	14.2	63.7	63.7	63.7	64	66.3	71.9	81.4	91.5	96.1	100		4410
2033	14.8	69.8	69.8	70.1	70.3	73.3	79.3	86.7	93.9	95.2	100		3860
2036	11.2	50.8	50.8	50.8	52.4	52.6	57.3	63.7	66.9	78.8	100		5450
2037	17.4	73.5	73.5	73.5	73.9	76.1	80.1	86.7	95.3	95.5	100		3750
2040	17.5	72.9	72.9	72.9	74.9	78.4	83.8	91.5	92.3	92.6	100		3240
2041	20.2	81.4	81.4	81.9	82.4	85.7	91.2	97.6	98.8	100			2750
2042	17.9	81.2	81.2	81.4	82	84.1	87.4	94.4	99	100			2890
2043	21.3	88.8	88.8	88.8	89	91	95	98.9	100				2800
2044	22.6	88.6	88.6	88.6	88.8	90.5	96	99.2	100				2560
2050	16.9	68.5	68.5	68.5	70.6	71.4	77.5	88	96.3	98.2	100		3610
2056	8.8	35.6	35.6	35.6	35.6	37.7	44.7	60.4	81	93.8	100		5440
2100	17.8	73	73	73	73	74.6	81.9	91.2	98.7	100			2940
2105	19	70.6	70.6	70.6	70.6	71.5	76.5	89.8	96.2	98.8	100		2010
2110	24	93.7	93.7	93.7	93.7	96.2	98.3	99.2	100				1880
2115	24.8	90.2	90.2	90.8	91	92.9	97.2	98.6	100				1780
2120	19.4	76.3	76.3	76.3	76.3	77.8	80.1	83.2	85.8	91	100		2340
2125	24.5	86.4	86.4	86.4	86.8	88.2	90.5	92.4	94.8	100			1470
2130	22.2	90.9	91.8	91.8	92.5	94.2	94.7	95.4	98	100			1590
2135	25.3	95.3	95.3	95.3	95.3	95.8	96.1	97.2	98.7	100			1500
2145	27	92.1	92.1	92.1	92.1	92.1	93.2	93.7	95.7	97.3	100		1260
2155	28.5	98.4	98.4	98.4	98.4	98.4	98.4	98.4	98.4	100			1320
2205	24.7	92.2	92.2	92.2	92.2	94.2	97.3	97.6	97.6	97.6	100		1250

Table D.4. Total Load Station Data for Goodwin Creek, Station 2

Time	Percent Finer than Indicated Size, mm													Sample Concentration
hrs	0.002	0.0625	0.088	0.125	0.177	0.25	0.354	0.5	0.707	1.0	2.0	4.0	8.0	ppm
1935	11	56.2	56.2	56.2	57.3	60.2	66.7	76.7	87.8	91.9	94.9	95.7	100	11400
1941	18.4	84.8	84.8	84.8	85.2	86.2	88.5	91.9	95.8	97.2	98.2	98.5	100	6360
1943	16.8	70.6	70.6	71.8	72.2	73	78.3	85.7	87.3	88.6	97.1	100		6580
1944	16.5	75.9	75.9	76.9	77.2	77.9	82.2	88.3	89.6	90.6	97.6	100		6120
1946	15	63.1	63.1	63.1	64.3	67.4	72.5	82.6	87.3	91.2	95.8	100		6870
1951	10.8	48	48	48	48.9	49.9	53.9	62.4	77.6	85.1	88.6	95.9	100	8330
1954	13.7	66	66	66	66.1	67.9	71.6	76.9	81.9	84.7	89.3	94.8	100	6070
1955	8.5	34.7	34.7	34.7	34.7	36.5	49.4	66.1	89.1	93.7	93.7	98.6	100	10100
1957	17.6	72.5	72.5	72.5	72.5	73.3	78.7	85.7	95.4	97.4	97.4	99.4	100	4790
2001	7.4	31.4	31.4	31.4	31.4	32.4	34.1	37.2	42.6	52.8	76.5	97.6	100	11000
2002	9.8	42.4	42.4	42.4	42.4	43.2	47.3	54.8	67.3	83.5	91.5	100		8280
2003	9	37.7	37.7	37.7	37.7	39	42.9	49.2	60.9	75.5	80.7	96.6	100	8720
2004	14.8	71	71	71	71.7	74.3	81.7	90.6	94.9	95.1	98.4	100		4820
2005	17.6	81.1	81.1	81.1	81.6	83.3	88.1	93.9	96.7	96.8	99	100		4130
2006	18.2	83	83	83	83.5	85	89.3	94.5	97	97.2	99	100		3990
2008	17.1	78	78	78.1	79.1	80.5	83.3	90.7	93.5	95.3	95.9	100		4140
2011	10.3	48.3	48.3	48.3	48.7	53	58.1	65.8	77.4	84.8	96.4	100		6570
2012	12.3	59.8	59.8	59.8	60.4	62.3	67.6	75.5	84.4	92.4	98.6	100		5180
2013	6	29.7	29.7	29.7	29.7	30.4	33.4	39.6	49.9	74.6	85	97.3	100	10200
2016	5.5	26.9	26.9	26.9	27	29.2	33.4	40.7	58.5	80	83.3	100		11200
2018	6.3	30.2	30.2	30.6	30.9	33	38	49.2	64.5	83.6	87.4	96.6	100	10300
2019	11	53	53	53.2	53.7	55.9	62.3	68.7	76	88.7	92.4	100		5490
2020	5.3	24.5	24.5	24.5	25	27	32.1	42.5	52.8	78.2	85.5	97.4	100	12500
2021	12.8	56.8	56.8	56.8	56.8	58.9	62.9	67.8	75.1	80.1	84.9	93.5	100	5280
2023	7.6	34.5	34.5	34.5	34.5	38.7	47.8	74.4	85.7	85.7	85.7	100		8870
2024	7.2	31.6	31.6	31.6	31.6	33.6	38.7	45.8	56.6	71.4	89.5	96.4	100	9750

(Continued)

Table D.4. (Concluded)

Time	Percent Finer than Indicated Size, mm													Sample Concentration
hrs	0.002	0.0625	0.088	0.125	0.177	0.25	0.354	0.5	0.707	1.0	2.0	4.0	8.0	ppm
2025	13.6	60.4	60.4	60.4	60.4	61.5	64.5	68.6	74.8	83.4	93.9	97.9	100	4860
2028	17.2	74.7	75.7	74.7	74.7	75.4	77.3	79.9	83.9	89.4	96.1	98.7	100	3920
2029	18	82	82	82	82	82.6	83.9	85.8	88.6	92.5	97.2	99	100	3500
2031	9.9	46.3	46.3	46.3	46.3	46.6	49.8	53.4	62.8	71.8	82.2	97.1	100	5950
2032	9.4	42.8	42.8	42.8	42.8	43.2	47.4	48.9	58	75.5	82.1	100		6350
2033	14.8	68.3	68.3	68.3	68.3	68.5	70.8	71.7	76.7	86.4	90.1	100		3790
2036	11	47.5	47.5	47.5	47.5	47.9	51.5	54.8	65.8	71.3	87.8	100		5620
2037	15.5	69.3	69.3	69.3	69.3	69.5	71.7	73.6	80	83.2	92.9	100		3750
2040	10	42.7	42.7	42.7	42.7	44.6	48.9	54.4	63.7	77.8	90.1	100		5840
2041	12.8	52.7	52.7	52.7	53.8	55.4	61.3	67.7	70.1	72.5	76.9	78.1	100	4640
2042	19.8	82.9	82.9	82.9	83.3	83.8	86	88.3	89.2	90	91.6	92	100	2950
2043	17.6	76.6	76.6	77.1	78	78.5	82.7	88.4	89.8	90.1	93.5	100		3150
2044	22.4	88.4	88.4	88.7	89.1	89.4	91.5	94.2	94.9	95.1	96.8	100		2670
2050	21.9	80.3	80.3	80.7	81.5	81.9	85.5	90.2	91.4	91.7	94.5	100		2770
2056	25.3	91	91	91.2	91.6	91.8	93.4	95.6	96.1	96.2	97.5	100		2320
2100	15.7	56.9	56.9	56.9	56.9	57.9	61.9	66.8	69.5	74.1	80.1	100		3850
2105	7.5	25.4	25.4	25.4	25.4	25.8	31.2	44	69.6	69.6	69.6	100		7710
2110	10.1	34.6	34.6	34.6	34.8	35.3	36.1	38.7	39.4	46	58.7	82.9	100	5680
2115	9.6	31.4	31.4	31.4	31.4	31.6	32.4	34.1	36.6	46.4	58.7	100		6260
2120	5.2	19.4	19.4	19.4	19.4	19.6	23.9	34.9	68.8	80.7	80.7	100		9790
2125	3.5	12.2	12.2	12.2	12.2	12.4	17.6	35.1	65.3	89.4	89.9	100		14800
2130	16.9	53.1	53.1	53.1	53.1	53.8	54.1	55.1	55.3	63	67.9	100		3260
2135	13.9	45.5	45.5	45.5	45.5	45.5	45.7	46.1	49.2	52.5	52.5	74	100	3770
2145	11	39.6	39.6	39.6	39.6	39.6	40	40.8	42.5	47.8	61.2	100		3990
2155	9.6	29.8	29.8	29.8	29.8	29.8	32.5	32.8	33.2	34.2	56.9	92.5	100	4670
2205	14	43.1	43.1	43.1	43.1	46.9	53.4	62.3	66.8	75.2	91.2	100		2960